

**ANTI-INFLAMMATORY PROPERTIES OF C-PEPTIDE.
A NEW THERAPEUTIC STRATEGY FOR REDUCING VASCULAR DAMAGE IN
TYPE 1 DIABETES PATIENTS**

by

Vincenza Cifarelli

M.S in Pharmaceutical Biotechnology, University of Modena and Reggio Emilia, Italy, 2005

Submitted to the Graduate Faculty of
Department of Human Genetics
Graduate School of Public Health in partial fulfillment
of the requirements for the degree of
Doctor of Philosophy

University of Pittsburgh

2011

UNIVERSITY OF PITTSBURGH
GRADUATE SCHOOL OF PUBLIC HEALTH

This dissertation was presented

by

Vincenza Cifarelli

It was defended on

May 5, 2011

and approved by

Micheal Barmada, PhD, Associate Professor, Department of Human Genetics, Graduate School of Public Health, University of Pittsburgh

David Finegold, M.D., Professor, Department of Human Genetics, Graduate School of Public Health, University of Pittsburgh

Patrizia Luppi, M.D., Research Assistant Professor, Department of Pediatrics, Children's Hospital of Pittsburgh, University of Pittsburgh

Massimo Trucco, M.D., Hillman Professor and Director of Division of Immunogenetics, Department of Pediatrics, School of Medicine, University of Pittsburgh

Dissertation Director: Robert Ferrell, PhD, Professor, Department of Human Genetics, Graduate School of Public Health, University of Pittsburgh

Copyright © by Vincenza Cifarelli

2011

**ANTI-INFLAMMATORY PROPERTIES OF C-PEPTIDE. A NEW
THERAPEUTIC STRATEGY FOR REDUCING VASCULAR DAMAGE IN TYPE 1
DIABETES PATIENTS**

Vincenza Cifarelli, PhD

University of Pittsburgh, 2011

C-peptide, historically considered a biologically inactive peptide, has been shown to exert insulin-independent biological effects on a number of cells proving itself as a bioactive peptide with anti-inflammatory properties. Type 1 diabetes (T1D) patients typically lack physiological levels of insulin and C-peptide and are at increased risk of developing complications affecting the vessels of the eye, the kidneys, and the peripheral nerves. Inflammation is an important factor for the development of diabetes-associated vascular complications, and there is increasing evidence that T1D patients, even at a young age and after short duration of T1D, have circulating activated monocytes and increased plasma levels of inflammatory cytokines.

It has been hypothesized that lack of circulating C-peptide might contribute to the development of diabetes-associated vascular complications by reducing the inflammatory response associated with T1D. In this study, we investigated the direct effect of C-peptide on several inflammatory processes of vascular damage, such as endothelial dysfunction and monocyte activation.

In an hyperglycaemia-induced model of vascular dysfunction, we found that C-peptide exerted its beneficial effect on a variety of inflammatory events such as cytokines secretions, adhesion molecules expression, oxidative stress generation, and cellular proliferation. Finally, to gain insights on the cell biology of C-peptide, we investigated its process of from the cell surface and its sub-cellular localization in target cells. Our findings indicate that C-peptide internalization from the cell surface within membrane-bound organelles of the endocytic pathway and excluded direct translocation across the plasma membrane. The importance of this finding is that endosomes represent intracellular sites from which C-peptide affects key signaling pathways in target cell.

The present evidences favor the view that replacement therapy with C-peptide in T1D patients has a critical public health impact for decreasing diabetic complications. In fact C-peptide therapy replacement offers an approach to retard the development of diabetes-associated vascular complications, for which no causal therapy is available today.

Much of the burden of diabetes is due to the development of microvascular complications including retinopathy, nephropathy and neuropathy. The prevention and treatment of microvascular complications are of critical importance to decrease the associated mortality and morbidity.

TABLE OF CONTENTS

| | |
|--|------------|
| ACKNOWLEDGMENTS..... | X |
| ABBREVIATIONS..... | XII |
| 1.0 INTRODUCTION..... | 1 |
| 2.0 REVIEW OF RELEVANT LITERATURE..... | 6 |
| 2.1 What is C-peptide..... | 6 |
| 2.2 Type 1 Diabetes as multifactorial disorder..... | 8 |
| 2.2.1 Genetics..... | 8 |
| 2.2.2 Epidemiology..... | 10 |
| 2.3 Players of the inflammation process during T1D..... | 11 |
| 2.4 Function of the endothelium layer in the vascular system..... | 13 |
| 2.5 T1D as risk factor for endothelial dysfunction..... | 13 |
| 2.6 Critical steps in vascular damage during T1D..... | 15 |
| 3.0 MATHERIALS AND METHODS..... | 17 |
| 4.0 HUMAN C-PEPTIDE ANTAGONIZES HIGH GLUCOSE ENDOTHELIAL DYSFUNCTION THROUGH NF-KB PATHWAY..... | 33 |
| 4.1 ABSTRACT..... | 34 |
| 4.2 INTRODUCTION..... | 34 |

| | |
|--|----|
| 4.3 RESULTS..... | 36 |
| 5.0 HUMAN PROINSULIN C-PEPTIDE REDUCES HIGH GLUCOSE-INDUCED PROLIFERATION AND NF-KB ACTIVATION IN VASCULAR SMOOTH MUSCLE CELL..... | 43 |
| 5.1 ABSTRACT..... | 44 |
| 5.2 INTRODUCTION..... | 44 |
| 5.3 RESULTS..... | 46 |
| 6.0 C-PEPTIDE REDUCES GLUCOSE-INDUCED ROS PRODUCTION IN ENDOTHELIAL CELL BY AFFECTING THE NADP(H) OXIDASE SUBUNIT RAC- 1..... | 55 |
| 6.1 FIGURES OF CHAPTER 6.0..... | 58 |
| 7.0 C-PEPTIDE REDUCES PRO-INFLAMMATORY CYTOKINE SECRETION IN LPS STIMULATED U-937 MONOCYTES IN CONDITION OF HYPERGLYCAEMIA..... | 65 |
| 7.1 FIGURES OF CHAPTER 7.0..... | 67 |
| 8.0 INTERNALIZATION OF C-PEPTIDE IN ENDOTHELIAL AND SMOOTH MUSCLE CELLS..... | 71 |
| 8.1 ABSTRACT..... | 72 |
| 8.2 INTRODUCTION..... | 72 |
| 8.3 RESULTS..... | 74 |
| 9.0 DISCUSSION..... | 83 |
| 10.0 CONCLUSION..... | 90 |
| BIBLIOGRAPHY..... | 91 |

LIST OF TABLES

| | |
|--|----|
| Table 1. Type 1 diabetes risk associated with HLA-DR and HLA DQ haplotypes..... | 10 |
|--|----|

LIST OF FIGURES

| | |
|---|----|
| Figure 1. C-peptide cellular targets documented in literature..... | 2 |
| Figure 2. Proinsulin C-peptide molecule..... | 7 |
| Figure 3. Endothelial dysfunction during atherosclerosis in diabetes..... | 16 |
| Figure 4. C-peptide decreases high glucose-stimulated VCAM-1 mRNA after 4h and 24h..... | 37 |
| Figure 5. C-peptide reduces high glucose-stimulated VCAM-1 protein expression on HAEC...38 | |
| Figure 6. C-peptide reduces adhesion of U-937 to HAEC in condition of hyperglycaemia..... | 39 |
| Figure 7. C-peptide decreases high glucose stimulated MCP-1 and IL-8 secretion..... | 40 |
| Figure 8. Expression of NF- κ B p65/p50 in HAEC cultured in high glucose in the presence of C-peptide..... | 41 |
| Figure 9. C-peptide reduces high glucose-induced proliferation of VSMCs..... | 48 |
| Figure 10. C-peptide stimulated proliferation of VSMCs under normal glucose..... | 49 |
| Figure 11. C-peptide reduces the number of Ki67 ⁺ cells..... | 50 |
| Figure 12. Expression of p65/p50 subunits of NF- κ B in UASMC..... | 51 |
| Figure 13. C-peptide treatment reduces high glucose induced nuclear translocation of p65 subunit in NF- κ B in UASMC..... | 53 |
| Figure 14. Inhibitory effect of C-peptide on phosphorylation of I κ B- α protein in UASMC..... | 54 |
| Figure 15. C-peptide decreases generation of histone-associated-DNA fragments in HAEC exposed to glucose for 48h..... | 56 |
| Figure 16. C-peptide decreases caspase-3 activity and expression in HAEC exposed to high glucose..... | 57 |
| Figure 17. C-peptide increases Bcl-2 expression in HAEC exposed to high glucose..... | 58 |
| Figure 18. Measurement of oxidative stress in HAEC exposed to high glucose..... | 60 |
| Figure 19. Effect of C-peptide on Rac-1 translocation exposed to high glucose..... | 62 |
| Figure 20. C-peptide decreases Rac GTPase activation in HAEC..... | 63 |

| | |
|---|----|
| Figure 21. C-peptide reduces LPS-stimulated secretion of cytokines in U937 monocyte..... | 67 |
| Figure 22. C-peptide reduces adhesion of U937 monocyte to HAEC..... | 68 |
| Figure 23. C-peptide diminishes nuclear traslocation of p65/p50 subunits of NF- κ B in LPS stimulated U937..... | 69 |
| Figure 24. Inibitory effect of C-peptide on phosphorylation of I κ B- α protein in LPS-stimulated U937 monocyte..... | 70 |
| Figure 25. C-peptide internalizes in HAEC and UASM as punctate structures..... | 76 |
| Figure 26. C-peptide internalization is inhibited at 4°C..... | 77 |
| Figure 27. Alexa Fluor 488-labelled C-peptide internalization is inhibited by an excess of unlabelled C-peptide..... | 78 |
| Figure 28. Effect of different pharmacological compounds on C-peptide entry into HAEC..... | 79 |
| Figure 29. Internalized Alexa Fluor546-labelled C-peptide co-localize with early endosomes in UASMC..... | 80 |
| Figure 30. Immunohistochemistry of C-peptide internalization and localization to early endosome..... | 81 |
| Figure 31. C-peptide co-localizes with isolated early endosomes in UASMC..... | 81 |
| Figure 32. Internalized AlexaFluor488-labelled C-peptide traffics to lysosomes in UASMC..... | 82 |

ACKNOWLEDGMENTS

I would like to acknowledge Dr. Patrizia Luppi for her endless support, instruction, and collaboration throughout my graduate studies. Dr Luppi has been always willing to share her knowledge, stimulating professional discussion and encouraging independent thoughts. She made me a more accountable researcher, a better critical thinker, and has inspired me throughout these years together. I will always be thankful for her exceptional mentoring on dedicating her time and intellectual energy to my graduate training. It has been a privilege to conduct research in her laboratory under her guidance.

This work could not have been possible without the guidance and support of Dr. Massimo Trucco, whose laboratory provided the financial, scientific, and intellectual resources for all of this research. Many technicians, students, fellows, and professors from the Diabetic Institute “Rangos Research Center” contributed in a myriad of ways to my intellectual growth during my time spent at the Diabetic Institute of the Children’s Hospital of Pittsburgh.

A special thanks goes to the Graduate School of Public Health and my instructors throughout the doctoral curriculum. I will always remember their genuine enthusiasm for science and critical thinking. Finally, I would like to thank my family for supporting my decision to pursue my scientific dreams overseas, as well as my husband Lamar for his emotional support and advice throughout the process.

ABBREVIATIONS

| | |
|----------------|--------------------------------------|
| T1D | Type 1 Diabetes |
| T2D | Type 2 Diabetes |
| EBM | Endothelial basal medium-2 |
| EGM | Endothelial growth media |
| HAEC | Human aortic endothelial cells |
| SMGM-2 | Smooth muscle cell basal medium-2 |
| UASMC | Umbilical artery smooth muscle cells |
| VCAM-1 | Vascular Cell Adhesion Molecule-1 |
| MCP-1 | Monocyte Chemoattractant Protein-1 |
| NF- κ B | Nuclear Factor (NF)- κ B |
| PBS | Phosphate Buffer Saline |
| MFI | Mean Florescence Intensity |
| mAb | Monoclonal antibody |
| PDTC | Pirrolydine Dithiocarbamate |
| ROS | Reactive Oxygen Species |
| RAB5A | RAB5A, member RAS oncogene family |
| EEA1 | Early endosome antigen 1 |
| MDC | Monodansylcadaverine |

1.0 INTRODUCTION

Human C-peptide is a 31 amino acid long peptide secreted by pancreatic β -cells. In healthy individuals, C-peptide is secreted in the peripheral circulation in equimolar amount with insulin in response to elevated blood glucose levels (hyperglycemia), but it is absent in the majority of T1D patients¹⁻³. C-peptide was considered biologically inactive and necessary only for proinsulin folding within beta-cells⁴⁻⁵. Research during the last years has provided direct and robust evidence that C-peptide is in effect capable of insulin-independent biological effects in many different cell types (Figure 1), where it affects activation of several intracellular pathways, such as, but not limited to, those involved in cellular proliferation and inflammation⁶⁻⁸.

Patients with T1D exhibit an increased susceptibility to develop a wide range of vascular complications, including microangiopathy and atherosclerosis, which account for the majority of deaths and disability in diabetic patients⁹⁻¹¹. To date, no treatment has been implemented in order to delay or prevent the development of vascular complications. It has been proposed that C-peptide exerts beneficial effects on the vasculature, especially when the vasculature is exposed to insults such as during T1D. Importantly, results from small clinical trials have demonstrated that C-peptide is beneficial when administered as replacement therapy to T1D patients who suffers from diabetic vascular complications, in particular in relation to nephropathy, neuropathy, and augmentation of blood flow¹²⁻¹⁵. Vascular disease in diabetes originates at the level of the endothelium with abnormalities in cellular function, a condition known as endothelial dysfunction that precedes the development of structural abnormalities and damage¹⁶. The healthy endothelium plays an important role in maintaining vessel wall homeostasis, synthesizing biologically active substances that modulate vascular tone and reactivity, preventing thrombosis, and influencing smooth muscle growth. In T1D some or all of these functions are altered.

Studies during the last decades have started unraveling the molecular mechanisms underlying the vascular effects of C-peptide. Several findings have shown that C-peptide affects leukocyte-endothelium interactions by reducing up-regulation of endothelial cell adhesion molecules typically observed under inflammatory conditions.

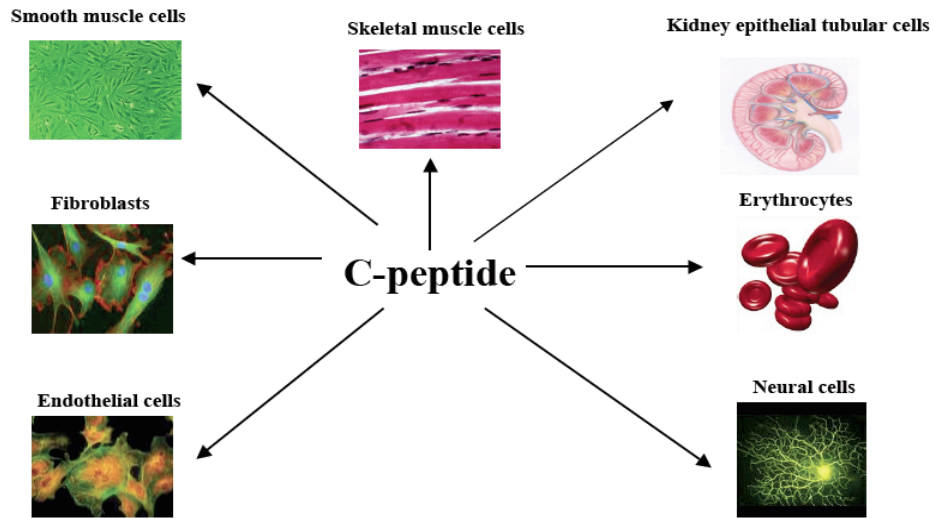


Figure 1. C-peptide cellular targets documented in literature.

The first evidence of this effect is from Scalia et al.¹⁷, who demonstrated that rats pretreated with C-peptide and injected with the inflammatory agents thrombin or N^G-nitro-L-L-arginine methyl ester (L-NAME), an agent causing acute endothelial dysfunction, resulted in reduced expression of ICAM-1 and P-selectin on the mesenteric microvascular endothelium. As a consequence, the number of rolling, adhering, and transmigrated leukocytes also decreased upon C-peptide administration to the animals. In another model of vascular injury, C-peptide decreased polymorphonuclear leukocyte (PMN) infiltration in isolated rat hearts following ischemia-reperfusion injury¹⁸. In this model, trans-endothelial migration of PMN to the sub-endothelial layers represents a prominent step in the inflammatory component of post-ischemic

injury. PMN infiltration induces endothelial and myocardial injury by releasing cytotoxic substances such as oxygen-derived free radicals, inflammatory cytokines and proteolytic enzymes. In neutrophil-depleted animals undergoing reperfused myocardial infarction, the infarct size was significantly decreased demonstrating that a significant amount of myocardial injury is induced by neutrophil-associated mechanisms^{18,19}. In the study by Young et al., systemic administration of C-peptide restored cardiac contractile function and postreperfusion coronary heart flow¹⁸ by reducing PMN infiltration to the myocardium.

Additionally, recent studies demonstrate the importance of C-peptide in modulating inflammatory pathways in the central nervous system. T1D patients may suffer impairments in learning, memory, problem solving, and mental and motor speed with primary diabetic encephalopathy recognized as a late complication of T1D²⁰. In the type 1 BB/Wor rat (rat model of human T1D), cognitive impairment is associated with apoptosis-induced neuronal loss in the hippocampus, an event associated with transcription nuclear factor (NF)- κ B and RAGE (Advanced Glycation End Products-Receptor) activation²¹. Elevated levels of the pro-inflammatory cytokines TNF- α , IL-1 β , IL-2, and IL-6 were also present in these animals²⁰. The up-regulation of RAGE and activation of NF- κ B, TNF- α , IL-1 β , IL-2, and IL-6 were significantly reduced when the diabetic rats received C-peptide replacement which was also associated with the prevention of astrocyte proliferation⁸ and reduction of apoptosis^{20,22}. However, the mechanisms able to produce the beneficial effects of C-peptide on vascular dysfunction during hyperglycaemia remain largely unknown.

This study aimed to develop an *in vitro* experimental model to investigate the direct effect of C-peptide on several processes of vascular damage, such as endothelial dysfunction and monocyte activation. We therefore initiated a study on the direct effect of C-peptide testing Vascular Cell Adhesion Molecule-1 (VCAM-1) expression, monocyte adherence, and secretion of IL-8 and Monocyte Chemoattractant Protein(MCP)-1 by endothelial cells exposed to short-term high glucose. As part of the endothelial dysfunction, we also evaluated the effects of short-term exposure of C-peptide on high glucose-induced proliferation of human aortic and human umbilical smooth muscle cells *in vitro*.

We then proceeded to study the process of human monocyte activation, a third component of the vascular damage. Specifically, we focused our investigation on the possible

anti-inflammatory effect(s) of C-peptide on cytokine release by Lypopolysaccharide (LPS)-activated human monocytes. We obtained strong evidence that C-peptide exerts anti-inflammatory properties on the endothelial and smooth muscle layers of vessel wall and circulating monocytes, neutralizing the deleterious effect inferred by hyperglycaemia.

Since activation of the transcription factor NF- κ B is involved in these pro-inflammatory responses, we also investigated the direct effect of C-peptide on nuclear translocation of the NF- κ B subunits p50/p65 in human endothelial cells, smooth muscle cells and monocyte. The study confirmed our hypothesis that physiologic concentrations of C-peptide protects the vasculature from high glucose-induced cellular dysfunction by decreasing NF- κ B activation thus inhibiting NF- κ B-dependent genes, such as VCAM-1, IL-8 and MCP-1 expression, and therefore affecting monocyte adhesion and smooth muscle cell proliferation.

However, which NF- κ B dependent upstream signaling event is affected by C-peptide in endothelial cells is not clear. Since reactive oxygen species (ROS) are powerful cellular activators of the NF- κ B pathway in condition of hyperglycaemia²³, we decided to investigate the effect of C-peptide on high glucose-induced ROS generation as the mechanism underlying its beneficial effects on endothelial cell dysfunction and apoptosis. We focused on the NAD(P)H oxidase pathway of ROS generation, which is the major pathway of ROS production in endothelial cells during diabetes.

Finally, since very little is known about the cell biology of C-peptide, we investigated the process of internalization of C-peptide from the cell surface and sub-cellular localization of C-peptide in target cells. Our findings indicate a process of C-peptide internalization from the cell surface within membrane-bound organelles of the endocytic pathway, and excluded direct translocation across the plasma membrane.

In summary, we provide evidence of an anti-inflammatory effect of C-peptide on several cellular targets involved in vascular damage in diabetes. Based on the current findings, we support a model in which C-peptide actively enters endothelial cell (mechanism also shown in smooth muscle), co-localizes with early endosomes, and it is degraded in lysosomes. The effect of C-peptide on the NF- κ B pathway might originate from a putative C-peptide/C-peptide-receptor complex signaling from the either the plasma membrane or endosomes, as it has been

demonstrated for certain Toll-like receptor pathways and other inflammatory pathways, which affect activation of the NF- κ B pathway from the endosomes^{24,25}. The mildly acidic pH of the sorting endosomes would then begin the dissociation of the C-peptide destined to lysosomes from its recycled receptor. C-peptide could inhibit the NF- κ B pathway through an effect on the activity of NAD(P)H oxidase, the major ROS producer in endothelial cells, thus decreasing apoptosis and several markers of endothelial dysfunction. Future research will have to determine the specific contribution of these mechanism(s) in C-peptide anti-inflammatory signaling.

2.0 REVIEW OF RELEVANT LITERATURE

2.1 What is C-peptide

C-peptide or connecting peptide is the 31 amino acid segment that links the A and B chains of proinsulin and serves to promote the efficient folding, assembly and processing of the insulin molecule in the beta cell endoplasmic reticulum in the course of insulin biosynthesis (Figure 2)¹. Equimolar amounts of insulin and C-peptide are subsequently stored in secretory granules of the beta cells and eventually released into the portal and systemic circulations. Unlike insulin, C-peptide escapes hepatic retention and circulates at a concentration approximately 10-fold higher than that of insulin. The peptide is primarily catabolized by the kidneys and the biological half-life of C-peptide is more than 30 min in adult humans, compared to 3-4 min for insulin².

Soon after its discovery in 1967 several investigators evaluated C-peptide for possible insulin-like effects but none were found. The apparent lack of physiological effects and consideration of the C-peptide structural variability and limited sequence conservation between species³ led to the general view that the peptide was devoid of physiological effects other than its role in insulin biosynthesis⁴. Instead, interest focused on the fact that it is co-secreted with insulin and that plasma concentrations of C-peptide effectively reflect the endogenous insulin secretion⁵. As a marker of insulin secretion, C-peptide has been of great value in furthering our understanding of the pathophysiology of both type 1 (T1D) and type 2 (T2D) diabetes. Even though C-peptide left the scientific limelight in the mid 1980s, interest in the possibility that the peptide may exert physiological effects remained. This notion was supported by the clinical observation of long standing that, compared to T1D patients in whom beta-cell function ceases totally, those patients who retain a low but detectable level of C-peptide are less prone to develop microvascular complications of the eyes, the kidneys and the peripheral nerves^{26, 27}.

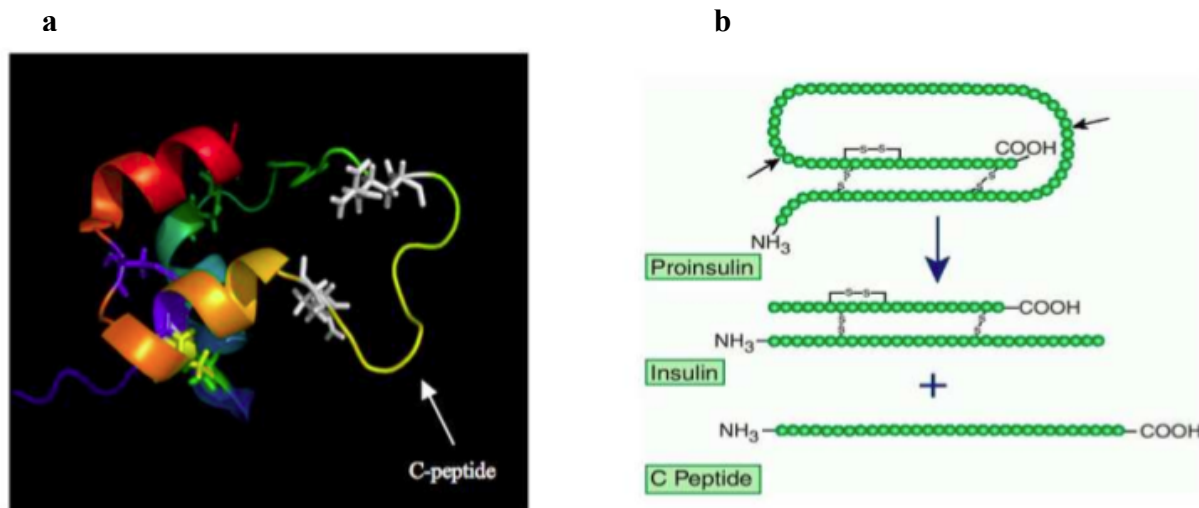


Figure 2. Proinsulin C-peptide molecule. In (a), is shown a tridimensional image of the proinsulin molecule, from which C-peptide is cleaved by endoproteases at the level of two Arginine residues linking the B-chain and C-peptide at the level of the Lysine-Arginine residues linking the C-peptide and the A-chain (in white). In Figure (b), is shown a schematic view of the proinsulin molecule. The black arrows indicate sites of cleavage by proteases at the level of Arginine residues. Once secreted into the bloodstream, C-peptide circulates at low nanomolar concentrations in healthy individuals, but it is absent in most patients with Type 1 Diabetes (T1D).

This view has recently received support from a study involving a large cohort of T1D patients treated uniformly at one medical center. The results show that a C-peptide level above 0.06 nM confers a statistically significant protective effect against the development of microvascular complications independently of glycemic control, duration of diabetes, age and sex²⁸. Moreover, pancreas or islet transplantation, with restoration of endogenous insulin and C-peptide secretion, are known to be accompanied by improvement of diabetes-induced abnormalities of nerve function, endothelial function and both structural and functional changes of the kidneys^{29, 30}.

2.2 Type 1 Diabetes as multifactorial disorder

T1D is a progressive autoimmune disease resulting from destruction of insulin-producing pancreatic beta cells³¹. The subsequent lack of insulin leads to a dramatic elevated blood glucose level (hyperglycemia) treated with exogenous long-life insulin treatment. The adjacent glucagon (alpha)- and somatostatin (delta)-producing cells in the pancreas are not affected. Hyperglycemia, glycosuria, polydipsia, and weight loss are some of the most significant early clinical signs and symptoms of the diabetic syndrome that arises when a major proportion of the beta-cells are destroyed. During the course of diabetes, most T1D patients gradually develop one or several histopathological lesions affecting the vasculature of both large and small blood vessels, leading to macro- and micro-vascular complications⁹. These lesions result in the development of accelerated atherosclerosis, coronary artery disease, visual impairment, renal dysfunction and sensory loss, all of which seriously affect the quality and life style of diabetic patients^{10,11,16,32}.

T1D is a multifactorial disease. Evidence so far indicates that the development of the disease is induced by a combination of genetic susceptibility, a diabetogenic trigger and exposure to a driving antigen^{33,60}. It is not known, however, whether all factors intervene concomitantly in a given individual or separately in a subset of patients or, whether a given environmental factor plays an etiological role in a selected genetic background³¹. A long list of environmental factors has been proposed and investigated mainly in case-control studies. Since increases in the occurrence of T1D are primarily seen in the youngest age groups in several countries, the focus of most investigators has been on exposures during the fetal, neonatal, and early childhood periods. The factors found to be associated with T1D include high birth weight, accelerated early growth, Coxsackie virus infection³³ and other pathogen exposure during gestation and early childhood, dietary factors such as breastfeeding, early exposure to cow's milk, intake of essential nutrients, climatological factors such as environmental toxins and contaminants^{34,35}. To date, none of these factors has been conclusively shown to influence the risk of T1D.

2.2.1 Genetics

Several lines of evidence indicate that the risk of developing T1D is at least partially determined by genetics. First, twin studies have revealed higher disease concordance rates among

monozygotic than dizygotic twins³⁶. However, data from the same study suggests that T1D is affected by environmental factors since the concordance rate for T1D development between monozygotic twins is less than 50%.

Genes for T1D provide both susceptibility towards, and protection from, the disease³⁷. Although many chromosomal loci have been identified, few true genes have been associated with such activity. The genetics of T1D cannot be classified according to a specific model of dominant, recessive, or intermediate inheritance of a specific set of genes³⁸.

Studies, conducted in the early-70', found that the Leukocyte Antigen (HLA) cluster region, on chromosome 6p21, is a critical susceptibility locus for T1D^{39,40}. This region, commonly termed IDDM1 (insulin-dependent diabetes mellitus locus) is located within the major histocompatibility complex (MHC) region and accounts for about 45% of genetic susceptibility for the disease⁴¹. The function of these genes in terms of immune response is well known (e.g. presentation of antigenic peptides to T lymphocytes), yet their specific contributions to the pathogenesis of T1D remain still under investigation.

After several decades of continuous progress since the discovery of HLA association, the class II genes remain the strongest genetic contributor⁴²⁻⁴⁴. T1D seems somewhat unique among autoimmune diseases in that in addition to forming susceptibility, certain MHC haplotypes provide significant protection, with protection dominant over susceptibility⁴⁵ (Table 1). The importance of class II haplotype not only depends on the well-known risk for disease associated with HLA-DR3 and HLA-DR4, but also on additional susceptibility associated with DQ α -chains and DQ β -chains⁴⁶.

T1D represents a heterogeneous and polygenic disorder, with a number (about 20) of non-HLA loci contributing to the disease susceptibility already identified⁴⁷. The IDDM2 region, on chromosome 11, maps to a variable number of tandem mini-satellite repeats (VNTR) in promoter region of insulin gene^{48,49}. The magnitude of risk correlates with the number of those tandem repeats: VNTR type I (with shorter repeats) homozygous individuals are in higher risk category and VNTR type III (longer repeats) protects carriers against the disease.

Another locus associated with T1D lies in the gene encoding for cytotoxic T lymphocyte-associated protein 4 (CTLA-4), located in the IDDM12 region which is responsible for modulating immune responsiveness⁵⁰. As with other regions, the risk association of allelic

variants in the CTLA-4 region is not exclusively confined to T1D, but has been replicated in several other autoimmune disorders, such as rheumatoid arthritis (RA)⁵¹, systemic lupus erythematosus (SLE)⁵² and multiple sclerosis (MS)⁵³.

Allelic variation in the interleukin (IL)-2 receptor- α gene (IL2RA)⁵⁴ and PTPN22, which encodes the lymphoid protein tyrosin phosphatase⁵⁵ are relatively new members of the T1D susceptibility gene set.

Table 1. Type 1 diabetes risk associated with HLA-DR and HLA-DQ haplotypes.

| Risk | HLA | | |
|------------------------------------|------------------------------|------------------------------|------------------------------|
| | HLA DRB1 | HLA DQA1 | HLA DQB1 |
| High risk | 0401, 0402,0405, 0301 | 0301 0501 | 0302 0201 |
| Moderate risk | 0801 0101 0901 | 0401 0101 0301 | 0402 0501 0303 |
| Weak or moderate protection | 0401 0403 0701 1101 | 0301 0301 0201 0501 | 0301 0302 0201 0301 |
| Strong protection | 1501 1401 0701 | 0102 0101 0201 | 0602 0503 0303 |

2.2.2 Epidemiology

T1D has historically been considered a disorder predominantly of children and young adults; the disease is commonly referred to as juvenile diabetes because of its peak expression between ages 10-14. However, several studies, conducted in the mid-90', support a different model in which the disease can occur at any age^{37, 56}. Additionally, the same studies found that 5-30% of adults patients initially diagnosed with type 2 diabetes actually had T1D, pointing a misclassification issue for the disease.

Disease onset generally occurs before the age of 30, commonly peaking around puberty (e.g. 10-14), with the peak age of onset being somewhat earlier in girls than in boy³⁴.

The incidence of T1D varies by age group. The incidence of childhood-onset T1D in the age group 0-14 years varies more than 100-fold worldwide, with Finland and Sardinia (Italy) having the highest rates (>40 and $37.8/10^5$, respectively), whereas the lowest rates have been reported from Venezuela ($0.1/10^5$) and China ($0.1-4.5/10^5$), with other Asian countries displaying a low frequency^{34,35}. In accordance with the European ancestry of much of their population, the USA, Canada, Australia and New Zealand have high to very high T1D incidence rates.

According to the America Center for Disease Control, the prevalence of T1D for residents of United States aged 0-19 years is 1.7/1,000. T1D incidence has been globally rising in the past decades, by as much as a 5.3% annually in the United States. If present trends continue, doubling of new cases of T1D in European children younger than 5 years is predicted between 2005 and 2020, and prevalence of cases in individuals younger than 15 years will rise by 70%⁵⁷ characteristic of a shift towards an earlier age⁵⁸. On this matter, The Diamond Study Group – in a study published in 2006 - commented that whatever event triggers the onset, is increasingly affecting susceptible individuals.

2.3 Players of the inflammation process during T1D

T1D is a chronic disease characterized by disruption of glucose homeostasis and by concomitant metabolic abnormalities as the result of insulin deficiency secondary to progressive autoimmune destruction of the insulin-producing pancreatic beta cells⁵⁹.

Although T cells are recognized to play a central role in the autoimmune destruction of the insulin-producing beta-cells⁶⁰, recent studies indicate that components of the innate immune system, including natural killer cells, monocytes, and inflammatory mediators have a much broader role in the pathogenesis of T1D and associated vascular complications than previously recognized⁶¹⁻⁶⁴. The primary role of monocytes in the early stages of T1D pathogenesis⁶⁵ has been demonstrated by showing that these cells are the first to accumulate in the pancreatic islets

of pre-diabetic BB rats⁶⁶. Subsequent T and B lymphocyte infiltration is dependent upon prior monocyte invasion of the islets⁶⁶, suggesting that monocytes and secreted inflammatory mediators might contribute to the early induction and amplification of the autoimmune assault against the pancreatic beta-cells⁶⁷.

A more generalized inflammatory response, with activation of monocytes and presence of oxidative stress has been found in the peripheral circulation of T1D patients. This inflammation is characterized by elevation of plasma levels of several inflammatory biomarkers, such as interleukin (IL)-1 β , IL-6, IL-8, tumor necrosis factor(TNF)- α , and C-reactive protein. Such inflammatory reactions have been detected both in recently diagnosed T1D children as well as in adult T1D patients well after the onset of diabetes⁶⁸⁻⁷³. These findings demonstrate that a generalized inflammatory response is present already in the very early stages of diabetes^{74, 75}. Many of the reported inflammatory changes are detected at the level of monocytes, which show up-regulation of the adhesion molecule CD11b (Mac-1)⁷⁵ and have aberrant constitutive and lipopolisaccharide (LPS)-stimulated expression of cyclooxygenase (COX)-2, a defect that may predispose to a chronic inflammatory response in T1D^{64,76}. The vascular endothelium represents a likely target of this inflammatory response by inducing endothelial cell activation, alteration of endothelial function, and monocyte adherence eventually leading to overt vascular damage in the later stages of T1D.

Indeed, inflammation is now considered a major component in the development of T1D-associated vascular dysfunction^{71,77-79}. It is therefore important to understand the origin of the inflammatory response characterizing T1D, since therapeutic strategies to decrease inflammatory activity in T1D will likely improve endothelial function. In particular, it is difficult to decide to what extent the inflammatory state is a primary pathogenic event contributing to the development of T1D or if it is the response to a metabolic derangement, i.e., a situation of poor glycaemic control and insulin-deficiency present at the early stages of the disease^{75, 80}. In the first case, the inflammatory state should precede overt diabetes and in this context the study of pre-diabetic subjects (i.e., autoantibody-positive individuals) should be characterized in respect to the inflammatory state.

2.4 Function of the endothelium layer in the vascular system

Endothelial cells form a continuous dynamic layer of the blood vascular system that operates to deliver blood-borne nutrients and necessary levels of oxygen into tissues and, at the same time, to remove waste⁸¹. The endothelial cell lining is continuously exposed to a variety of biomechanical forces and stimuli and is thereby designated to be the homeostatic organ for the regulation of vascular tone and structure⁸². In addition, the endothelium has a regulatory role on leukocyte-endothelium interactions, leukocyte extravasation and subendothelial accumulation, all important events in the inflammatory cascade underlying vascular damage⁸³.

Chronic exposure of endothelial cells to insults and stressors shifts the normal endothelial function to a pathological degree, called endothelial dysfunction⁸³. Endothelial dysfunction refers to a condition in which the ability of the endothelium to properly maintain vascular homeostasis is impaired⁸⁴. Several pathological conditions have been identified as potential risk factors for the development of endothelial dysfunction, such as hypertension⁸⁵, chronic renal failure⁸⁶, T1D and T2D^{87,88}, sedentary life style⁸⁹, and smoking⁹⁰. These observations suggest that the pathophysiology of endothelial dysfunction is complex and involves multiple mechanisms.

2.5 T1D as a risk factor for the development of endothelial dysfunction

Diabetes is a well-established risk factor for vascular diseases. Patients with T1D exhibit an increased susceptibility to develop a wide range of vascular complications, including microangiopathy and atherosclerosis, which account for the majority of deaths and disability in diabetic patients⁸⁸. Diabetes causes vascular compromise secondary to endothelial dysfunction. A major hallmark of diabetes is an abnormally elevated blood glucose level, i.e. hyperglycemia, which is one important factor causing endothelial dysfunction in diabetes. Acute (i.e., spike of hyperglycemia after a meal) and prolonged exposure of endothelial cells to high blood glucose are toxic to endothelial cells because they trigger massive changes in cellular phenotype, state of activation, metabolism and physiology. High glucose can exert a direct toxic effect on

endothelial cells or through the generation of intermediate products such as advanced glycation end-products (AGE)^{9,11,91,92}. These changes are initially characterized by modification of endothelial cell function, such as by an increased vascular tone and permeability due to an impaired bioavailability of vasodilator factors such as nitric oxide and of vasoconstrictor factors such as endothelin (ET)-1⁹³. High glucose exposure also modulates availability of permeability factors such as vascular endothelial growth factor (VEGF)⁹⁴.

A second sign of endothelial dysfunction is the modification of cell molecule expression on the surface of endothelial cells. These molecules are essential for leukocyte-endothelium interaction, the first step in atherosclerosis plaque formation. Generally, these adhesion molecules, such as VCAM-1, intercellular adhesion molecules(ICAM)-1, and selectins (L-selectine; or P-selectine), are expressed at low levels on endothelial cells and are up-regulated upon cellular activation, such as after exposure to high glucose or inflammation. Activated endothelial cells also increase secretion of certain pro-inflammatory cytokines, such as IL-6, IL-8 and MCP-1, which are pivotal in initiating leukocyte interactions with endothelial cells and their subsequent recruitment in the subendothelial layer (Figure 3)⁹⁵. The migrated monocyte phagocyte oxidize-low density lipoprotein(LDL), become foam cells and keep secreting inflammatory mediators that maintain inflammation by recruiting more immune cells from the bloodstream to the vessel wall. In the meantime, smooth muscle cells proliferate and migrate from the media to the intima of the vessel wall where the new atherosclerotic plaque is developing. IL-8 and MCP-1 are usually found in human atherosclerotic plaques⁹⁶. Simultaneously, adipocyte cells are also recognized to secrete circulating cytokines (adipokines) such as IL-6, tumor necrosis factor-alpha, leptin and plasminogen activator inhibitor(PAI-1), exacerbating the on-going vascular inflammation in the vessel wall of diabetic patients^{9,97}.

Additional players in the pathogenesis of hyperglycaemia-induced endothelial dysfunctions are reactive oxygen species (ROS). Hyperglycaemia increases oxidative stress and up-regulates the antioxidant enzyme machinery²³. It has been shown that hyperglycaemia-induced generation of ROS in endothelial cells occurs mainly through a NAD(P)H oxidase-dependent mechanism. NAD(P)H oxidase is an enzymatic complex made up by several subunits localized in the cytoplasm and plasma membrane. Specifically, NAD(P)H oxidase is composed by 2 membrane subunits (p22phox and gp91phox) and 4 cytosolic subunits (p40phox, p47phox,

p67phox and Rac-1). In a scenario of hyperglycaemia, NAD(P)H oxidase is stimulated and the cytosolic subunits translocate from the cytosol to the plasma membrane to induce ROS production⁹⁸. Excessive ROS production is toxic to endothelial cells and leads to decreased cellular proliferation⁹⁹ and acceleration of the apoptotic process. One of the mechanism(s) underlying ROS toxicity in the endothelium involves activation of transcription factors such as NF- κ B and activating protein(AP)-^{191,101-103}, which ultimately lead to activation of genes that increase production of inflammatory mediators and inflammatory responses in general. Increased oxidative stress is observed in peripheral blood monocyte from T1D patients suffering from microvascular complications compared to those without microvascular complications, as demonstrated by elevated levels of nitrotyrosine, monocyte superoxide anion,⁷¹ DNA and protein oxidation^{104,105}. Inflammation is now considered a major component in the endothelial dysfunction underlying vascular complications in T1D.

2.6 Critical steps in vascular damage during T1D

As shown in Figure 2, the endothelial dysfunction gravitates on the altered behavior of the cells of the artery wall, the endothelial cells and smooth muscle cells, and inflammatory leukocytes that join them in the arterial intima during the atherogenic process. Endothelial cells play an active role in the recruitment of inflammatory cells into the vessel wall, by producing cytokines and expressing cellular adhesion molecules (Fig. 2) (i.e. VCAM-1), and secretion of inflammatory cytokines as Il-8 and MCP-1.

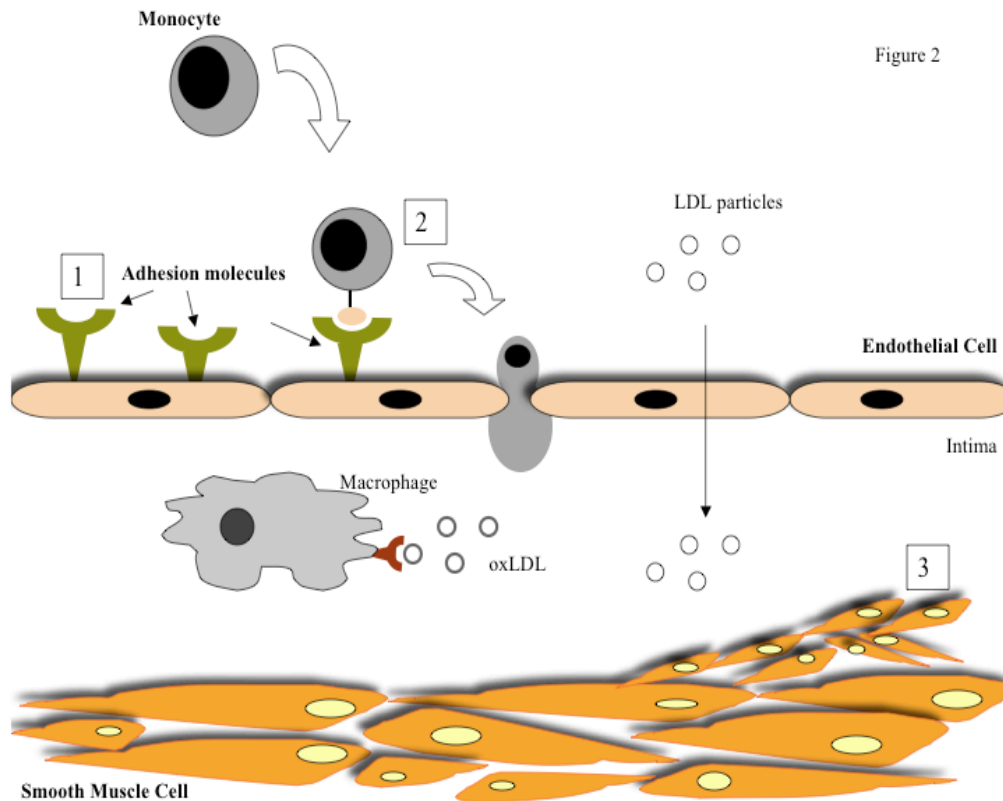


Figure 2

Figure 3. Endothelial dysfunction during atherosclerosis in diabetes. Endothelial cells play an active role in the recruitment of inflammatory cells into the vessel wall, by producing cytokines and expressing cellular adhesion molecules (1) (i.e. VCAM-1, vascular cell adhesion molecule-1) and secretion of inflammatory cytokines as IL-8 and MCP-1. Subsequently, leukocytes will migrate to the subendothelial space, and will phagocytose oxidized-LDL, becoming foam cells (2). At the same time, smooth muscle cells proliferate and migrate (3) from the media to the intima of the vessel wall where a new atherosclerotic plaque is developing.

These events will capture leukocytes (i.e. monocyte) and assist their passage into the sub-endothelial space. Subsequently, leukocytes migrate to the subendothelial space, phagocytose oxidized-LDL and become foam cells. Smooth muscle cells proliferate and migrate from the media to the intima of the vessel wall where the new atherosclerotic plaque is developing.

3.0 MATERIALS AND METHODS

3.1 EFFECT OF C-PEPTIDE ON ENDOTHELIAL DYSFUNCTION DURING HYPERGLYCAEMIA

3.1.1 Cell Cultures

Human Aortic Endothelial Cell (HAEC) were obtained from Lonza (Lonza Bioscience Walkersville Inc., Walkersville, MD) and grown into 75 cm² culture flasks (250,000/flask) (Corning Incorporated, Corning, NY, USA) at 37°C, 5% CO₂ in the presence of EBM-2 supplemented with EGM SingleQuots (Lonza) containing FBS (2%), hydrocortisone (0.04%), human fibroblast growth factor (0.4%), vascular endothelial growth factor (0.1%), R³-insulin – like growth factor (0.1%), ascorbic acid (0.1%), heparin (0.1%), human epidermal growth factor (0.1%), gentamicin sulfate amphotericin-B (0.1%). EBM-2 contains 5.6 mmol/L glucose. Fresh EBM-2 was replaced every 2-3 days, and HAEC were used at passage 2-6.

Human Umbilical Artery Smooth Muscle Cell (UASMC) and Human Aortic Smooth Muscle Cell (AoSMC) were obtained from Lonza and grown into 75cm² cell culture flasks (Corning Incorporated, NY, USA) at 37°C, 5% CO₂ in the presence of Smooth Muscle Cell Basal Medium-2 (SMGM-2) (Lonza) additioned with 5% of FBS, 0.1% of antibiotics GA-1000 (gentamicyn, amphotericin B), 0.2% of human basic fibroblastic growth factor (hFGF-b), 0.1% insulin, and 0.1% of human epidermal growth factor (hEGF) (Cambrex Bio Science). Cells were used at passage 4 to 10 for the experiments¹¹⁰.

Human monocytic U-937 cells were purchased from the American Type Culture Collection (Rockville, MD) and grown in complete RPMI 1640 (Lonza Walkersville Inc, Maryland, USA) supplemented with 10% FBS, 100µl/mL streptomycin, 100IU/mL penicillin,

250ng/mL fungizone, 1mmol/L Sodium Pyruvate and 10mmol/L HEPES (all from Gibco Invitrogen, Carlsband, CA) in T75 cm² flasks (Corning, NY, USA) at 37°C, 5% of CO₂.

3.1.2 IL-8 and MCP-1 detection in culture supernatant by ELISA

HAEC were maintained in 6-well plates (50,000/well) (Corning) in the presence of EBM-2 (Cambrex) until 80-90% confluent. On the day of the experiment, medium was replaced with fresh EBM-2 containing either 5.6 mmol/L or 25 mmol/L glucose (Sigma). Human C-peptide (Sigma) (0.5 nmol/L) was added to the high glucose medium. HAEC were also exposed to the NF-κB inhibitor PDTC (10 μM) (Sigma). HAEC were incubated at 37°C, 5% CO₂ for 4 hours. Supernatant was collected and kept at -20°C until tested by ELISA (Quantikine[®], R&D Systems, MN, USA). Three independent experiments were performed. In each experiment, each condition was tested in triplicate. Concentration of the chemokines (pg/mL) was assessed by calculating values according to the values obtained in the standard curve. Data from three separate experiments were averaged.

3.2 DETECTION OF VCAM-1

3.2.1 RT-PCR

HAEC confluent monolayers were grown into 75 cm² culture flasks (250,000/flask) (Corning) and stimulated with 25 mmol/L glucose (high glucose condition) (Sigma, St. Louis, MO) in the presence or absence of physiological concentrations of human C-peptide (Sigma) (0.5 nmol/L and 1nmol/L)¹⁰⁶ for 24 hours at 37°C, 5% CO₂. HAEC cultured in regular EBM-2 were used as a baseline for VCAM-1 expression. As a positive control, HAEC were exposed to human recombinant TNF-α(10 ng/mL) (R&D System, Inc., MN, USA), which up-regulates VCAM-1. As a control for C-peptide activity, C-peptide (1 nmol/L) was heat-inactivated by boiling it for 1 hour. RNA extraction was performed using the RiboPure[™]-Blood kit (Ambion, Texas, USA). 1μg of RNA was used for RT-PCR using Oligo(d)T (RETROscript, Ambion). VCAM-1 was

amplified from 1 μ l of cDNA using the following oligonucleotides: sense 5'-CCCTTGACCGGCTGGAGATT-3', and antisense 5'-CTGGGGGGCAACATTGACATAAAGTG-3'¹⁰⁷. TITANIUM™ Taq PCR Kit (Clontech Laboratories, Inc. Mountain View, CA) was used for PCR amplification. PCR conditions were: 94°C for 40s, 60°C for 30s, and 68°C for 3min. Amplification of GAPDH was performed as internal control using the following oligonucleotides: sense 5'-ACCACACAGTCCATGCCATCAC-3', and antisense 5'-TCCACCACCCTGTTGCTGTA-3'¹⁰⁷. PCR conditions were: 94°C for 40s, 58°C for 30s, and 68°C for 3 min. After 30 cycles, PCR products were detectable by electrophoresis. Three independent experiments were performed. Densitometry was performed with UN-SCAN-IT gel software (Silk Scientific, Orem, UT). Data were averaged and expressed as means \pm SD.

3.2.2 Surface staining by flow cytometry

HAEC were maintained in 6-well plates (50,000/well) in the presence of EBM-2 until 80-90% confluent. On the day of the experiment, medium was replaced with 2 mL of fresh EBM-2 containing either 5.6 mmol/L or 25 mmol/L glucose (Sigma). Human C-peptide (Sigma) (0.5 and 1 nmol/L) was added to the high glucose medium and cells were kept at 37°C, 5% CO₂ for 24 hours. Heat-inactivated human C-peptide (1 nmol/L) was used as control. HAEC were also exposed to human recombinant TNF- α (10 ng/mL) (R&D System). After 24 hours, HAEC were harvested and assayed for VCAM-1 expression. Determination of VCAM-1 expression was performed on PFA-fixed HAEC monolayers following a methodology shown to preserve single cell integrity, which is a prerequisite for flow cytometric determination of surface adhesion molecules¹⁰⁸. Briefly, after incubation of the cells in the different conditions, HAEC were washed with PBS (Gibco BRL, Life Technologies Inc., Rockville, MD) and fixed with 0.5% cold PFA. Cells were then stained for 30 minutes with saturating concentration of PE conjugated anti-human mAb to CD106 (VCAM-1) (BD Pharmigen, San Diego, CA). A PE isotype control (BD Pharmigen) was added at the same concentration of the specific mAb. HAEC were washed, trypsinized and the pellet fixed in cold 0.5% PFA and run on a Becton Dickinson FACSCalibur (Becton Dickinson, San Jose, CA). For each sample, at least 5,000 events were acquired.

Data were analyzed by CELLQuest software (Becton Dickinson). Dot-plot graphs of SSC versus FSC were drawn, and a gate was created around the HAEC. Within this gate, HAEC were analyzed for cells positive for CD106. Lower limits for antibody positivity were determined using the negative isotype control. Fluorescence was measured using a log₁₀ scale. Results were expressed as MFI (brightness of fluorescence) of the positive cells for CD106. Since mAb to CD106 was used at saturating concentration, the MFI of the antibody binding could be used as a semi quantitative measure of the amount of antigen detected. Three sets of independent experiments were performed. Within each experiment, each condition was tested in triplicate. Data were averaged and expressed as means ± SD.

3.3 MONOCYTE ADHESION ASSAY

HAEC confluent monolayers were grown on 48-well plates (12,000/well) (Corning) and stimulated with EBM-2 (Cambrex) with 25 mmol/L glucose in the presence of absence of 0.5 nmol/L of human C-peptide for 4 hours. Heat inactivated human C-peptide (0.5 nmol/L) was used as control for C-peptide activity. HAEC were also exposed to human recombinant TNF- α (10 ng/mL) (R&D System). Human monocytic U-937 cells were purchased from the American Type Culture Collection (Rockville, MD) and grown in RPMI 1640 (Cambrex) containing 10% FCS, 100 μ l/mL streptomycin, 100 IU/mL penicillin, 250 ng/ml fungizone, 1 mmol/L Sodium Pyruvate, 10 mmol/L HEPES (all from Gibco Invitrogen, Carlsband, CA) at 37°C, 5% of CO₂. On the day of the experiment, medium was removed from each well, cells were washed with PBS and fresh medium containing U-937 cells (1 x 10⁶ cells/mL) was added to each well and incubated for 1 hour at room temperature on a rocking plate. Non-adherent U-937 cells were removed and adherent cells fixed in 1% glutaraldehyde. To determine the number of adherent cells, three random 40x field/well were counted and averaged by a blinded investigator, avoiding areas of non-confluence and cell clusters. Three experiments were performed. Within each

experiment, each condition was tested in triplicate. Results were averaged and showed as means \pm SD.

3.4 WESTERN BLOTTING ANALYSIS

HAEC were cultured in 75 cm² culture flasks (250,000/flask) in the presence of 25 mmol/L glucose alone or in combination with C-peptide (0.5 nmol/L) for 24 hours. Heat-inactivated C-peptide (0.5 nmol/L) was used as control. Cells were harvested at 4 and 24 hours and pretreated with 25 μ l of protease inhibitor cocktail (Pierce, Rockford, IL). Nuclear and cytoplasmic fractions were separated using NE-PER[®] Nuclear and Cytoplasmic extraction kit (Pierce). Protein content of the extract was measured using a bicinchoninic acid assay kit (Pierce Biotechnology). A minimum of three independent experiments were performed. NF- κ B immunoblot was performed as previously described¹⁰⁹ with 10 μ g of nuclear protein extracts. Densitometry was performed with UN-SCAN-IT gel software (Silk Scientific). For each set of data, a minimum of three experiments was performed. Data were averaged and expressed as means \pm SD. Activation of the NF- κ B p50 subunit was detected on 3 μ g of nuclear protein extracts using a EZ-Detect[™] Transcription Factor Kit (Pierce Technology). For each set of data, a minimum of three experiments was performed. Data were averaged and expressed as means \pm SD.

For Bcl-2 and cleaved caspase-3 proteins detection, HAEC were grown into T-75cm² flasks and exposed overnight to the treatment conditions as above. For Rac-1 protein detection, HAEC were serum starved overnight before treatment for 30min. Cytosolic and membrane proteins were extracted using Qproteome Cell Compartment kit (QIAGEN, Valencia, CA) and protein content was measured using a bicinchoninic acid assay kit (Pierce Biotechnology). Aliquots of protein extracts (30 μ g) were subject to immunoblot analysis using rabbit polyclonal anti-Rac-1 (1:1000), anti-cleaved caspase-3 (1:500), anti-Bcl-2 antibodies (all from Cell Signaling Technology, Danvers, USA) and mouse monoclonal anti- β -actin antibody (1:10,000;

Sigma). Densitometry was performed with UN-SCAN-IT gel software (Silk Scientific, Orem, UT). A minimum of three independent experiments was performed.

3.5 COMMON EXPERIMENT TREATMENT FOR VASCULAR SMOOTH MUSCLE CELLS

SMGM-2 containing 25mmol/L glucose (Sigma Chemical S. Louis, MO, USA) was used as a high glucose condition in all the experiments, while basal SMGM-2, which contains 5.6mmol/L glucose, was used as normal glucose control. In all experiments, cells were serum-deprived for 24 hours with SMGM-2 containing 1% FBS and 0.1% antibiotics GA-1000. Cells were then replaced with SMGM-2 containing 25mmol/L glucose in the presence or absence of human C-peptide (0.5 and 1nmol/L) (Sigma Chemical) for 48 hours. Basal SMGM-2 containing 5.6mmol/L glucose was used as control. Insulin was not added to the culture medium. The effects of two different NF- κ B-inhibitors, such as (E)-3-(4-Methylphenylsulfonyl)-2-propenenitrile (1 μ M) (Bay11-7082; Sigma) and pyrrolidine dithiocarbamate (PDTC, Sigma) (20 μ M) were also tested in VSMCs. These NF- κ B-inhibitors were added to SMGM-2 with 25mmol/L glucose for 48 hours. Separate sets of experiments were performed in which C-peptide (0.5 and 1nmol/L) was added to medium containing normal glucose. Purity of C-peptide was $\geq 95\%$ as assessed by the manufacturer by HPLC evaluation. Human scrambled C-peptide (Sigma-Genosys, Texas, USA) was used as a control. The scrambled C-peptide has an identical amino acid composition to that of the human C-peptide, but the sequence was randomized (110).

3.6 PROLIFERATION STUDY

3.6.1 Cell counting

33,000 UASMC/well were seeded in 6-well plates (Corning Incorporated) and left overnight in an incubator at 37°C, 5% CO₂. Cells were then serum-deprived and exposed to the indicated treatment conditions and then counted using a Neubauer Hemocytometer (Hausser Scientific, Horsham, PA), as previously published^{11,112}.

3.6.2 BrdU measurement

Proliferation of VSMCs was evaluated by uptake of bromo-2'-deoxy-uridine (BrdU) using an ELISA kit (Roche Diagnostic, Mannheim, Germany) following manufacturer's instructions. Briefly, UASMC and AoSMC were seeded (6×10^4 cells/100 μ L) in 96 well flat-bottomed plate (FALCON[®] Becton Dickinson and Company, Franklin Lakes, NJ) and kept them at 37°C, 5% CO₂ overnight. Cells were then exposed to the indicated treatment conditions in the presence of 10 μ mol/L of BrdU. Each condition was tested in triplicate. Results were expressed as proliferative response (fold induction versus 5.6mmol/L) and final data averaged (mean values \pm SD).

3.6.3 Ki-67 staining

As another technique to assess VSMC proliferation, we used Ki-67 immunofluorescence staining for proliferating cells. UASMC were seeded into a glass bottom culture dish (35 mm diameter, poly-d-lysine coated) (MatTek Corporation, Ashland, MA) (~100,000 cells/dish) and then cultured following treatment conditions. Cells were permeabilized with 0.02% of Triton-X100 (Sigma), fixed with 2% paraformaldehyde (PFA) (USB Corporation, Cleveland, OH, USA) and stained with a monoclonal mouse anti-human Ki-67 primary antibody overnight (1:100, DakoCytomation, Denmark). A carboxymethylindocyanine 3(Cy3)-conjugated goat anti mouse secondary antibody (1:500, Jackson Immuno Research Lab INC. West Grove, PA) was then added for 1 hour. DAPI stain (Molecular Probes, Eugene, OR) was used to stain the nuclei. Images were recorded with a confocal laser-scanning microscope (Nikon, Eclipse E800, Japan).

The number of Ki67⁺ cells was counted in 5 different fields per dish by one of the investigator blind to the study. A Ki67-labeling index was calculated by dividing the number of Ki67⁺ cells by the total number of cells in each of the 5 fields. An averaged Ki-67-labeling index (\pm SD) was then obtained for each section. Four different independent experiments were performed.

3.7 IMMUNOFLUORESCENCE ANALYSIS FOR NF-kB P65

UASMC were seeded into a glass bottom culture dish (~100,000 cells/dish) (MatTek Corporation). After the indicated treatments, cells were fixed with 2% PFA (USB Corporation), and stained with a rabbit polyclonal primary antibody against NF-kB p65 (1:150, Santa Cruz Biotechnology, Inc) at 4°C overnight. A carboxymethylindocyanine 3(Cy3)-conjugated goat anti-rabbit secondary antibody (1:500, Jackson Immuno Research Lab INC.) was then added for 1 hour, in the dark, at room temperature. DAPI stain (Molecular Probes, Eugene, OR) was used to stain the nuclei. Fluorescence staining was evaluated using Nikon, Eclipse E800 epifluorescence microscope connected to a digital camera and interfaced with a computer.

3.8 DETECTION OF APOPTOSIS IN ENDOTHELIAL CELL

3.8.1 Treatment conditions

In all experiments, HAEC were exposed to regular EBM-2 media, or high glucose medium, or high glucose medium with either C-peptide (Phoenix Pharmaceuticals, Burlingame, CA) or scrambled C-peptide (Sigma-Genosys, Texas, USA) (10nmol/L) for a time period ranging from 30 min to 12-48 hours, as specified in each experiment, at 37°C in a humidified atmosphere of 95% air and 5% CO₂. In experiments to detect Rac-1 GTPase activity, Rac-1 mRNA expression, Rac-1 protein levels, and NAD(P)H oxidase activity, hEGF was removed from the EBM-2 media to avoid aspecific Rac activation.

3.8.2. Detection of cytoplasmic histone-associated-DNA fragments

HAEC were seeded in 96-well plates overnight and the next day treated as above for 48 hours. Apoptosis was detected by using Cell Death Detection ELISA^{PLUS} (Roche Diagnostics GmbH, Mannheim, Germany), which detects cytoplasmic histone-associated-DNA-fragments after induced-cell death. Results were expressed as absorbance raw data and percentage of apoptosis versus high glucose condition. Three different experiments were run in which each condition was tested in triplicate.

3.8.3 Caspase-3 enzyme activity

HAEC were maintained in 96-well plate until confluency, and exposed to treatment conditions as above overnight. Caspase-3 activity was assessed using Caspase-3 Activity Assay Kit following manufacturer's instructions (Calbiochem, EMD Chemicals, Gibbstown, NJ). Results were expressed as caspase-3 activity fold induction versus normal glucose condition.

3.9 DETERMINATION OF REACTIVE OXIGEN SPECIES

3.9.1 Measure of intracellular ROS

HAEC (50,000/well) were seeded in 6-well plates and treated as specified above overnight. Intracellular hydrogen peroxide (H₂O₂) production was monitored by flow cytometry using CM-H₂-DCFDA (Molecular Probes, Invitrogen, cat. C6827), a membrane-permeable indicator for ROS that is non-fluorescent until removal of the acetate groups by intracellular esterases and oxidation occurs within the cell. CM-H₂-DCFDA was added to each well at a final concentration of 10µmol/L in phosphate buffer saline (PBS) (Gibco). Cells were put in the incubator for 30min to allow uptake of the dye. After cellular detachment, cells were collected in 12x75mm flow tubes (Falcon), and centrifuged at 1,000rpm for 5 min. Cells were resuspended in freshly prepared regular EBM-2, or high glucose medium, or high glucose with C-peptide (10nmol/L) and immediately run at the flow cytometer (time 0) (Becton Dickinson FACSARIA II, BD Biosciences, San Jose, CA). HAEC were maintained at 37°C and intracellular ROS production monitored every hour until 5 hours. Results are expressed as mean fluorescence of CM-H₂-

DCFDA in HAEC. At least 4 experiments were run in which each condition was tested in duplicate.

3.9.2 NADPH oxydase activity detection

NADPH oxidase activity was measured in cells using lucigenin-derived chemiluminescence, as described previously¹¹³. HAEC were seeded into T-25cm² flasks, serum starved overnight and exposed to treatment conditions as above for 30 minutes. Pre-treatment for 2 hours with the pharmacological inhibitors of NAD(P)H oxidase apocynin (10µM; Sigma) and diphenyliodonium (DPI) (100µM; Sigma) were tested as well. After detachment from the flasks, cells were resuspended in Krebs–Henseleit buffer (10 mmol/L glucose, 0.02 mmol/L Ca-Triplex, 25 mmol/L NaHCO₃, 1.2 mmol/l KH₂PO₄, 120 mmol/L NaCl, 1.6 mmol/L CaCl₂·2H₂O, 1.2 mmol/L MgSO₄·7H₂O, and 5 mmol/L KCl, pH 7.4) and seeded in white 96-well plates (10⁵ cells/well). Superoxide anion production was measured in the presence of lucigenin, (5 µmol/L, incubated for 20 min). The reaction was started by the addition of NADPH (100 µmol/L), and the relative light units (RLU) luminescences were measured over a period of 30 minutes in a Victor3 multi-well reader (PerkinElmer, Shelton, USA). Three experiments were performed in which each condition was tested in quadruplicate. Results were expressed as percent of NAD(P)H oxidase activity.

3.9.3 Measure of mRNA expression by qRT-PCR

HAEC were grown into T-75cm² flasks, then were serum starved overnight and exposed to treatment conditions as above for 30 minutes. Total RNA was isolated using a commercial kit (RNAqueous-4PCR kit; Ambion, Austin, TX) and quantified by spectrophotometry. One microgram of RNA was reverse transcribed to cDNA (5 min at 65°C, 50 min at 50°C and 5 min at 85°C) using oligo(dT) primers (Invitrogen, Carlsband, CA). Using the LightCycler system (Roche Diagnostics) according to the manufacturer's instruction, quantitative real time PCR was performed using the following primers: *Rac-1* sense 5' AGGAAGAGAAAATGCCTG-3' and antisense 5'-AGCAAAGCGTACAAAGGT-3' and housekeeping gene *GAPDH* sense 5'-TCGGAGTCAACGGATTTGGTCGTA-3' and antisense 5'-TGGCATGGACTGTGGTCATGAGTC-3'¹¹⁴. Aliquots of the cDNA were loaded into capillary

tubes and amplified for 40 cycles. The PCR products were further analyzed by agarose gel electrophoresis to confirm the correct length of the amplified products. Rac-1 data were normalized using GAPDH housekeeping gene and results were expressed as fold induction versus normal glucose condition.

3.9.4 Assessment of Rac-1 GTPase activity

HAEC were grown into T-75cm² flasks until confluency, serum starved overnight and exposed to treatment conditions as above for 30 minutes. Rac GTPase activity was measured in 10µg of cell lysates using a commercially available Rac G-LISATM Activation Assay kit which measures the GTP form of Rac-1 from HAEC lysates following manufacturer's instructions (Cytoskeleton, Inc, Denver, CO). At least 4 experiments were run in which each condition was tested in duplicate. Results are expressed as GTPase activity-fold induction compared to normal glucose condition.

3.10 CITOKINE SECRETION STUDY IN U-937 MONOCYTE

3.10.1 Luminex Assay Analysis

U-937 cells (50,000 cells/well/mL) were seeded in 24-well plates in presence of RPMI-1640 supplemented with 30mmol/L glucose and stimulated with 0.5ng/µL of LPS from E.Coli (E25:B55) in the presence or absence of 1µmol/L C-peptide (Sigma Chemical, St. Louis, MO) for 24 hours at 37°C, 5% of CO₂. A randomized version of the full-length C-peptide containing the same amino acid residues but randomly ordered (scrambled C-peptide; Sigma Genosys), was used as control at the same concentration of the C-peptide. Supernatant was collected in 1.5mL cryovials and stored at -20°C until tested for cytokine concentration. Luminex multiplex assays were used to assess levels of IL-6, IL-8, macrophage inflammatory protein (MIP)-1α and MIP-1β (Millipore Human Cytokine kit, Millipore Corp. Billerica, MA) in the culture supernatants of LPS-stimulated U-937 cells following manufacturer's instructions. A minimum of 4 independent experiments was performed. Each condition was tested in duplicate.

3.10.2 Adhesion of U-937 monocytes to HAEC

Human Aortic Endothelial Cells (HAEC) were purchased from Lonza and maintained in EBM-2 media at 37°C, 5% CO₂ as previously described. HAEC (200,000cells/well) were then seeded on 48-well plates and grown until they reached 90% confluency. U-937 monocytes were exposed to low (5.6mmol/L), or intermediate (11mmol/L), or high glucose (30mmol/L) medium, in the presence or absence of C-peptide (2µmol/L) for 4 hours at 37°C, 5% CO₂. As a positive control to induce adhesion, U-937 monocytes were stimulated with IL-1β (1ng/mL, Sigma Chemical) for 4 hours at 37°C, 5% CO₂. After the allotted time, U-937 cells were added on top of the HAEC for 1 hour at room temperature on a rocking plate. Non-adherent U-937 cells were removed by washing and adherent cells fixed in 1.25% glutaraldehyde. The number of adherent U-937 monocytes was evaluated by counting five random 40X fields per well. At least three experiments were performed. Within each experiment, each condition was tested in triplicate.

3.10.3 Immunoprecipitation of IκB-α and Phosphorylated IκB-α

Cytoplasmic extracts (50 µg) were incubated overnight at 4°C with anti-IκB-α IgG (1:100). The samples were then treated with 10µl of protein A agarose beads (Sigma) for 2 h at 4°C after which the samples were centrifuged and washed 5 times in PBS (Gibco). The beads were boiled in SDS-PAGE sample treatment buffer and electrophoresed on a 4-20% SDS-PAG as described above. The PVDF membranes were then blotted and incubated with either monoclonal P-IκB-α or IκB-α antibodies (both from Santa Cruz Biotechnology; 1:1000) followed by incubation with an anti-rabbit peroxidase secondary antibody (1:10,000, Jackson Laboratories, Bar Harbor, USA).

3.11 INTERNALIZATION OF C-PEPTIDE IN ENDOTHELIAL CELL (HAEC) AND SMOOTH MUSCLE CELLS (UASMC)

3.11.1 Cell culture

HAEC and UASMC were obtained from Cambrex (Cambrex Bioscience Walkersville Inc., Walkersville, MD) and grown into 75 cm² flasks (Corning Incorporated, Corning, NY, USA) at 37°C, 5% CO₂ as previously described. HAEC were used at passage 2-6 and UASMC were used at passage 4-10. Unless differently specified, in all experiments HAEC and UASMC (~100,000 cell/dish) were seeded on 35 mm diameter, poly-d-lysine coated MatTek plates (MatTek Corporation, Ashland, MA) and allowed to settle overnight at 37°C, 5% CO₂ in their specific medium. Next day, cells were washed with fresh medium before starting with the specific experimental conditions.

3.11.2 Preparation of AlexaFluor-labelled C-peptide and culture conditions

Two AlexaFluor-labelled C-peptide probes were customized, one labeled with AlexaFluor488 and the other with AlexaFluor546, and had them synthesized by Molecular Probes (Invitrogen Corporation, Carlsbad, CA). Unless differently specified, 1 µmol/L of AlexaFluor488- or AlexaFluor546-labelled C-peptide (Molecular Probes, Invitrogen Corporation) was added to each MatTek plate in serum-free medium. Cells were incubated at 37°C, 5% CO₂ for the designated time. After incubation, fluorescent probe was discarded and cells were washed with fresh medium before analysis under a confocal microscope. The concentration of fluorescent probe corresponded to the minimum concentration of fluorescent probe that we were able to easily detect in our experimental system, and had also been previously used by other¹¹⁵.

3.12 LIVE-CELL CONFOCAL IMAGING

3.12.1 Time course of C-peptide internalization

Confocal fluorescence microscopy was performed using an Olympus Fluoview 300 Confocal Laser Scanning head with an Olympus IX70 inverted microscope (Melville, NY, USA).

Cells were incubated with the fluorescent C-peptide probe for a minimum of 5 min and a maximum of 1 h. As a control for specificity of the staining, 1 $\mu\text{mol/L}$ of free AlexaFluor488 (cat.#A10235) or AlexaFluor546 fluorescent dye (cat.#A20002) (Molecular Probes, Invitrogen Corporation) was added to separate plates. Cells were studied in an “open” cell cultivation system at 37°C by live-cell confocal microscopy after 5 min, 10 min, 20 min, 30 min, and 1 h from uptake of the C-peptide probe. At least 8 independent experiments were performed, with a minimum of 6 MatTek plates with adherent cells each.

3.12.2 Effect of temperature on AlexaFluor-labelled C-peptide internalization

Cells were cooled at 4°C in a fridge for 1 h and then incubated with the fluorescent C-peptide probe at 4°C for 30 min. Uptake of the fluorescent probe by live-cells was studied under a confocal microscope. Cells were then incubated at 37°C, 5% CO₂ for 1 h and analyzed again with a confocal microscope. At least 4 independent experiments were performed, with a minimum of 6 MatTek plates for each experiment.

3.12.3 Inhibition of AlexaFluor-labelled C-peptide uptake by excess of unlabelled C-peptide

Cells were incubated with either 30 $\mu\text{mol/L}$ of unlabelled, native, C-peptide (Sigma) or 30 $\mu\text{mol/L}$ of scrambled C-peptide (Sigma Genosys) for 1 h at 37°C, 5% CO₂. This latter peptide (purity of >95%) represents a randomized version of the native C-peptide containing the same amino acid residues but randomly ordered, as follows: ADQVELGAPQSAGLGGSQLPQGLGLVLGE. After 1 h of incubation, fluorescent C-peptide probe was added for 30 min. Live-cells were then analyzed under a confocal microscope. Uptake of C-peptide in these cells was compared with uptake of fluorescent C-peptide in the absence of any pre-incubation with either unlabelled, native, or scrambled C-peptide.

3.12.4 Uptake of AlexaFluor-labelled C-peptide in the presence of pharmacological compounds

Cells were pre-treated for 30 min at 37°C, 5% CO₂ with either Monodansylcadaverine (MDC; 43 µmol/l), which inhibits the clathrin-coated pit pathway, Filipin (5 µg/mL), which blocks caveolae pathway, Nocodazole (10 µmol/L), which disrupts microtubule assembly, or Cytochalasin D (30 µmol/L), which disrupts actin filaments. The dose and time of treatment for each compound, which showed no toxic effect, was determined experimentally on the basis of previous reports¹¹⁶⁻¹¹⁹. After 30 min, fluorescent C-peptide was added for 30 min and cells put back in the incubator. Cells were then examined under a confocal microscope. The response of cells to each condition was highly consistent with inhibition of C-peptide uptake with MDC and Nocodazole. We therefore analyzed the mean fluorescence per cell in only 3 cells/plate (total of 9 cells) for each condition by using Olympus Fluoview 300 Software. Repeated Measures ANOVA was applied to determine statistical significance.

3.13 SUB-CELLULAR ORGANELLES CO-LOCALIZATION STUDY

3.13.1 Endosome transduction

Cells were transduced with 500 µL of Organelle Lights™ Endosomes-GFP reagent (Invitrogen Corporation, cat.#010104), which target Rab5a, an early endosomal marker, following manufacturer's instructions. The plates were incubated for 2 h on a plate shaker at room temperature. After removing the medium, 500 µL of 1:1000 dilution of enhancer was added to the cells and incubated at 37°C, 5% CO₂ for 2 h. Cells were kept in the incubator for 2 days in fresh medium to allow expression of the fluorescence protein and then incubated with fluorescent C-peptide for 30 min before confocal microscopy analysis. At least 5 independent experiments were performed for each organelle, with a minimum of 6 MatTek plates with adherent cells each.

3.13.2 Immunohistochemistry of early endosomes

HAEC (~100,000 cell/dish) seeded on MatTek plates (MatTek Corporation) were fixed with paraformaldehyde (PFA), and incubated with rabbit anti-human antibody to C-peptide (Millipore Corporation, Billerica, MA) together with a mouse anti-human monoclonal antibody to the early endosome antigen 1 (EEA1) (Santa Cruz Biotechnology, Inc., Santa Cruz, CA) for 2 h. Appropriate secondary antibodies were then applied. Cells were washed and imaged by using confocal microscopy. At least 4 independent experiments were performed, with a minimum of 6 MatTek plates with adherent cells each.

3.13.3 Isolation of endosomes and analysis of C-peptide content

To identify early endosomes, we followed internalization of AlexaFluor488-conjugated human transferrin, a ligand known to enter the cells by clathrin-mediated endocytosis and a specific marker of early endosomes¹²⁰ in the presence of AlexaFluor546-labelled C-peptide in UASMC in the incubator for 10 min. Endosomes were isolated from other sub-cellular compartments by centrifugation¹²¹ and an aliquote of both the pellet and the endosome-containing supernatant used to quantitate AlexaFluor488-transferrin and AlexaFluor546-C-peptide fluorescence spectra by using a scanning spectrofluorimeter. Repeated Measures ANOVA was applied to determine statistical significance. Three independent experiments were performed.

3.14 STATISTICAL ANALYSIS

Two-tailed paired t-test was used to assess differences between the different conditions tested by using GraphPad Prism 4 program (GraphPad Software, Inc. San Diego, CA). Values of $p < 0.05$ were considered to be statistically significant.

4.0 HUMAN C-PEPTIDE ANTAGONIZES HIGH GLUCOSE ENDOTHELIAL DYSFUNCTION THROUGH NF- κ B PATHWAY

Patrizia Luppi[§],MD; Vincenza Cifarelli[§], Hubert Tse[‡],PhD; Jon Piganelli[§],PhD; and Massimo Trucco[§]MD

[§]Division of Immunogenetics, Department of Pediatrics, Rangos Research Center, Children's Hospital of Pittsburgh, University of Pittsburgh, School of Medicine, Pittsburgh, PA15213, USA; [‡] Department of Microbiology, University of Alabama–Birmingham School of Medicine, Birmingham, Alabama.

Diabetologia 51(8):1534-43

This study was supported by: the Henry Hillman Endowment Chair in Pediatric Immunology (M.T) and by grants DK 024021-24 from the National Institute of Health and NIH 5K12 DK063704 (P.L. and M.T.), and W81XWH-06-1-0317 from the Department of Defense (M.T.)

4.1 ABSTRACT

Aims: Endothelial dysfunction in diabetes is predominantly caused by hyperglycemia leading to vascular complications through overproduction of oxidative stress and activation of the transcription factor nuclear factor (NF)- κ B. Many studies have suggested that decreased circulating levels of C-peptide may play a role in diabetic vascular dysfunction. To date, the possible effect of C-peptide on endothelial cells and intracellular signaling pathways are largely unknown. We therefore investigated the effect of C-peptide on several biochemical markers of endothelial dysfunction *in vitro*. To gain insights on potential intracellular signaling pathways affected by C-peptide, we tested NF- κ B activation, since it is known that inflammation, secondary to oxidative stress, is a key component of vascular complications and NF- κ B is a redox-dependent transcription factor. **Methods:** Human Aortic Endothelial Cells (HAEC) were exposed to 25 mmol/L glucose in the presence of C-peptide (0.5 nmol/L) for 24 hours and tested for expression of vascular cell adhesion molecule (VCAM)-1 by RT-PCR and flow cytometry. Secretion of interleukin(IL)-8 and monocyte chemoattractant protein (MCP)-1 was measured by ELISA. NF- κ B activation was analyzed by immunoblotting and ELISA. **Results:** Physiologic concentrations of C-peptide impact high glucose-induced endothelial dysfunction by: a) decreasing VCAM-1 expression and U-937 cell adherence to HAEC; b) reducing secretion of IL-8 and MCP-1; and c) suppressing NF- κ B activation. **Conclusions:** During hyperglycemia, C-peptide directly affects VCAM-1 expression, and MCP-1 and IL-8 secretion by HAEC through a reduced NF- κ B activation. These effects suggest a physiologic anti-inflammatory (and potentially anti-atherogenic) activity of C-peptide on endothelial cells.

4.2 INTRODUCTION

It is well established that diabetic vascular disease is characterized by changes in small (microangiopathy) as well large vessels (macroangiopathy) with common biochemical changes in the tunica media. In the large vessels, the changes are supposed to increase the susceptibility to

atherogenic insults and thereby pave the way for an increased presence of atherosclerosis in patients with diabetes. In the small vessels, the disease principally affects the eye, kidney and heart and dysfunction, as a result of the diabetic state, contributes significantly to the morbidity associated with diabetes¹⁰.

Diabetes causes vascular compromise secondary to endothelial dysfunction, measured by *in vivo* studies of flow-mediated vasodilation¹³³ and increased circulating levels of biochemical markers, such as, but clearly not limited to VCAM-1⁹¹. Generally, VCAM-1 is expressed at a low level on endothelial cells and is up-regulated upon cellular activation, such as the one observed after exposure to inflammatory stimuli or high glucose⁹². VCAM-1 binds to the leukocyte integrin $\alpha_4\beta_4$ (also called Very Late Antigen-4; CD49d), and has a principal role in the early stages of monocytes adhesion to the vascular endothelium, one of the first steps in atherosclerosis plaque formation¹⁰⁸. A major hallmark of diabetes is an abnormally elevated high blood glucose level (i.e., hyperglycemia) and hyperglycemia has been proposed as one factor causing endothelial dysfunction in diabetes. In endothelial cells, acute and chronic hyperglycemia works through ROS production^{91,104,105} that leads to activation of the transcription factor NF- κ B^{91,146} and ultimately the production of inflammatory mediators¹⁰¹.

In the unstimulated state, NF- κ B exists in its canonical form as a heterodimer composed of p50 and p65 subunits bound to I κ B. Upon activation, I κ B is phosphorylated and degraded causing the release of p50/p65 components of NF- κ B⁹³. The active p50/p65 heterodimer translocates to the nucleus and initiates the transcription of a gamut of genes involved in the inflammatory response, such as pro-inflammatory cytokines, cell surface adhesion molecules, and chemokines, including IL-8 and MCP-1^{91,95}. IL-8 and MCP-1 expression is present in human atherosclerotic plaques^{85,96} and participates in the development of atherosclerosis by recruiting monocytes into the subendothelial cell layer⁹⁵.

It has been suggested that proinsulin C-peptide, may possess cytoprotective effects on the microvasculature during inflammatory events⁶. In line with this, it has been reported that T1D patients with circulating levels of C-peptide closer to the physiological level of 0.5 nmol/L² or receiving whole pancreas²⁹ or allogeneic islet transplantation³⁰ show a reduced incidence of microvascular complications. The mechanisms underlying the beneficial effect of C-peptide on

vascular dysfunction in diabetes remains largely unknown. One study performed *in vivo* in a rat inflammatory model of vascular dysfunction, showed that a single i.v. dose of C-peptide significantly inhibited leukocyte-endothelium interaction via decreased expression of endothelial cell adhesion molecules¹⁷. Similar results were obtained in isolated ischemic and reperfused rat hearts, where addition of C-peptide attenuated polymorphonuclear cells adherence to the vascular endothelium¹⁸. To date, no data are available on the effects of C-peptide on human endothelial cells exposed to the damaging insult of hyperglycemia, a common condition in diabetes.

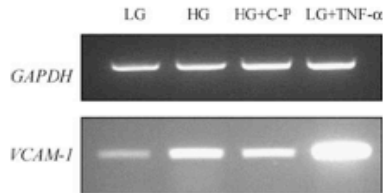
We therefore initiated a study on the direct effect of C-peptide testing VCAM-1 expression, monocyte adherence, and secretion of IL-8 and MCP-1 by HAEC exposed to short-term high glucose. Since activation of the transcription factor NF- κ B is involved in these pro-inflammatory responses, we also investigated the direct effect of C-peptide on nuclear translocation of the NF- κ B subunits p50/p65 in HAEC. We hypothesized that physiologic concentrations of C-peptide protects HAEC from high glucose-induced cellular dysfunction by decreasing NF- κ B activation thus inhibiting NF- κ B-dependent genes, such as VCAM-1, IL-8 and MCP-1 expression.

4.3 RESULTS

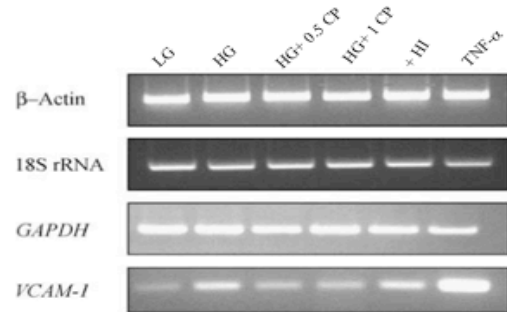
We observed that C-peptide is able to decrease the expression of the adhesion molecule VCAM-1 on endothelial cells exposed to high glucose (25 mmol/L glucose). VCAM-1 expression and secretion was assessed by RT-PCR (Figure 4a-1c) and ELISA (Figure 5a) measurements after 4 and 24h treatment with C-peptide. Heat inactivated C-peptide was used as a positive control. When C-peptide was added to low glucose medium (5.6 mmol/l glucose), it did not cause a significant change in VCAM-1 (Figure 5b) (107).

To determine whether C-peptide-induced inhibition of VCAM-1 was associated with a decrease adherence of monocytes, we evaluated the adherence of human the monocytic cell lines U-937 to HAEC exposed to high glucose, in presence or absence of C-peptide.

a) *VCAM-1* expression in HAEC by RT-PCR (4h)



b) *VCAM-1* expression in HAEC by RT-PCR (24h)



c) Densitometry *VCAM-1* expression (24h)

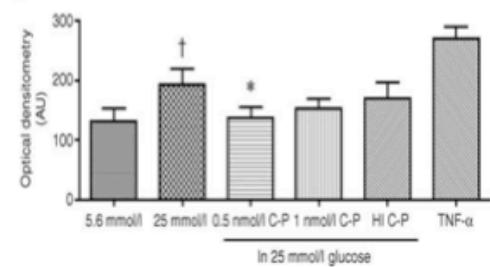


Figure 4. C-peptide decreases high glucose-stimulated VCAM-1 mRNA after 4h and 24h.

In (a) a representative example of RT-PCR detecting VCAM-1 mRNA expression in HAEC treated for 4h. b RT-PCR was used to detect VCAM-1 mRNA in HAEC treated with: low glucose (5.6 mmol/l; LG); high glucose (25 mmol/l; HG); HG+ 0.5 nmol/l C-peptide (C-P); HG + 1 nmol/l C-P; HG+ 1 nmol/l heat-inactivated C-P (HI); LG + 10 ng/ml TNF- α . *GAPDH*, 18S rRNA and β -actin were used as internal controls. c Densitometric analysis of *VCAM-1* mRNA expression. Boxplot graphs showing the median values (limits of the lines are the 5th and 95th centiles of arbitrary units [AU]). C-peptide decreased high glucose-induced VCAM mRNA expression compared to high glucose alone. * $p < 0.05$, † $p = 0.008$ vs 5.6 mmol/l.

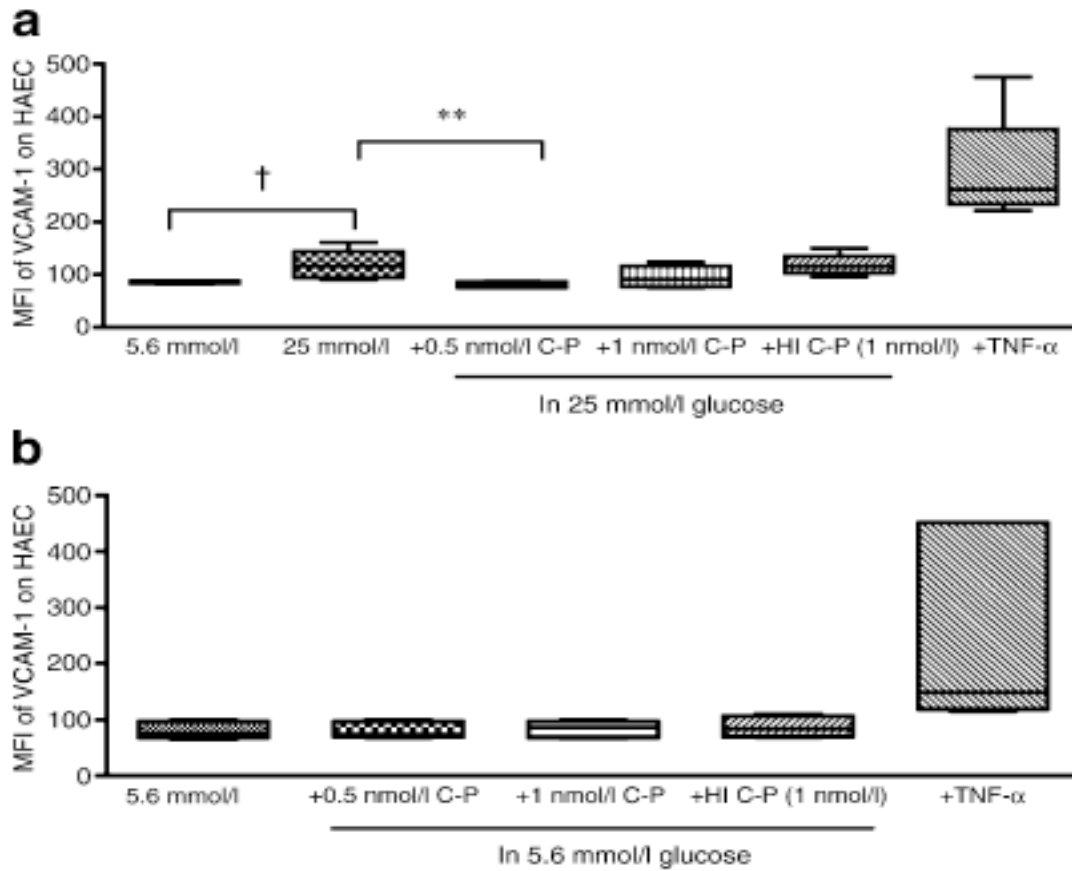


Figure 5. C-peptide reduces high glucose-stimulated VCAM-1 protein expression on HAEC. Boxplot graphs showing the median values (limits of the lines are the 5th and 95th centiles) of MFI of VCAM-1 expression in HAEC exposed to (a) 25 mmol/l glucose or (b) 5.6 mmol/l glucose with and without C-peptide (C-P) for 4 h as determined by flow cytometry (n=3 independent experiments). (a) HAEC exposed to 25 mmol/l glucose significantly increased VCAM-1 expression; †p=0.03 vs 5.6 mmol/l. This increase was significantly inhibited by 0.5 nmol/l C-peptide; **p<0.01. No significant changes in VCAM-1 were observed when C-peptide was added to basal medium containing 5.6 mmol/l glucose (b). HI, heat-inactivated

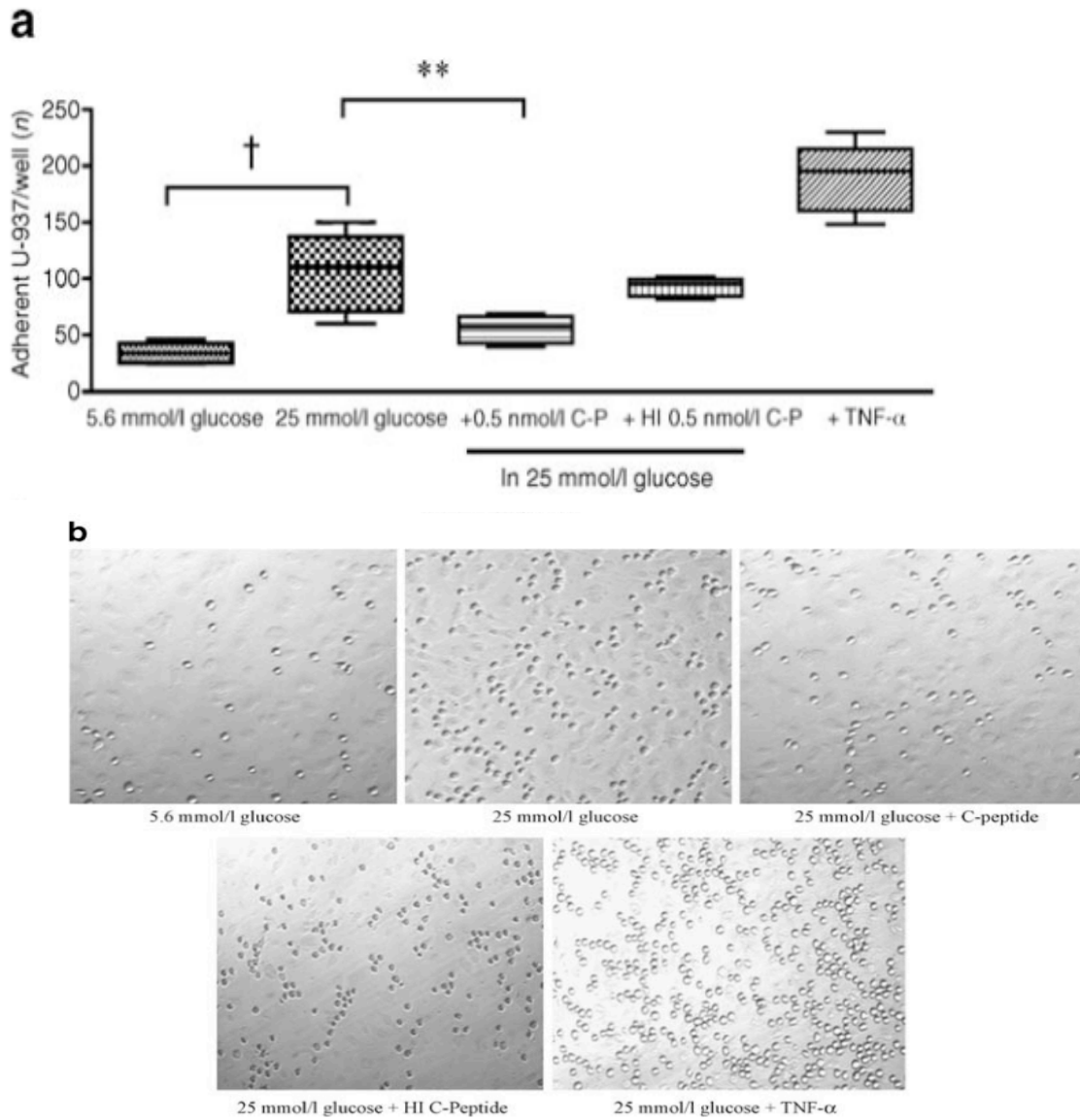
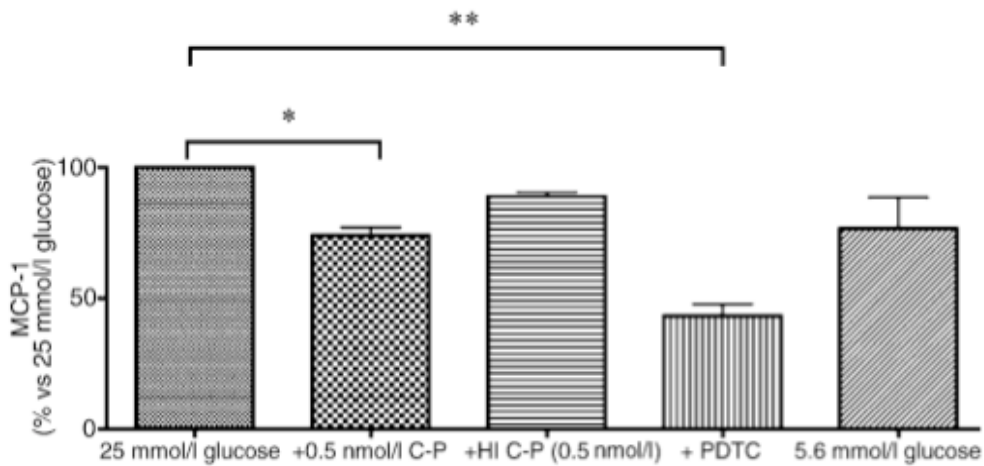


Figure 6. C-peptide reduces adhesion of U-937 to HAEC in condition of hyperglycaemia. HAEC were cultured in 25 mmol/l glucose in thpresence or absence of 0.5 nmol/l of C-peptide (C-P) for 4 h. U-937 were added for 1 h and then counted. a Boxplot graphs showing the median values of number of adherent U-937 per well (n=3 sets of independent experiment). High glucose increased the number of adherent U-937; **p<0.01 vs. 25 mmol/l glucose alone. Heat-inactivated (HI) C-peptide (0.5 nmol/l) did not significantly alter adherence of U-937. TNF-α (10 ng/ml) produced more than a fivefold increase in adherent U-937 in comparison to normal glucose. b Photographic view of U-937 adherent to HAEC.

A



b

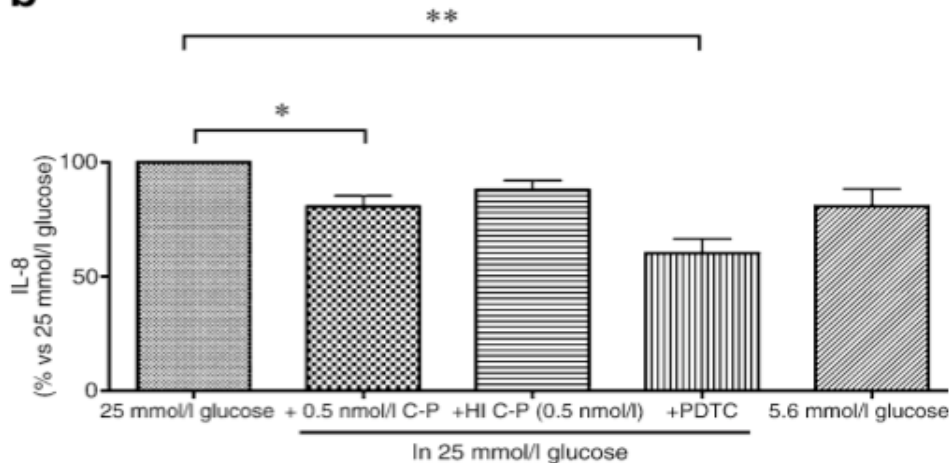


Figure 7. C-peptide decreases high glucose stimulated MCP-1 and IL-8 secretion by HAEC. HAEC were cultured with high glucose (25 mmol/L) alone or combined to C-peptide (0.5 nmol/L) for 4 hours and secretion of MCP-1 and IL-8 in the supernatant assessed by ELISA. (a) Boxplot graphs showing the median values of secreted MCP-1 or IL-8 (on the Y axis) in the supernatant of HAEC exposed to 25mmol/L glucose compared to 5.6 mmol/L glucose ($p=0.04$). (b) Levels of IL-8 in supernatant of C-peptide-treated HAEC. HAEC treated with 25 mmol/L glucose in the presence of C-peptide showed a significant decrease in the levels of IL-8 in the supernatant, approaching levels measured in 5.6 mmol/L glucose ($p < 0.05$ vs. 25 mmol/L). A significant decrease in secreted MCP-1 and IL-8 was also found in HAEC treated with the NF- κ B inhibitor PDTC (10 μ M). On the Y axis, MCP-1 and IL-8 levels expressed as percent versus the appropriate control at 25 mmol/L. Shown are the average \pm SD of a set of three independent experiments run in triplicate.

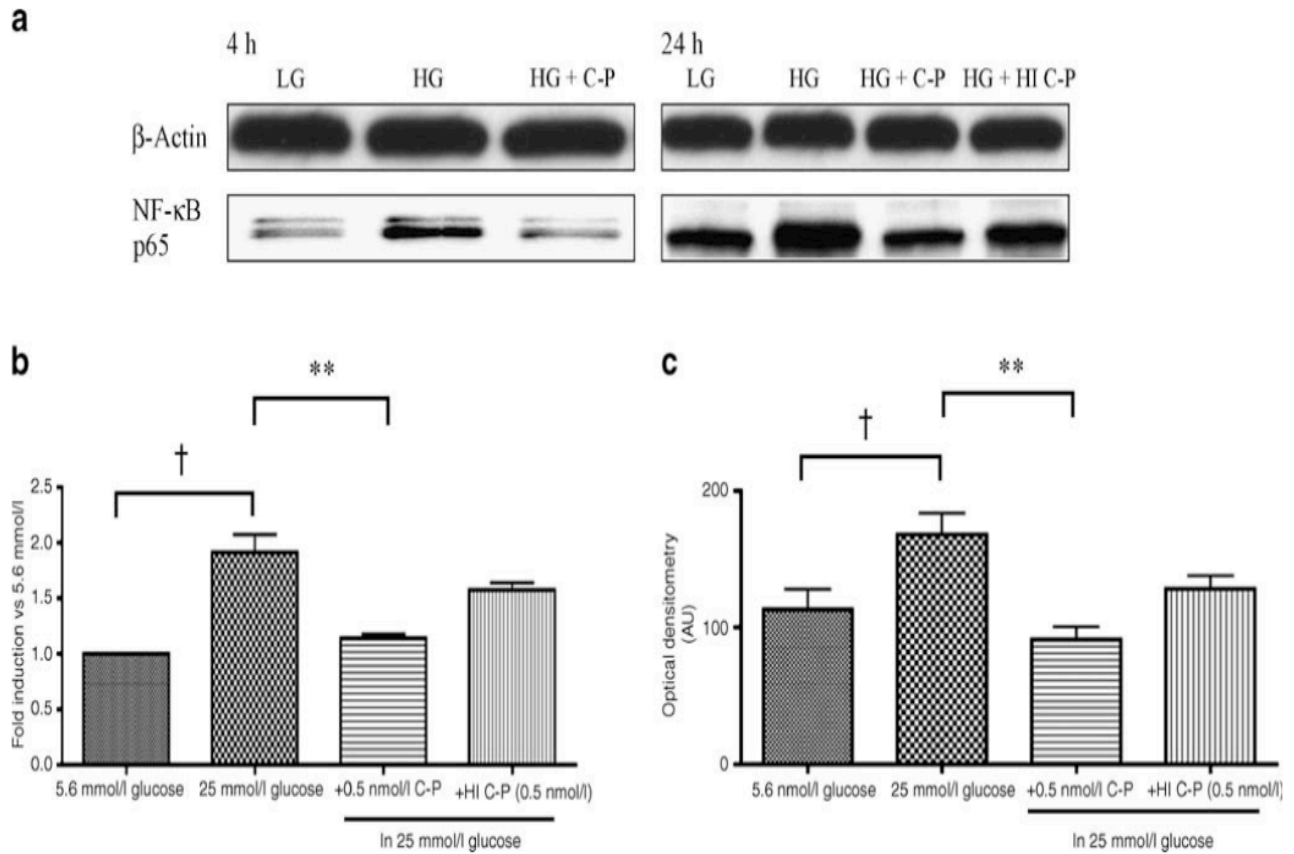


Figure 8. Expression of p65/p50 subunits of NF-κB in HAEC cultured in high glucose for 24 hours in the presence of C-peptide. HAEC were cultured in low glucose (LG; 5.6mmol/L) or high glucose (HG; 25 mmol/L) in the presence or absence of 0.5 nmol/L C-peptide for 24 hours. Cellular nuclear extracts were subjected to: a Western blotting to detect the 65-kDa band of the p65 subunit using a specific antibody (1:1,000); b Bar graph showing the densitometric quantitation of the bands. In cells exposed to HG there was a two-fold increase in NF-κB p65 nuclear translocation compared to cells in LG ($p = 0.03$). A decrease in NF-κB p65 nuclear translocation is observed when HAEC are exposed to HG + 0.5 nmol/L C-peptide ($p < 0.05$). Results are means \pm SD ($n = 3$). Heat-inactivated (HI) C-peptide (0.5 nmol/L) was used as control; c Detection of the NF-κB p50 binding activity by using a EZ-Detect™ Transcription Factor kit (Pierce Biotechnology). Results were expressed as fold induction of NF-κB p50 activity in respect to control at 5.6mmol/L. In cells exposed to HG there was a two-fold increase in NF-κB p50 nuclear translocation compared to cells in LG ($p = 0.002$). A decrease in NF-κB p50 nuclear translocation is observed when HAEC are exposed to HG + 0.5 nmol/L C-peptide (C-P) ($p < 0.01$). Results are expressed as means \pm SD ($n= 3$). Heat-inactivated C-peptide (HI C-P) was used as control of C-peptide activity.

We observed a threefold increase in the number of adherent U-937 under high glucose as compared to 5.6 mmol/L glucose. When C-peptide was added to the high glucose medium, the number of adherent U-937 cells was reduced (Figure 6a).

Addition of heat inactivated C-peptide did not alter significantly the number of adherent cells as compared with 25mmol/L glucose alone. The adhesion of U-937 to HAEC exposed to different conditions was also photographed (Figure 6b). As expected, TNF- α , which activates endothelial cells, produced a fivefold increase in U-937 adherence to HAEC compared to high glucose alone. Moreover, we found that C-peptide was able to decrease the secretion of the inflammatory cytokines IL-8 and MCP-1 from high glucose-exposed HAEC (Figure 7a-7b), which are important mediators in the process of monocyte adherence during endothelial dysfunction eventually leading to plaque formation.

These effects were mediated by a reduced activation of NF- κ B pathway by C-peptide (Figure 8), a pathway involved in inflammatory responses by decreasing its translocation into the nucleus. In the unstimulated state, in fact, NF- κ B exists in its canonical form as a heterodimer composed of p50 and p65 subunits bound to I κ B in the cytoplasm. Upon activation, I κ B is phosphorylated and degraded causing the release of p50/p65 components of NF- κ B. The active p50/p65 heterodimer translocates to the nucleus and initiates the transcription of a gamut of genes involved in the inflammatory response, such as pro-inflammatory cytokines, cell surface adhesion molecules, and chemokines, including IL-8 and MCP-1

**5.0 HUMAN PROINSULIN C-PEPTIDE REDUCES HIGH GLUCOSE-INDUCED
PROLIFERATION AND NF- κ B ACTIVATION IN VASCULAR SMOOTH MUSCLE
CELLS**

Vincenza Cifarelli[§], Patrizia Luppi[§], Hubert M. Tse[‡], Jing He[§], Jon Piganelli[§], Massimo Trucco[§]

[§]Division of Immunogenetics, Department of Pediatrics, University of Pittsburgh, School of Medicine, Pittsburgh, PA 15213, USA; [‡] Department of Microbiology, University of Alabama–Birmingham School of Medicine, Birmingham, Alabama.

Atherosclerosis 201(2):248-57

This work was supported in part by the Henry Hillman Endowment Chair in Pediatric Immunology and Department of Defense grant # W81XWH-06-1-0317 to M.T.

5.1 ABSTRACT

Aim: Excessive proliferation of vascular smooth muscle cells (VSMCs) is one of the primary lesions in atherosclerosis development during diabetes. High glucose triggers VSMC proliferation and initiates activation of the transcription factor nuclear factor (NF)- κ B. Recently, clinical studies have demonstrated that replacement therapy with C-peptide, a cleavage product of insulin, to Type 1 diabetic (T1D) patients is beneficial on a variety of diabetes-associated vascular complications. However, the mechanisms underlying the beneficial activity of C-peptide on the vasculature in conditions of hyperglycemia are largely unknown.

Material/Methods: The effects of C-peptide on the proliferation of human Umbilical Artery Smooth Muscle Cell (UASMC) and Aortic Smooth Muscle Cell (AoSMC) lines cultured under high glucose for 48 hours were tested. To gain insights on potential intracellular signaling pathways affected by C-peptide, we analyzed NF- κ B activation in VSMCs since this pathway represents a key mechanism for the accelerated vascular disease observed in diabetes.

Results: High glucose conditions (25mmol/L) stimulated NF- κ B-dependent VSMC proliferation since the addition of two NF- κ B-specific inhibitors, BAY-117082 and PDTC, prevented proliferation. C-peptide at the physiological concentrations of 0.5 and 1nmol/L decreased high glucose-induced proliferation of VSMCs that was accompanied by decreased phosphorylation of I κ B and reduced NF- κ B nuclear translocation.

Conclusions: These results suggest that in conditions of hyperglycemia C-peptide reduces proliferation of VSMCs and NF- κ B nuclear translocation. In patients with T1D, physiological C-peptide levels may exert beneficial effects on the vasculature that, under high glucose conditions, is subject to progressive dysfunction.

5.2 INTRODUCTION

Patients with type 1 diabetes (T1D) exhibit an increased susceptibility to develop a wide range of vascular complications, including microangiopathy and atherosclerosis, which account for the

majority of deaths and disability in diabetic patients⁹. Elevated blood glucose levels (hyperglycemia) are considered one of the major causes of vascular complications in T1D patients¹¹.

Together with endothelial dysfunction, the proliferation of vascular smooth muscle cells (VSMCs) is one of the characteristic features of human atherosclerosis¹¹¹. Under high glucose conditions, human, porcine and rat VSMC proliferate and migrate from the media to the subendothelial space of the vessel wall where early atherosclerotic lesions are localized¹¹¹⁻¹¹².

In VSMCs, high glucose initiates the activation of the transcription factor NF- κ B¹⁰², which leads to the transactivation of a number of genes involved in VSMC proliferation. Several studies have pointed to an involvement of the NF- κ B pathway in the process of atherosclerosis by acting at different pathophysiological levels during plaque development. The activated p65 subunit has been found in macrophages, endothelial cells, and VSMCs within human atherosclerotic lesions⁷¹. Other studies mostly point to a role of NF- κ B in regulating apoptosis of VSMCs and fine-tuning of the inflammatory response present in the injured vessel wall¹¹². Overall, these studies support the idea that NF- κ B activation in VSMCs represent a key mechanism for the accelerated vascular disease observed in diabetes. Strategies targeting NF- κ B pathway activation to inhibit VSMC proliferation for the prevention or the treatment of cardiovascular diseases are emerging¹¹².

Despite intensive insulin treatment and well-controlled glucose levels, vascular complications are still common among T1D patients¹²⁷. As well as reduced endogenous insulin, the level of C-peptide is also decreased in the plasma of T1D patients. This peptide is cleaved from proinsulin and released from the pancreas into the circulation in equimolar amounts to insulin. C-peptide was initially believed to have no biological effects apart from its role in insulin biosynthesis. However, recent evidence suggests that C-peptide may have a physiological role on a variety of cell types including the vasculature⁶⁻⁷. Moreover, results from small clinical trials where C-peptide was administered to T1D patients, showed that C-peptide ameliorates renal dysfunction¹², stimulates skeletal muscle microcirculation¹⁴, and improves functional and structural abnormalities in peripheral nerves¹³. It was then proposed that C-peptide may represent an important factor in reversing or preventing microvascular damage associated with diabetes.

Supporting this hypothesis, was evidence that T1D patients receiving whole pancreas or islet transplantation exhibited improvement in vascular disease in comparison to patients receiving daily insulin injections to control their hyperglycemia^{26,27, 29,30}.

Several studies have focused on the direct effects of C-peptide on the vasculature, often with contradicting results. For example, while there seems to be concordance on the vasodilatory properties of C-peptide⁷, it is still controversial whether C-peptide exerts pro-atherogenic effects on the vasculature or vice versa. Other observations point instead to a protective role of C-peptide on vascular dysfunction in diabetes. For example, Kobayashi *et al.*¹²³ demonstrated that 3 weeks exposure to C-peptide inhibited high glucose-induced hyperproliferation of rat VSMCs. Another group showed that rat C-peptide inhibits leukocyte-microvascular endothelium interaction *in vivo*¹⁷.

This study evaluated 1) the effects of short-term exposure of C-peptide on high glucose-induced proliferation of human VSMCs *in vitro*, and 2) determined whether the NF- κ B pathway is involved in the intracellular signaling events associated with C-peptide in VSMCs, since to date, no data identifies or excludes NF- κ B signaling as a molecular event associated with C-peptide effects on VSMCs under high glucose conditions.

5.3 RESULTS

Excessive proliferation of vascular smooth muscle cells (VSMCs) is one of the primary lesions in atherosclerosis development during diabetes. Together with endothelial dysfunction, the proliferation of VSMCs is one of the characteristic features of human atherosclerosis development.

Proliferation was assessed using Bromodeoxyuridine (BrdU) (Figure 9) which is incorporated into the newly synthesized DNA of replicating cells (during the S phase of the cell cycle), substituting for thymidine during DNA replication. Exposure of UASMC to 25 mmol/L glucose for 48 h significantly increased BrdU incorporation compared with control cells exposed to 5.6 mmol/L glucose ($p=0.002$). Administration of C-peptide at a dose of 0.5 ($p<0.01$), and 1

nmol/L ($p < 0.01$) for 48 h significantly suppressed high glucose-induced increase in BrdU incorporation in UASMC compared to untreated and scrambled C-peptide-treated cells (Figure 9a) (110). These findings were observed, as well, in aortic smooth muscle cells (AoSMC) when cultured for 48 h with 25 mmol/L glucose in the presence of 0.5 nmol/L ($p < 0.01$) and 1 nmol/L ($p < 0.01$) C-peptide (Figure 9b). High glucose conditions stimulated NF- κ B-dependent VSMC proliferation since the addition of two NF- κ B specific inhibitors, BAY11-7082 and pyrrolidine dithiocarbamate (PDTC), prevented proliferation (Figure 9a-9b).

In contrast, when UASMCs were cultured with regular medium (containing 5.6 mmol/L of glucose) in the presence of C-peptide we detected increased BrdU incorporation as compared to regular medium in the absence of C-peptide ($p < 0.05$) (Figure 10a). No significant increase in BrdU incorporation was detected in AoSMC exposed to regular medium in the presence of C-peptide (Figure 10b).

As additional prove of proliferation, Ki67⁺ immunostaining was performed (Figure 11). Ki67⁺ is a nuclear marker of proliferation in living cells and tissues. A significant increase in Ki67⁺ cells was observed under high glucose conditions ($p = 0.01$ vs. 5.6 mmol/L), while addition of C-peptide reduced Ki67⁺ cell number (19.8% \pm 2.88) in comparison to cells exposed to 25 mmol/L glucose only (26.8% \pm 2.91) ($p = 0.02$) (Figure 11a-11b). The increase in Ki67⁺ cells from UASMC grown under high glucose conditions was mediated by NF- κ B activation since treatment with PDTC (20 μ M), an NF- κ B inhibitor, reduced the number of Ki67⁺ cells to basal levels detected in normal glucose conditions ($p < 0.01$). To determine if high glucose-induced proliferation of UASMC was associated with activation of the NF- κ B signaling pathway, immunoblot analysis and NF- κ B-specific ELISAs were performed with nuclear extracts from stimulated-UASMC. As shown in Fig. 12a, high glucose (25 mmol/L) induced an increase in NF- κ B p65 nuclear translocation in comparison to normal glucose (5.6 mmol/L) stimulated UASMC. The addition of C-peptide to the high glucose cultures decreased NF- κ B p65 nuclear translocation to normal glucose levels (Figure 12a), while the addition of scrambled C-peptide did not suppress NF- κ B activity (Figure 12a).

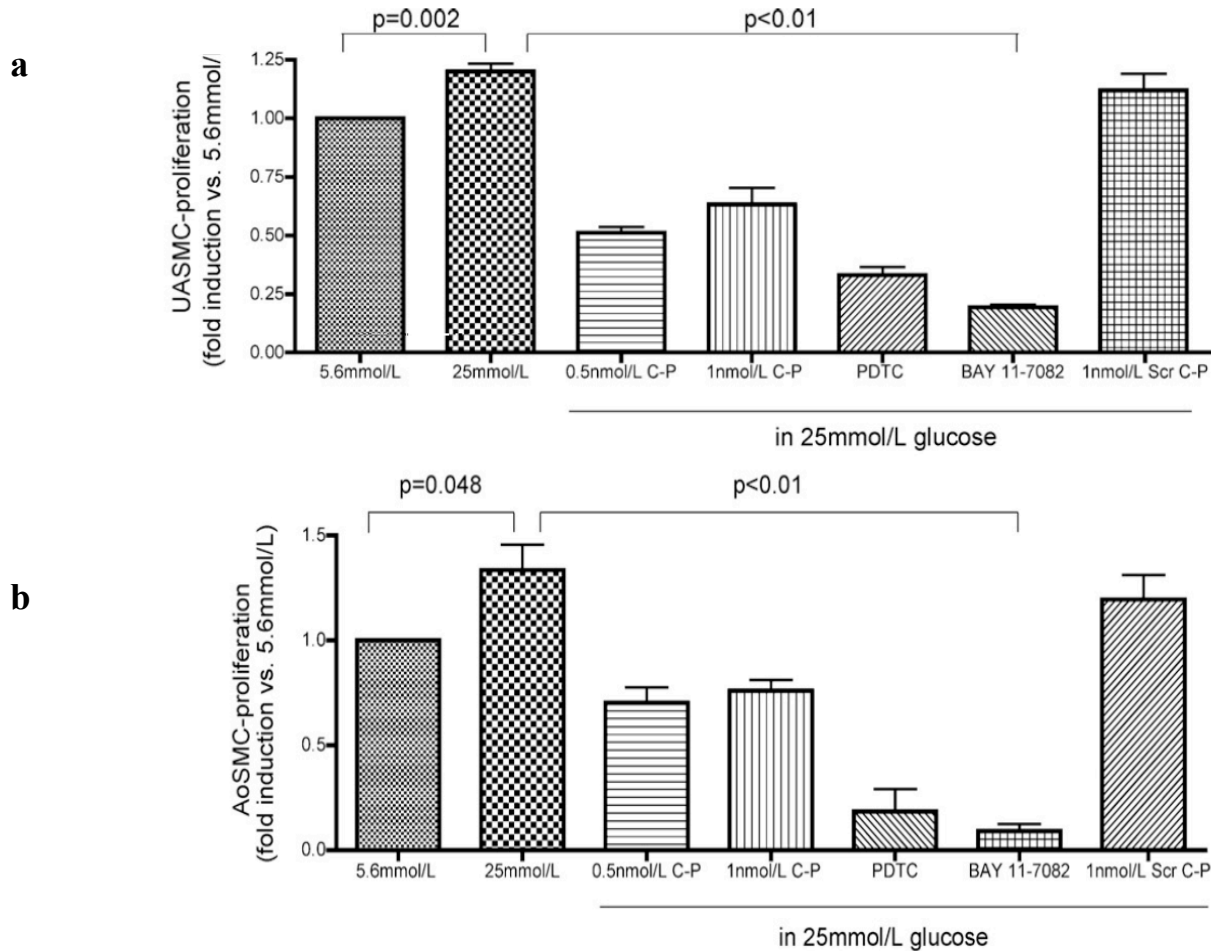


Figure 9. C-peptide reduces high glucose-induced proliferation of VSMCs. VSMCs were incubated with 25mmol/L glucose in the presence or in the absence of C-peptide (C-P) for 48 hours and assayed for proliferation. In (a) BrdU incorporation shows cellular proliferation in high glucose ($p=0.002$ vs. 5.6mmol/L). C-peptide reduced high glucose-induced UASMC proliferation ($p<0.01$), while addition of scrambled C-peptide (Scr C-P) did not have any significant effect. Addition of the NF- κ B inhibitors PDTC (20mM) and BAY-11078 (1mM) also showed a decrease in proliferation ($p<0.01$ vs. 25mmol/L glucose). In (b) BrdU incorporation in AoSMC demonstrates that high glucose stimulated cellular proliferation ($p=0.048$ vs. 5.6mmol/L). C-peptide significantly reduced high glucose-induced UASMC proliferation ($p<0.01$ vs. 25mmol/L), while addition of scrambled C-peptide (Scr C-P) did not have any effect. Addition of PDTC (20mM) and BAY-11078 (1mM) also showed a decrease in proliferation ($p<0.01$ vs. 25mmol/L glucose). Values are mean \pm SD of 10 different experiments run in triplicate.

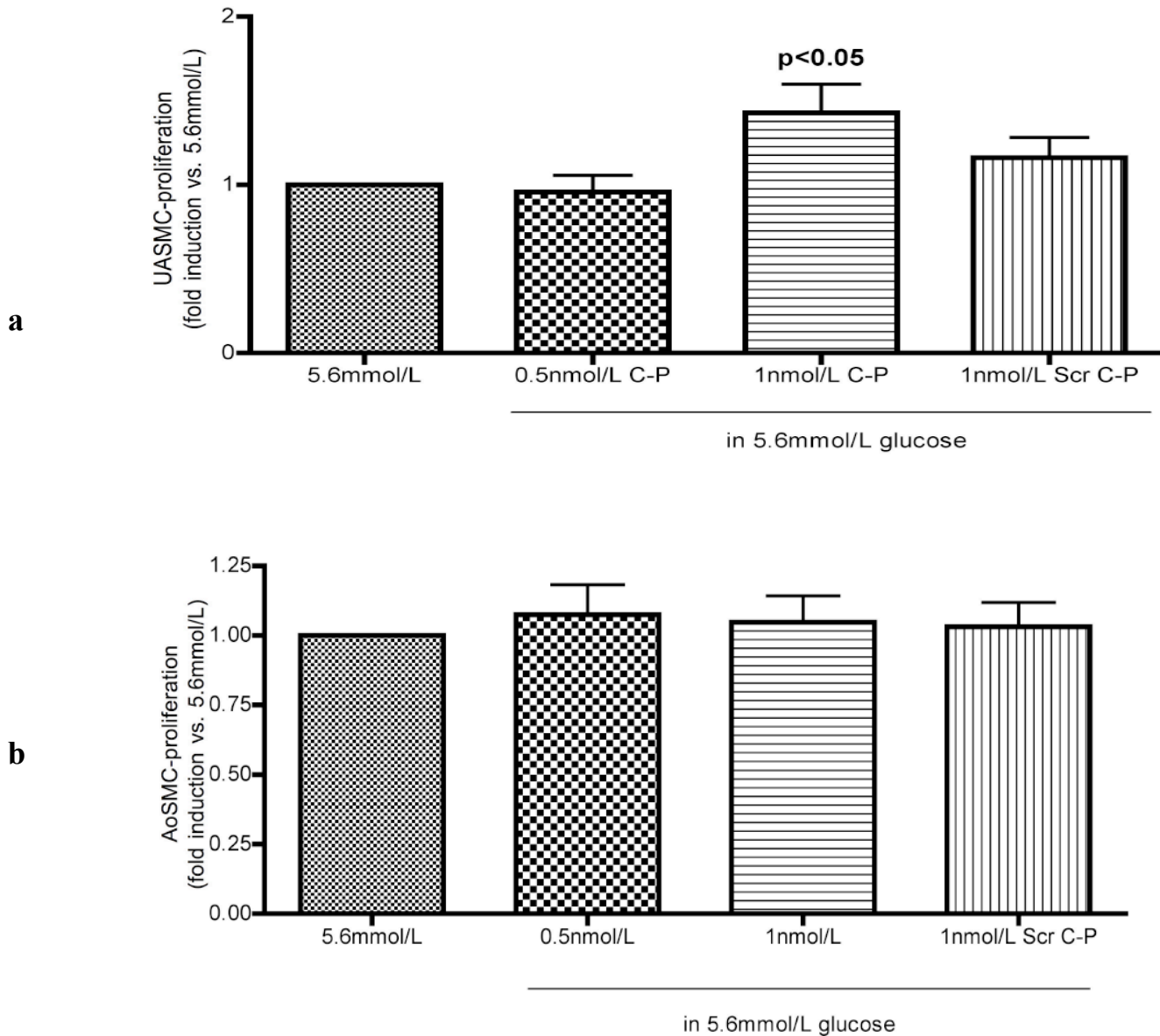


Figure 10. C-peptide stimulates proliferation of VSMCs under normal glucose. VSMCs were incubated with 5.6 mmol/L in the presence or in the absence of C-peptide (C-P) for 48 h and assayed for proliferation. In (a), BrdU incorporation in UASMC shows increased proliferation in the presence of 1 nmol/L C-peptide ($p < 0.05$ vs. 5.6 mmol/L glucose), while addition of scrambled C-peptide (Scr C-P) did not have any significant effect. In (b), BrdU incorporation in AoSMC shows no significant effect of C-peptide on cellular proliferation under normal glucose.

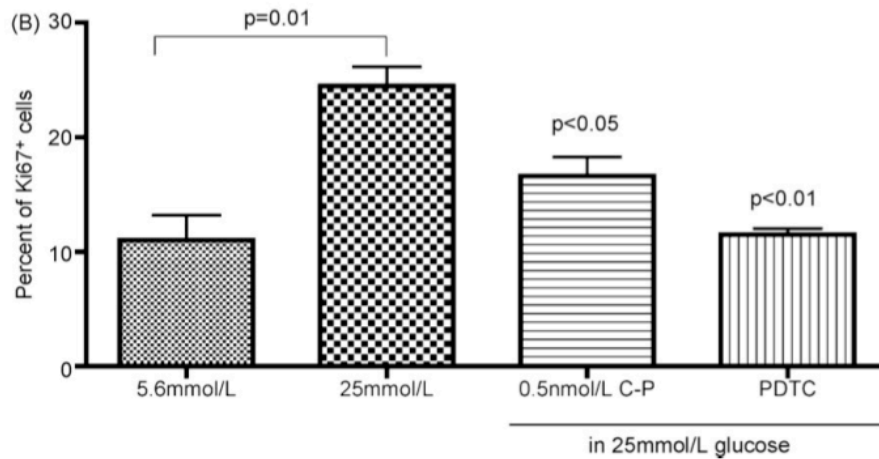
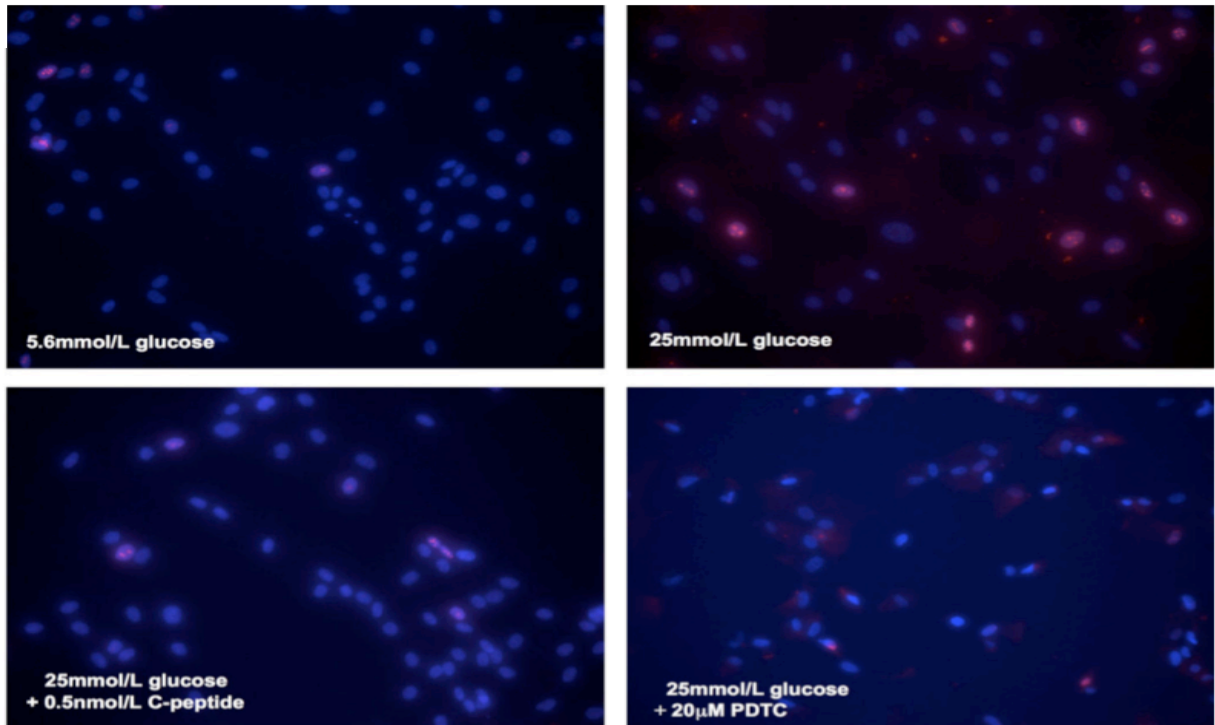


Figure 11. C-peptide reduces the number of Ki67⁺ cells. In (a) Images of Ki-67-immunostaining (in red) in UAMSC exposed for 48 hours to the different conditions, as stated. DAPI staining was used to stain the nuclei (in blue). C-peptide addition to the high glucose medium reduced Ki67⁺ cell number. In (b) quantitation of Ki67⁺ cells. Bar graph shows percent of Ki-67⁺ cells (mean±SD) compared to DAPI staining (blue) from five random fields of four independent experiments. Exposure of UAMSC to 25mmol/L glucose increased number of Ki-67⁺ cells compared to normal glucose (p=0.01), while addition of C-peptide significantly reduced the number of Ki-67⁺ proliferating cells (p<0.05 vs. 25mmol/L glucose). Addition of the NF-κB inhibitor PDTC to the high glucose medium also reduced the number of Ki-67⁺ cells (p<0.01 vs. 25mmol/L glucose).

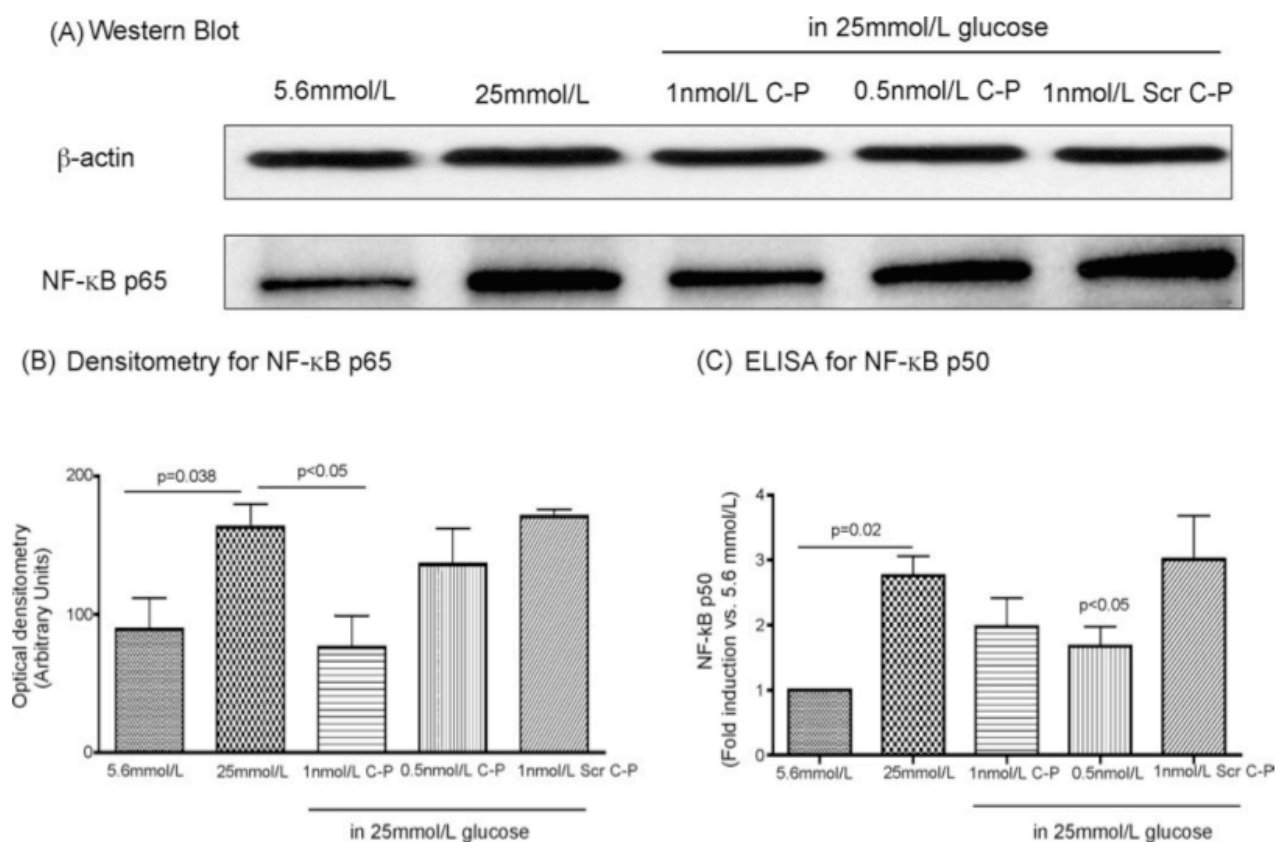


Figure 12. Expression of p65 and p50 subunits of NF- κ B in UASMC cultured in high glucose in the presence of C-peptide. UASMC were cultured in 5.6mmol/L or 25mmol/L glucose in the presence or absence of C-peptide (C-P) for 48 hours. Cellular nuclear extracts were subjected to Western immunoblotting to detect p65 levels using a specific antibody (1:1,000). Scrambled C-peptide (Scr C-P) was used as control. In (a) Representative immunoblot depicting the 65-kDa band of the p65 subunit. To show equal loading of the gel, staining for b-actin is also shown. In (b) Bar graph showing the densitometric quantitation of the bands (n=4 different experiments). There is a significant increase in NF- κ B p65 nuclear translocation in cells under 25mmol/L glucose (p=0.038 vs. 5.6mmol/L) that is reduced with addition of C-peptide (p<0.05). Results are means \pm SD. In (c) NF- κ B binding activity of the p50 subunit was examined using a EZ-DetectTM Transcription Factor kit (Pierce Biotechnology). Results were expressed as fold induction of NF- κ B p50 activity respect to control at 5.6mmol/L. High glucose increased NF- κ B p50 activation as compared to normal glucose (p=0.02). This activation is decreased by addition of C-peptide to the high glucose medium (p<0.05 vs. 25mmol/L glucose alone).

Densitometry of the NF- κ B p65 immunoblot demonstrated that high glucose-stimulated NF- κ B p65 nuclear translocation ($p = 0.038$ vs. normal glucose) and that the addition of C-peptide (1 nmol/L) during high glucose exposure reduced NF- κ B p65 nuclear translocation by 2-fold as compared to high glucose alone ($p < 0.05$) (Figure 12b).

NF- κ B activation was also assessed with a NF- κ B p50-specific ELISA with nuclear extracts from glucose-stimulated UASMCs, as shown in Fig. 12c. High glucose-induced a significant increase in NF- κ B p50 binding activity in contrast to normal glucose ($p = 0.02$) and was efficiently ablated by the addition of C-peptide ($p < 0.05$). Similar results were obtained with AoSMC (data not shown).

Nuclear translocation of NF- κ B p65 was also determined by immunofluorescence staining. UASMC cultured in 25 mmol/L glucose resulted in an increase in NF- κ B p65 nuclear translocation as demonstrated by the intense green fluorescence localized in the cell nuclei (Figure 13) and also from superimposing photomicrographs of DAPI-stained nuclei (blue) (Figure 13b) with green fluorescence (Figure 13c). Cells in normal glucose (5.6 mmol/L) retained NF- κ B p65 in the cytoplasm (green fluorescence) with very little staining observed in the nuclei (Figure 13a). The addition of C-peptide (0.5 nmol/L) to high glucose-treated cells prevented NF- κ B. The mechanism underlying NF- κ B nuclear translocation from the cytoplasm to the nucleus is based on the phosphorylation of I κ B- α . The effect of C-peptide on high glucose-induced phosphorylation of I κ B- α was therefore investigated by Western blotting on cytoplasmic extracts from UASMC (Figure 14). As expected, an increase in the level of phosphorylated I κ B (p-I κ B- α) was observed in the cytoplasmic extracts after UASMC treatment (48 h) with 25mmol/L glucose as compared to UASMC cultured in low glucose (5.6mmol/L) (Figure 14). Addition of C-peptide to the high glucose medium caused a decrease in the level of I κ B- α as compared to cells exposed to high glucose in the absence of C-peptide (Figure 14). These results suggest that in conditions of hyperglycemia C-peptide reduces proliferation of VSMCs and NF- κ B nuclear translocation.

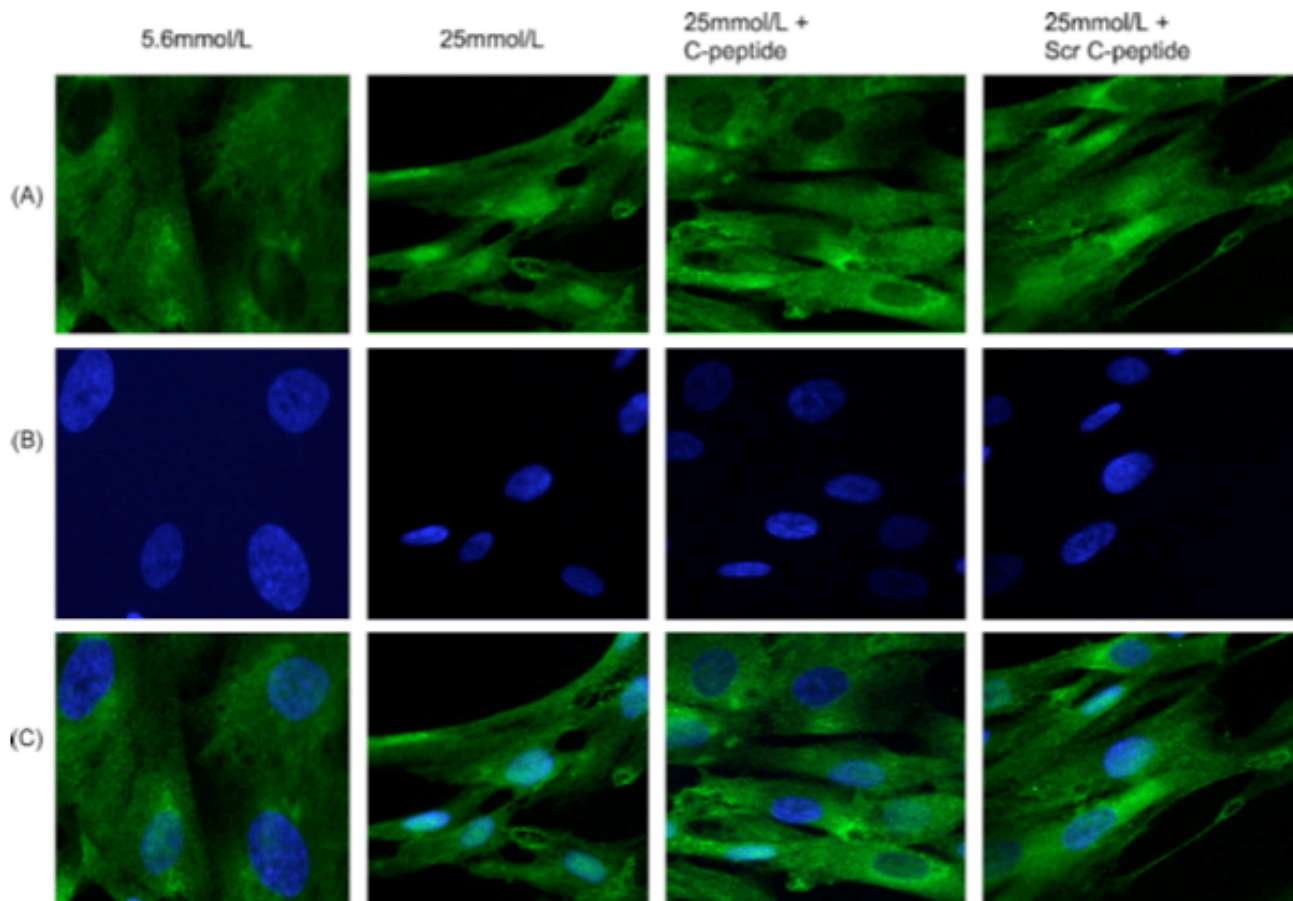


Figure 13. C-peptide treatment reduces high glucose-induced nuclear translocation of NF- κ B p65 subunit in UASMC. UASMC were serum-starved for 24 hours and then treated for 48 hours with either normal glucose, or high glucose, or high glucose in the presence of 0.5nmol/L C-peptide. Scrambled C-peptide (0.5nmol/L; Scr) was used as positive control. In (a) localization of NF- κ B immunostaining using a monoclonal antibody against the p65 subunit (green fluorescence); (b) UASMC nuclei stained with DAPI; (c) Composite images generated by superimposing photographs in A and B. As shown in (a), the green fluorescence corresponding to the p65 subunit was localized mostly in correspondence of the nuclei when cells were treated with 25mmol/L glucose. This was clearly shown by superimposing the DAPI nuclear staining in (b) with the green fluorescence. On the contrary, UASMC treated with C-peptide showed green fluorescence mostly localized in the cytoplasm, rather than in the cell nuclei. Three independent experiments were performed, and one representative photomicrograph sets (30x) is shown.

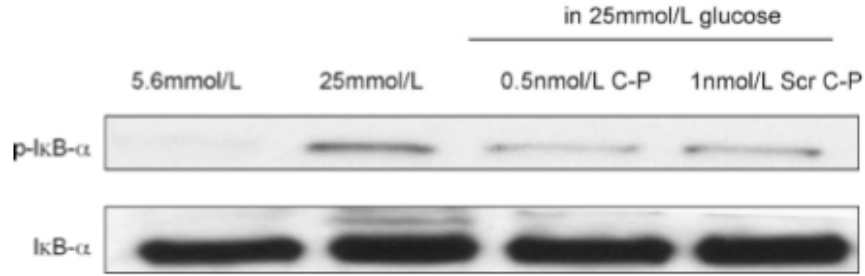


Figure 14. Inhibitory effect of C-peptide on phosphorylation of IκB-α protein in UAMSC. UAMSC were serum-starved for 24 h and then treated for 48 h with either 5.6 mmol/L glucose or 25 mmol/L glucose or 25 mmol/L glucose + 0.5 nmol/L C-peptide (C-P) or 25 mmol/L glucose + 1nmol/L C-P. Cellular cytoplasmic extracts were subjected to Western immunoblotting to detect phosphorylated IκB-α (p-IκB-α) using a specific antibody. In this figure, it is shown a representative immunoblotting depicting decreased phosphorylation of p-IκB-α with C-peptide. Immunoblot for total IκB-α is also shown. Similar results were obtained in at least two independent experiments.

6.0 C-PEPTIDE REDUCES GLUCOSE INDUCED ROS PRODUCTION IN ENDOTHELIAL CELL BY AFFECTING THE NAD(P)H OXIDASE SUBUNIT RAC-1

In this section, we investigated the effect of C-peptide to reduce cell death (apoptosis) and ROS generation in endothelial cells (HAEC) exposed to hyperglycaemia. We also investigated whether C-peptide affects the activity of the enzymatic complex called NAD(P)H oxidase, which is considered to be one of the major sources of ROS production in EC after exposure to hyperglycemia⁸⁴.

Exposure of HAEC to high glucose medium (25mmol/L) for 48 hours significantly increased DNA fragmentation as compared to cells in normal glucose ($p<0.01$), as shown in Figure 15a. Addition of C-peptide to the high glucose media significantly reduced HAEC apoptosis, as compared to high glucose alone ($p<0.05$). This corresponded to a 25% reduction of apoptosis by C-peptide as compared to high glucose (Figure 15b).

One crucial mediator of apoptosis is the activated caspase-3 proteases, which catalyzes the specific cleavage of many key cellular proteins. We evaluated endogenous levels of the large fragment (17/19kD) of activated (cleaved) caspase-3 by Western blotting in cell lysates from HAEC exposed to high glucose overnight. As shown in Figure 16a, expression of cleaved caspase-3 was higher in cell lysates from HAEC under high glucose compared to normal glucose conditions ($p<0.05$). Addition of C-peptide reduced endogenous levels of activated caspase-3 in cell lysates of HAEC compared to high glucose alone ($p<0.05$), a result that was not observed with scrambled C-peptide (Figure 16a-16b).

Caspase-3 activity in high glucose-exposed HAEC was also assessed *in vitro* on cell lysates by ELISA. As shown in Figure 16c, exposure to high glucose overnight significantly increased

caspace-3 activity compared to normal glucose ($p < 0.01$). Addition of C-peptide to the high glucose medium, significantly reduced caspace-3 activity ($p < 0.01$ vs. high glucose alone), while scrambled C-peptide was without significant effects (Figure 16c). Analysis of expression of the product of the survival gene Bcl-2 by Western blotting showed a decreased level of protein expression in cell lysates of HAEC exposed to high glucose overnight (Figure 17a) ($p < 0.05$). Addition of C-peptide to the high glucose medium increased Bcl-2 protein expression as compared to high glucose alone (Figure 17a) ($p < 0.05$).

Intracellular ROS produced by HAEC was assessed using a fluorescent dye called carboxy-DCFDA, which is a cell-permeant indicator for ROS. Treatment with high glucose on HAEC was found to increase CM-H₂-DCFDA fluorescence in a time-manner, as compared to normal glucose. Figure 18a shows that CM-H₂-DCFDA fluorescence in HAEC exposed to high glucose increased progressively from time 0 to 5 hours after addition of the dye, as compared to control levels of glucose ($p < 0.05$ vs. normal glucose at 3 hours). C-peptide addition to the high glucose medium completely significantly suppressed the increased in CM-H₂-DCFDA fluorescence induced by high glucose at all time points and reaching statistical significance at 3 hours ($p < 0.01$ vs. high glucose) and 4 hours ($p < 0.01$ versus high glucose) (Figure 18a). When scrambled C-peptide was added to high glucose, no significant decrease in CM-H₂-DCFDA fluorescence was detected in HAEC as compared to high glucose alone (Figure 18a). Figure 18b shows representative histograms of flow cytometry analysis of CM-H₂-DCFDA fluorescence in HAEC under the different treatment conditions after 4 hour.

We also tested the effect of C-peptide to decrease the level of oxidative stress in hyperglycaemia-induced HAEC generated by the activity of NAD(P)H oxidase. Percent of NAD(P)H oxidase activity in HAEC upon different treatment conditions (30 min) are shown in Figure 18c. NAD(P)H oxidase activity decreased in presence of C-peptide (<60% less; $p < 0.01$ vs. HG) compared to high glucose alone. Pre-incubation of HAEC with NAD(P)H oxidase inhibitors Apocynin (10mmol/L) and DPI (100mmol/L) for 2 hours, drastically reduced NAD(P)H oxidase activity in HAEC successively exposed to high glucose for 30 minutes. We then decided to focus our investigation on Rac-1, a small GTPase, which is a cytosolic subunit that upon stimulation translocates to plasma membrane in order to form the NAD(P)H oxidase enzymatic complex together with other subunits.

To determine if high glucose-induced translocation of Rac-1 from cytoplasm to plasma membrane was affected by C-peptide, we performed immunoblot analysis on plasma membrane and cytosolic proteins from stimulated-HAEC.

We showed that high glucose induced the translocation of Rac-1 subunit from the cytoplasm to the plasma membrane (Figure 19a-b) ($p < 0.05$ compared to NG) after 30 minutes treatment. Addition of C-peptide to HAEC previously exposed to high glucose, led to a decreased localization of Rac-1 on the membrane and higher presence of Rac-1 in the cytoplasm ($p < 0.05$ vs high glucose condition) while scrambled C-peptide was without significant effects (Figure 19a-b). We tested whether C-peptide treatment for 30 min had any effects on mRNA gene expression of Rac-1 in high glucose-exposed HAEC. As shown in Figure 6C, we did not find any significant differences in mRNA expression for Rac-1 in HAEC exposed to C-peptide as compared to high glucose alone (Figure 19c).

The activity of Rac-1 using 10 μg of cell lysates was evaluated by G-LISATM assay. We observed that after serum starvation, high glucose increased Rac GTPase activity in HAEC after 30 minutes treatment compared to normal glucose condition (Figure 20) ($p < 0.01$). Addition of C-peptide to HAEC exposed to high glucose, reversed the activation of Rac GTPase activity to basal level ($p < 0.01$ vs high glucose) while scrambled C-peptide was without significant effects (Figure 20). As further control of high glucose-induced Rac-1 translocation and activity, these experiments were performed using cell culture medium that lacked hEGF, known as Rac activator, during both serum starvation and treatments

6.1 FIGURES OF CHAPTER 6.0

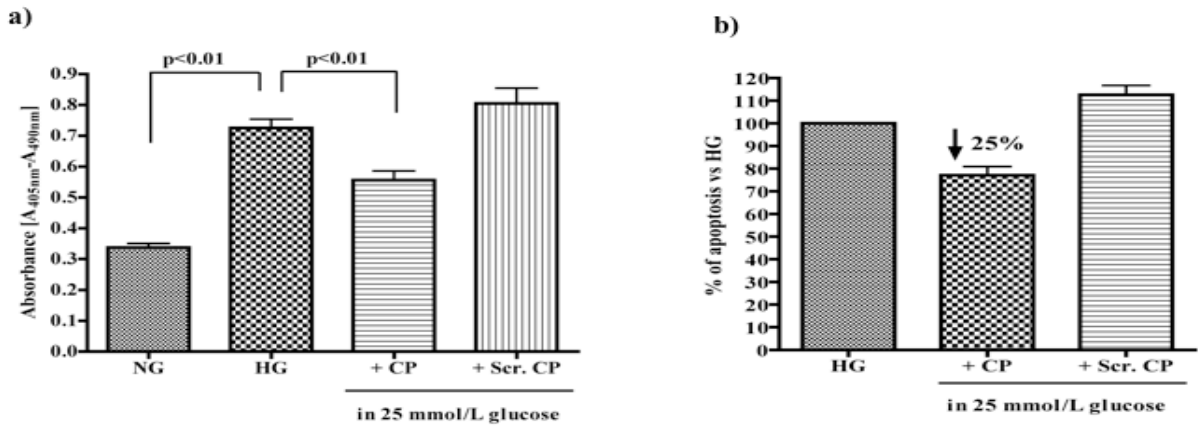


Figure 15. C-peptide decreases generation of histone-associated-DNA fragments in HAEC exposed to high glucose for 48 h. HAEC were seeded in 96 well-plate and exposed to either normal glucose, or high glucose (25 mmol/L) or high glucose + C-peptide (10 nmol/L) or high glucose + Scrambled C-peptide for 48 h. Changes of cytoplasmic histone-associated-DNA fragments upon different treatment conditions were detected using DNA fragmentation ELISA. In (a), significant increase of DNA fragments in HAEC exposed to high glucose for 48h compared to normal glucose ($p < 0.01$ vs. 5.6 mmol/L glucose). DNA fragments decreased in the presence of 10 nmol/L C-peptide ($p < 0.01$ vs. 25 mmol/L glucose), while addition of scrambled C-peptide (Scr. CP) did not have any significant effect. In (b), percent of DNA fragmentation in HAEC exposed to high glucose + C-peptide compared to high glucose alone (25 % less). Values are mean \pm S.D. of three different experiments run in triplicate.

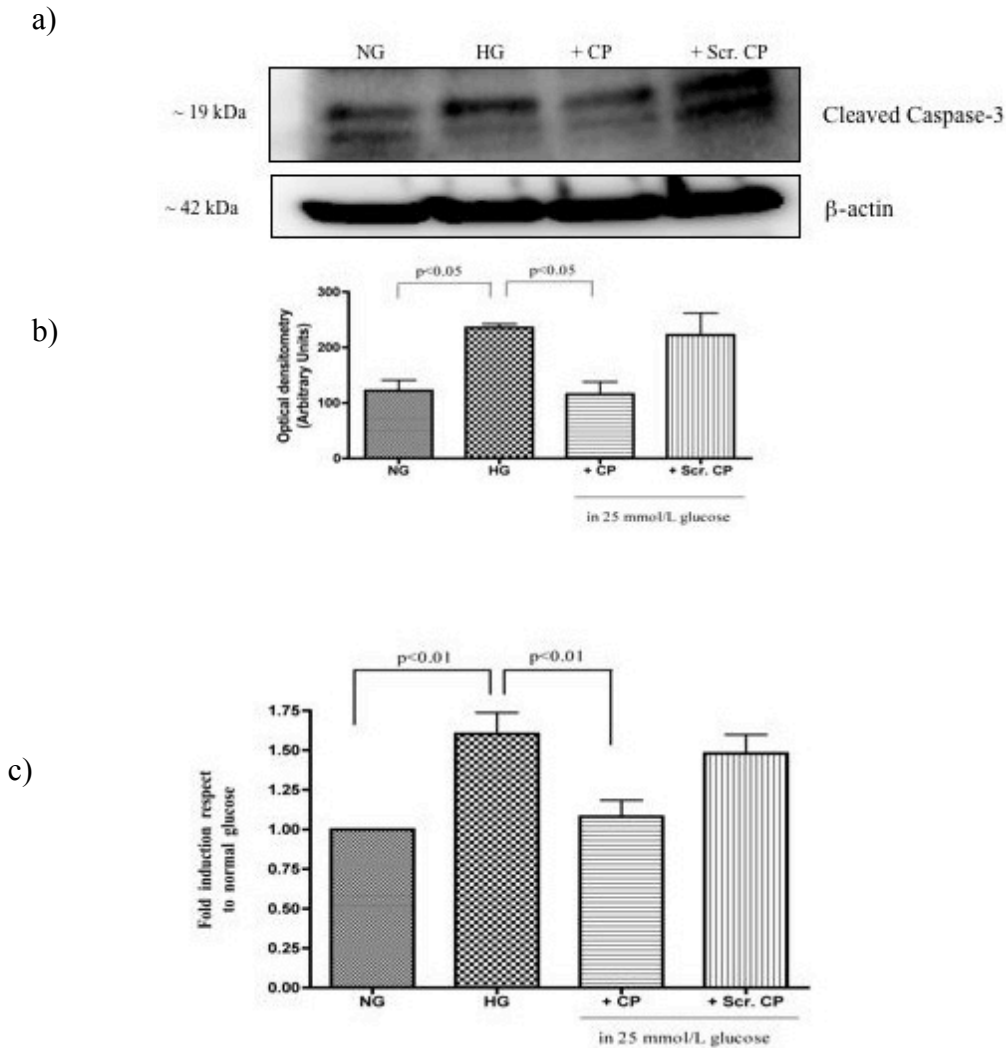


Figure 16. C-peptide decreases caspase-3 activity and expression in HAEC exposed to high glucose. HAEC were cultured in normal glucose (NG; 5.6mmol/L) or high glucose (HG; 25 mmol/L) in the presence or absence of 10 nmol/L C-peptide overnight. Cellular cytoplasmic extracts were subjected to Western blotting (a) to detect the 19-kDa band of the cleaved caspase-3. In (b) bar graph showing the densitometric quantitation of the bands. In cells exposed to HG there was a two-fold increase in cleaved caspase-3 compared to cells in NG ($p < 0.05$). A decrease in cleaved caspase-3 is observed when HAEC are exposed to HG + 10 nmol/L C-peptide ($p < 0.05$). Results are means \pm SD ($n = 3$). Scrambled (Scr. Cp) C-peptide (10 nmol/L) was used as control; c Detection of the caspase 3 activity by using a kit (Calbiochem). Results were expressed as fold induction of caspase-3 activity in respect to control at 5.6mmol/L. In cells exposed to HG there was a 1.5-fold increase in caspase-3 activity compared to cells in NG ($p <$

0.01). ^{a)} A decrease in caspase-3 activity is observed when HAEC are exposed to HG + 10 nmol/L C-peptide ($p < 0.01$). Results are expressed as means \pm SD ($n = 3$). Scrambled C-peptide (Scr. CP; 10 nmol/L) was used as control.

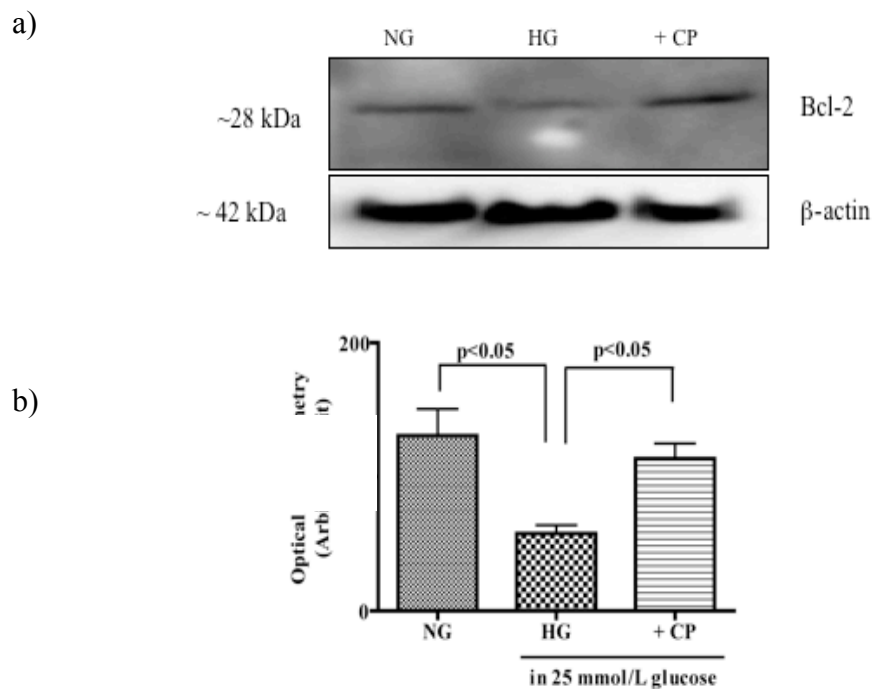
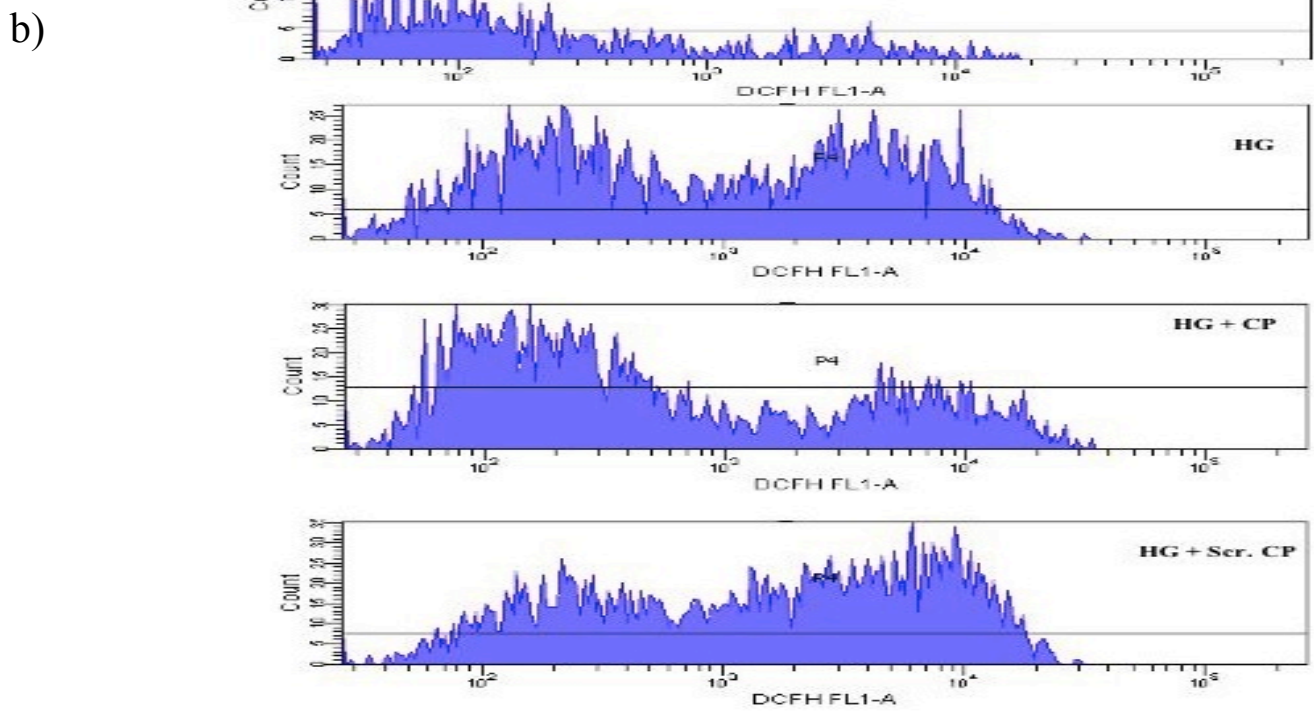
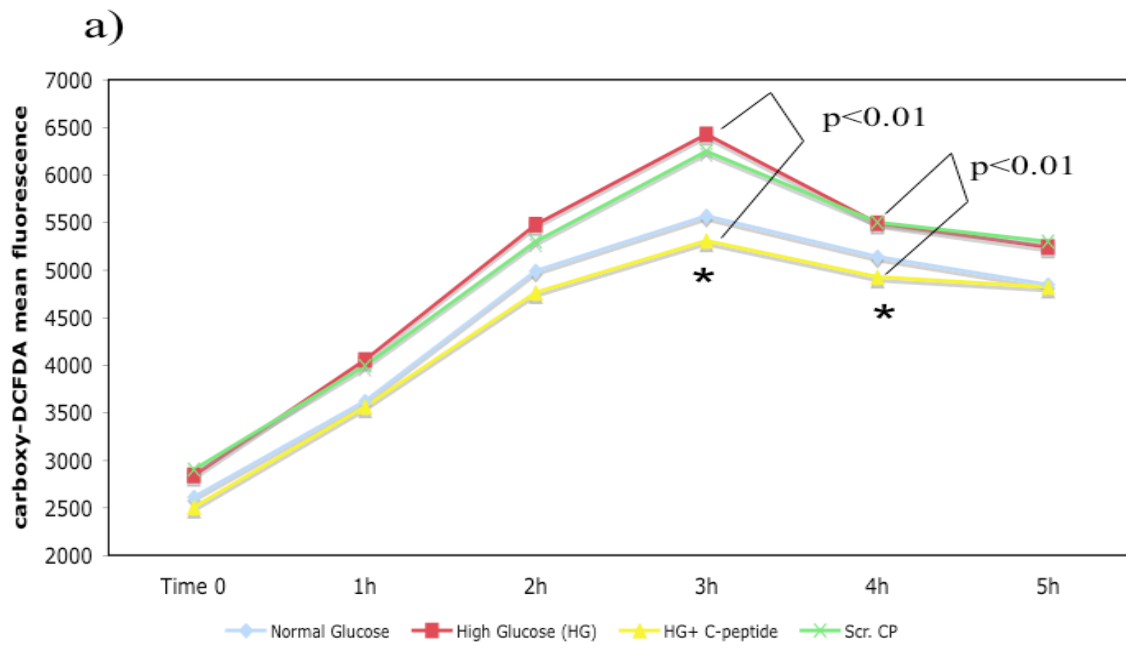


Figure 17. C-peptide increases Bcl-2 expression in HAEC exposed to high glucose. In (a) a typical western blot of Bcl-2 and β -actin in endothelial cells treated in high glucose overnight. In (b) Bar graph showing the densitometric quantitation of the bands. Bcl-2 expression was significantly decrease in condition of high glucose ($p < 0.05$ compared to NG)., On the other hand, addition of C-peptide to HAEC previously exposed to high glucose, led to an increased expression of Bcl-2 suggesting an activation of the cell survival pathway ($p < 0.05$).



E

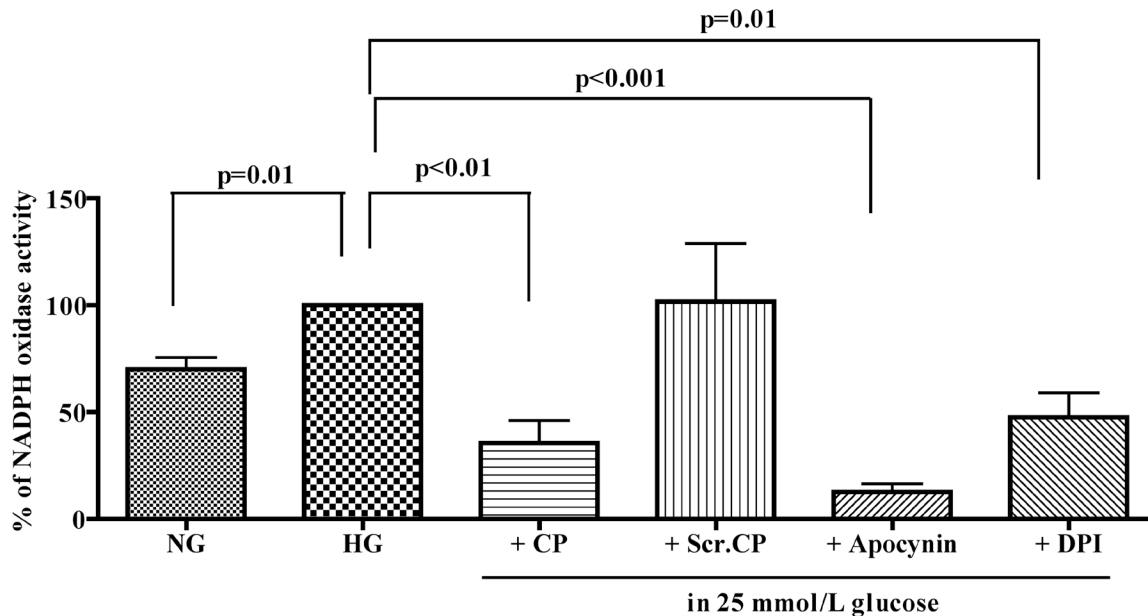


Figure 18. Measurements of oxidative stress in HAEC exposed to high level of glucose. In (a) detection of ROS accumulation in culture HAEC was performed using a carboxy-dichlorodi-hydrofluorescein diacetate (carboxy-H₂-DCFDA). Briefly, HAEC were treated with the indicated treatment overnight and the following day, incubated with the carboxy-H₂-DCFDA dye (10 μ mol/L) for 30min. After incubation time, HAEC were immediately read at the flow cytometer (time 0). HAEC were then maintained at 37 $^{\circ}$ C and intracellular ROS production monitored every hour until 5 hours. As shown in (a) high glucose was able to increase the production of ROS vs. normal glucose condition in HAEC (paired t-test: 3h p=0.01; 4h p<0.01). C-peptide treatment showed to decrease ROS production in HAEC exposed to high glucose overnight. In (b), a representative fluorescence emission graph of oxidized dye for ROS detection. In (c) percent of NAD(P)H oxidase activity in HAEC upon different treatment conditions (30 min). NAD(P)H oxidase activity decreased in presence of C-peptide (<60% less; p<0.01 vs. HG) compared to high glucose alone. Inhibitors Apocynin (10 μ M) and DPI 100 μ M) drastically reduced NAD(P)H oxidase activity in HAEC exposed to high glucose. Scrambled C-peptide was used a control.

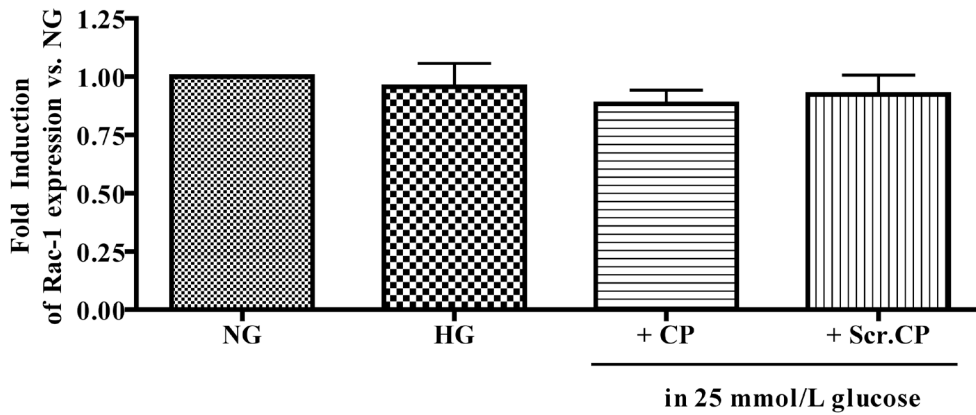
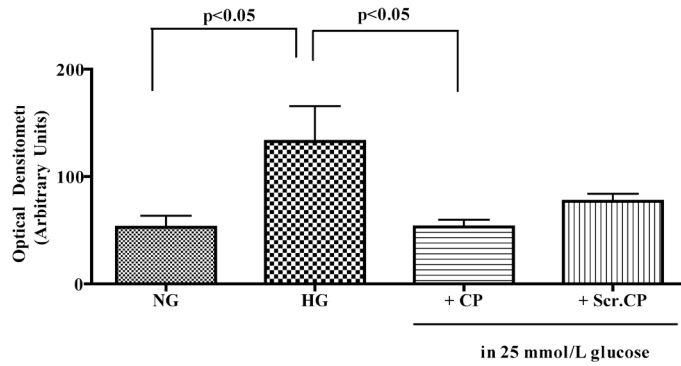
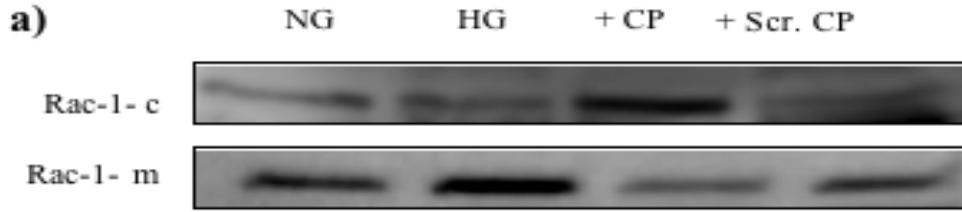


Figure 19. Effect of C-peptide on Rac-1 translocation in HAEC exposed to high glucose. In (a) western blot of cytoplasmic (Rac-1-c) and membrane (Rac-1-m) Rac-1 expression in endothelial cells treated in high glucose, in presence or absence of C-peptide (10 nmol/L) for 30 minutes. In (b) Bar graph showing the densitometric

quantitation of the bands. High glucose condition induced the translocation of Rac-1 subunit from the cytoplasm to the plasma membrane ($p < 0.05$ compared to NG). Addition of C-peptide to HAEC previously exposed to high glucose, led to a decreased localization of Rac-1 on the membrane and higher presence of Rac-1 in the cytoplasm ($p < 0.05$ vs high glucose condition). In c) effect of treatment condition on Rac-1 mRNA in HAEC

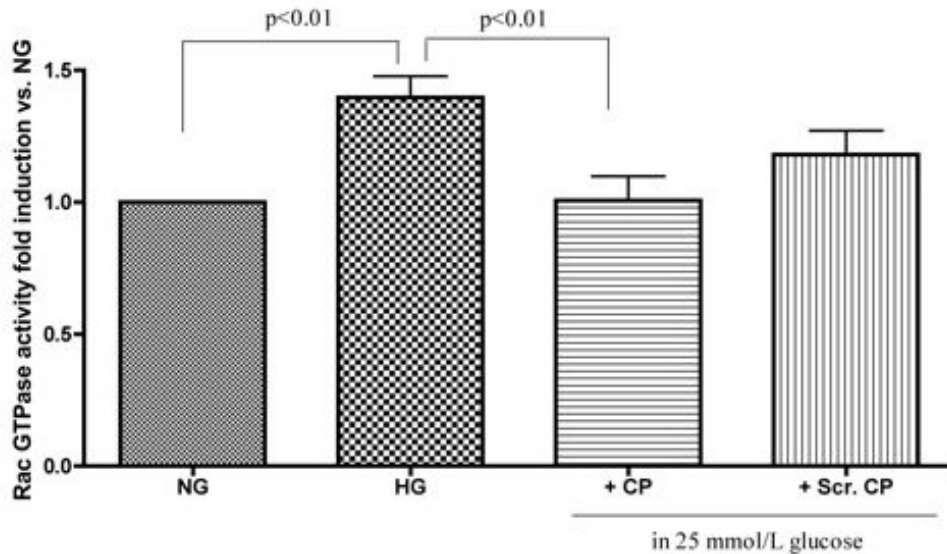


Figure 20. C-peptide decreases Rac GTPase activation in HAEC exposed to hyperglycaemia after 30 minutes.

HAEC were serum starved overnight and exposed to regular EBM-2 media containing either normal glucose, or high glucose, or high glucose+ C-peptide (10 nmmol/L) or scrambled C-peptide (10nmol/L) for 30 minutes at 37°C. EGF, known as Rac activator, was removed from the EBM-2 media during both serum starvation and treatments. 10 µg of cell lysates were then subjected to the G-LISA™ assay and absorbance was read at 490 nm. High glucose condition increased Rac GTPase activity in HAEC after 30 min of treatment compared to normal glucose condition ($p < 0.01$). Addition of C-peptide to HAEC exposed to high glucose, reversed the activation of Rac GTPase activity to basal level ($p < 0.01$ vs high glucose).

7.0 C-PEPTIDE REDUCES PRO-INFLAMMATORY CYTOKINE SECRETION IN LPS-STIMULATED U937 MONOCYTES IN CONDITION OF HYPERGLYCEMIA

We investigated the effect of C-peptide on pro-inflammatory cytokine secretion by LPS-treated U-937 monocytes. As expected, exposure of U-937 cells to high glucose and LPS for 24 hours significantly stimulated secretion of several pro-inflammatory cytokines, such as IL-6, IL-8, macrophage inflammatory protein (MIP)-1 α , and MIP-1 β (Figure 22a-d). Addition of C-peptide (1 μ mol/L) to the LPS-treated U-937 monocytes statistically significantly reduced secretion of IL-6, IL-8, MIP-1 α and MIP-1 β (Fig. 21a-d). Addition of scrambled C-peptide (1 μ mol/L) to the culture medium did not significantly affect LPS-induced cytokine secretion after 24 hours incubation (Figure 21a-d).

We then assessed adherence of U-937 monocytes to HAEC after exposure of monocytes to C-peptide and glucose at various concentrations. When C-peptide was added to 30mmol/L glucose, there was a significantly decreased number of adherent monocytes as compared to high glucose alone ($p < 0.05$), (Figure 22a). As a positive control, IL-1 β was used to stimulate adherence of U-937 monocytes to HAEC ($p < 0.01$ vs. high glucose). In low and intermediate glucose conditions, C-peptide did not show significant effects on U-937 monocyte adherence. In Figure 22b, are shown images of U-937 monocyte adhesion under the different conditions tested. The signal transduction pathway leading to mRNA synthesis of adhesion molecules and chemokines involves activation of NF- κ B. To determine whether C-peptide affected high glucose-induced NF- κ B nuclear translocation in LPS-stimulated U937 monocytes, immunoblot analysis and NF- κ B-specific ELISAs were performed with nuclear extracts from LPS-stimulated U-937. As shown in Figure 23a, exposure of U-937 to LPS for 24 hours induced an increase in

NF- κ B nuclear translocation in comparison to cells without LPS stimulation. A two-fold increase in NF- κ B p65 activation was found after 24 hours stimulation with LPS as compared to incubation with 30mmol/L glucose alone ($p < 0.05$) (Figure 23a-b). Addition of C-peptide significantly decreased NF- κ B p65 nuclear translocation (Figure 23a). Densitometric analysis of this NF- κ B p65 immunoblot demonstrated that C-peptide (1 μ mol/L) reduced NF- κ B p65 nuclear translocation as compared to stimulation with LPS ($p < 0.05$) (Figure 23b). Addition of C-peptide to LPS-treated U937 monocytes also reduced NF- κ B p50 subunit nuclear translocation as compared to LPS-treatment alone, as detected by ELISA ($p=0.0042$) (Figure 23c).

The mechanism underlying NF- κ B nuclear translocation from the cytoplasm to the nucleus is based on the phosphorylation of I κ B- α . We therefore investigated the effects of C-peptide on LPS-induced phosphorylation of I κ B- α by Western blotting on cytoplasmic extracts from U-937 cells (Figure 24). As expected, an increase in the level of phosphorylated I κ B- α (p-I κ B- α) was observed in the cytoplasmic extracts of LPS-stimulated U937 monocytes after 24 hours treatment compared to U937 cells cultured in 30mmol/L glucose alone (Figure 24). Addition of C-peptide caused a decrease in the level of p-I κ B- α as compared to cells exposed to LPS in the absence of C-peptide (Figure 24).

7.1 FIGURES OF CHAPTER 7.0

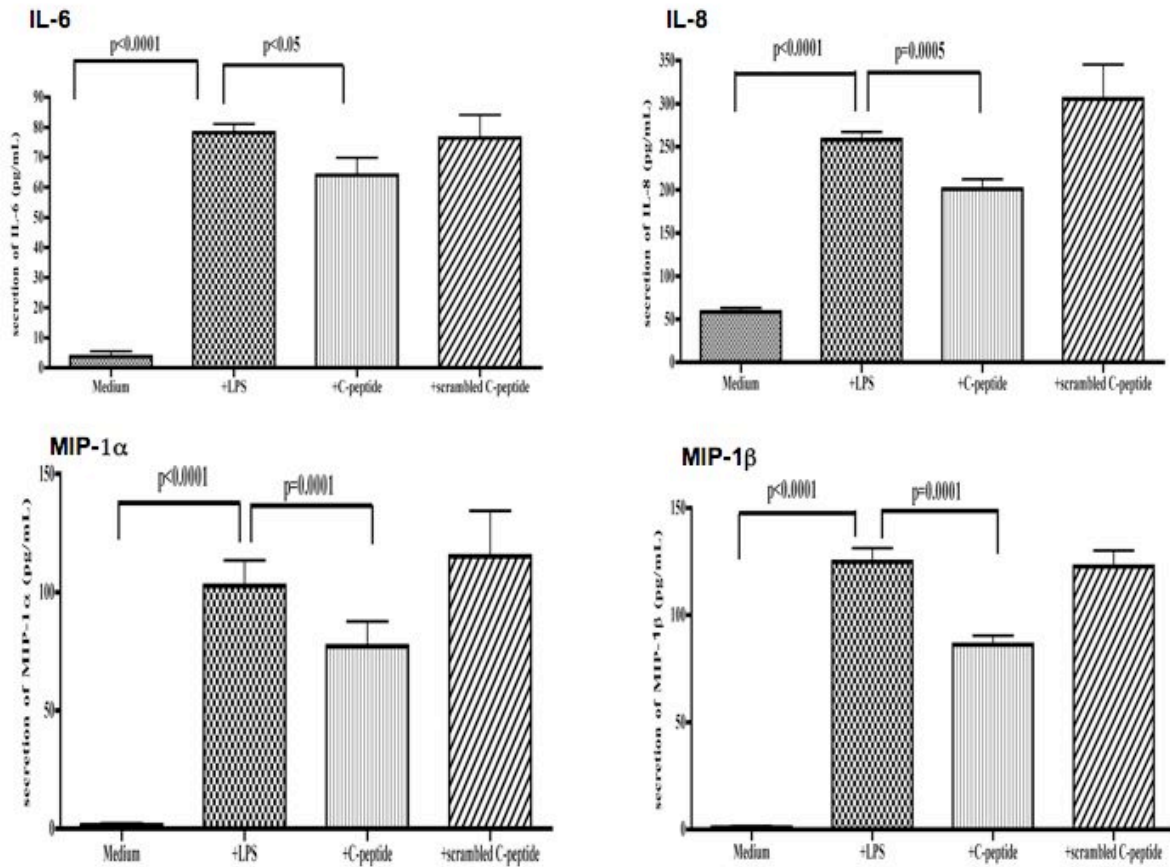


Figure 21. C-peptide reduces LPS-stimulated secretion of IL-6, IL-8, MIP-1a, and MIP-1b in U937 monocytes. U-937 cells were cultured with 30mmol/L glucose and stimulated with 0.5 ng/mL of Lipopolysaccharide in the presence or absence of 1 μ mol/L C-peptide for 24 hours. Scrambled C-peptide (1 μ mol/L) was used as a control. Luminex multiplex assays were used to assess levels of IL-6, IL-8, MIP-1a and MIP-1b in the culture supernatants of LPS-stimulated U937 cells. Bar graphs demonstrate cytokine secretion (pg/mL). Cells exposed to LPS produced more cytokines than cells exposed to high glucose alone ($p < 0.001$). Addition of C-peptide to the LPS-treated U-937 monocytes reduced secretion of IL-6, IL-8, MIP-1a and MIP-1b ($p < 0.05$, $p = 0.0005$, $p = 0.0001$, $p = 0.0001$, respectively). Addition of scrambled C-peptide to the culture medium did not significantly affect LPS-induced cytokine secretion. A minimum of 4 independent experiments was performed. Each condition was tested in duplicate. Results are expressed as mean \pm SD.

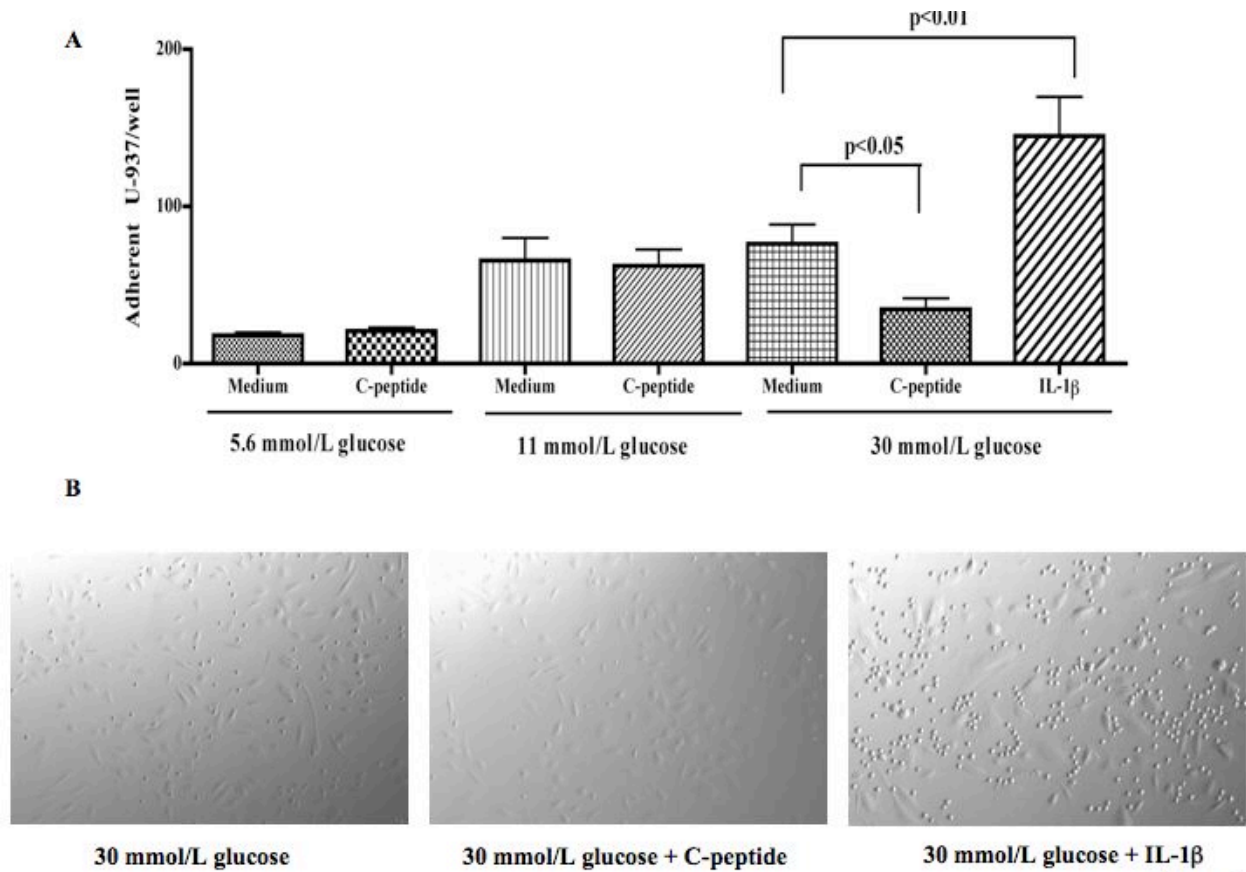


Figure 22. C-peptide reduces adhesion of U937 monocytes to HAEC. U-937 monocytes were cultured in either low (5.6mmol/L), intermediate (11mmol/L), or high glucose (30mmol/L) medium, in the presence or absence of C-peptide for 4 hours. Subsequently, the U937 were added to confluent HAEC and allowed to incubate for 1 hour and then counted. (A) Bar graphs demonstrating the number of adherent U937 per well (n =at least 3 sets of independent experiments with each condition tested in triplicate). Intermediate and high glucose increased the number of adherent U937 compared to low glucose. The addition of C-peptide to U937 cultured in low- or intermediate-glucose did not demonstrate a significant affect on adhesion. When C-peptide was added to high glucose, there was a decreased number of adherent monocytes as compared to high glucose alone ($p<0.05$). As a positive control, IL-1 β was used to stimulate adherence of U-937 monocytes to HAEC ($p<0.01$ vs. high glucose). Results are expressed as mean \pm SD. (B) Photographic images of U-937 monocyte adhesion under the various conditions tested.

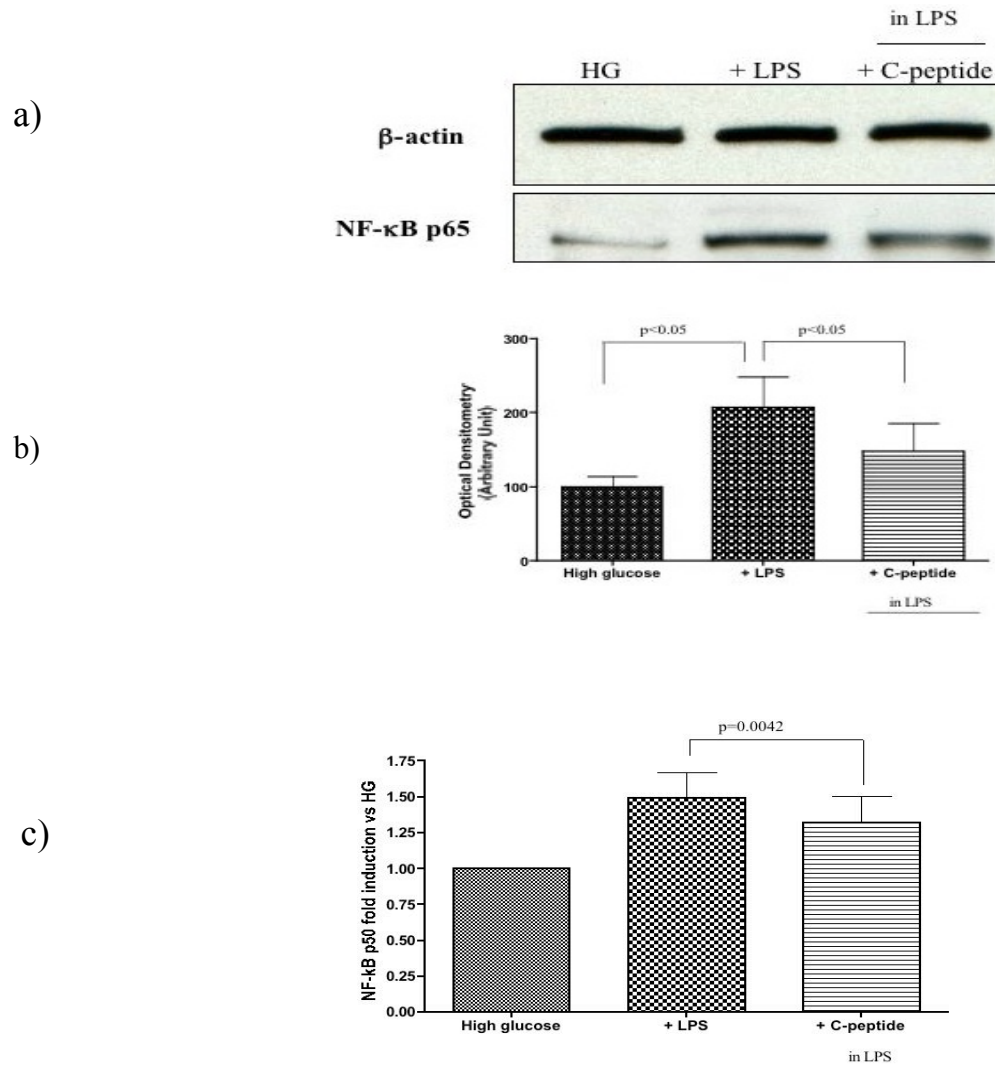


Figure 23. C-peptides diminishes nuclear translocation of p65/p50 subunits of NF-κB in LPS-stimulated U937. U-937 cells were cultured in complete RPMI-1640 with 30 mmol/L glucose and exposed to LPS (0.5ng/μL) in the presence or absence of C-peptide for 24 hours. (a) Nuclear extracts were subjected to western blotting to detect p65 subunits of NF-κB. (b) Densitometric quantification of the band at 24 h. In cells exposed to LPS there was a two-fold increase in NF-κB p65 nuclear translocation compared with cells in HG alone ($p < 0.05$). A decrease in p65 nuclear translocation was observed in the presence of 1 μmol/L C-P: $p < 0.05$ vs LPS. Results are expressed as means±SD (n=3). (c) Detection of the NF-κB p50 binding activity by ELISA after 24 h. Results are expressed as fold induction of NF-κB p50 activity in respect to 30 mmol/L glucose. In cells exposed to LPS there was a 1.5 increase in NF-κB p50 nuclear translocation compared to cells in HG alone. A decrease in NF-κB p50 nuclear translocation was observed in the presence of 1 μmol/L C-peptide (C-P); $p = 0.0042$ vs LPS condition.

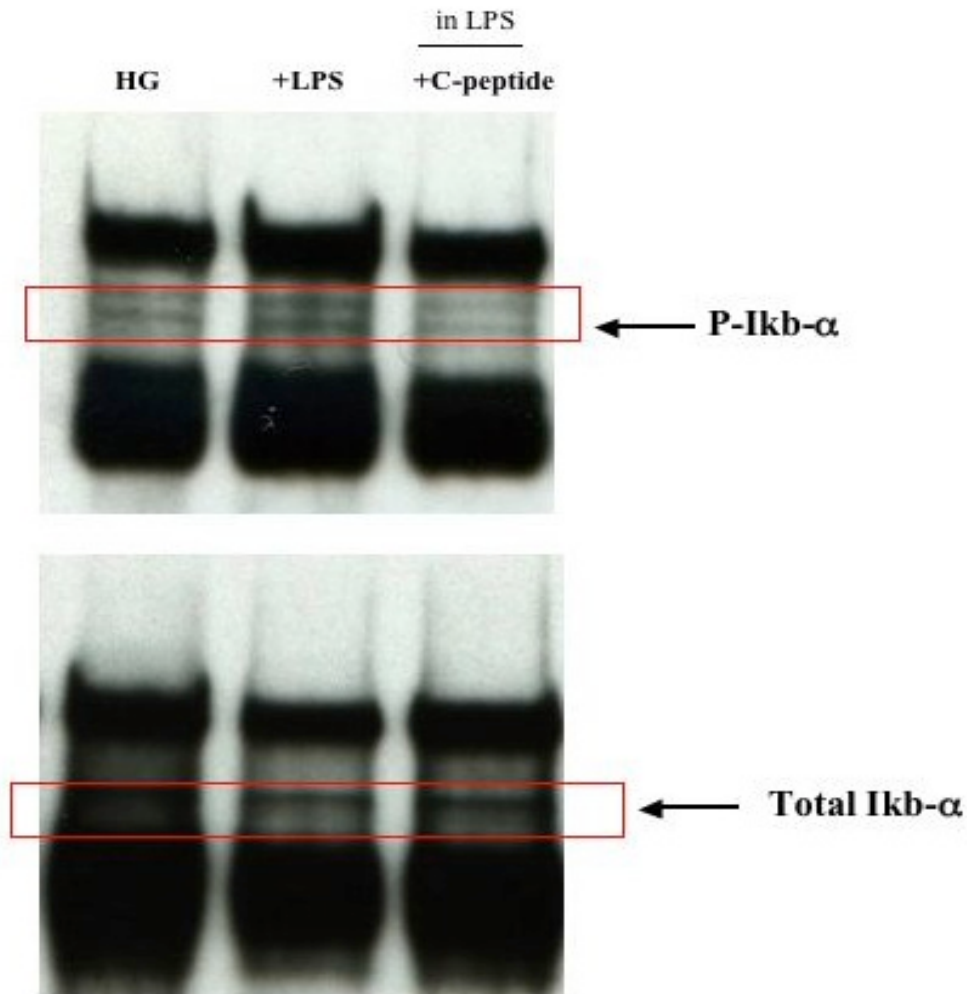


Figure 24. Inhibitory effect of C-peptide on phosphorylation of IκBα protein in LPS-stimulated U937 monocytes. Cytoplasmic extracts (50 μg) were incubated overnight at 4°C with anti-IκBα IgG (1:100). The samples were then treated with 10 μl of protein A agarose beads for 2 h at 4°C after which the samples were centrifuged and washed in PBS. The beads were boiled in SDS-PAGE sample treatment buffer and electrophoresed on a 4-20% SDS-PAGE. The gel was blotted and incubated with either monoclonal P-IκBα or IκBα antibodies (both from Santa Cruz Biotechnology; 1:1000). (Upper panel) An increase in the level of phosphorylated-IκB-a (p-IκBa) was observed in the cytoplasmic extracts of LPS-stimulated U937 monocytes after 24 hours treatment compared to U937 cells cultured in 30mmol/L glucose alone. Addition of 1mmol/L C-peptide caused a decrease in the level of p-IκBa as compared to cells exposed to LPS in the absence of C-peptide. (Lower panel) Total IκB-a levels did not change upon treatment conditions.

8.0 C-PEPTIDE IS INTERNALIZED IN ENDOTHELIAL AND SMOOTH MUSCLE CELLS VIA EARLY ENDOSOMES

P. Luppi[‡], X. Geng*, V. Cifarelli[‡], P. Drain*, and M. Trucco[‡]

[‡]Division of Immunogenetics, Department of Pediatrics, Rangos Research Center, Children's Hospital of Pittsburgh, and *Department of Cell Biology and Physiology, University of Pittsburgh, School of Medicine, Pittsburgh, PA 15213, USA

Diabetologia 52(10):2218-28

This study was supported by: the Henry Hillman Endowment Chair in Pediatric Immunology (to MT) and by grants DK 024021-24 from the National Institute of Health, W81XWH-06-1-0317 from the Department of Defense (to MT), and 1-06-RA-39 from the American Diabetes Association (to PD).

8.1 ABSTRACT

Aims: There is increasing evidence that C-peptide exerts intracellular effects in a variety of cells and could be beneficial in patients with type 1 diabetes. How exactly C-peptide achieves these effects, however, is still unknown. Recent reports showed that C-peptide internalizes in the cytoplasm of HEK-293 and Swiss 3T3 cells, where it is not degraded for at least 1 hour from uptake. In this study, we investigated the hypothesis that C-peptide is internalized via an endocytic pathway and traffics to classic endocytic organelles, such as endosomes and lysosomes. **Methods:** We studied internalization of C-peptide in vascular endothelial and smooth muscle cells, two relevant targets of C-peptide activity, by using AlexaFluor-labelled C-peptide probes in live-cells and immunohistochemistry employing confocal laser-scanning microscopy. To examine trafficking to sub-cellular compartments, we used fluorescent constructs tagged to Rab5a to identify early endosomes, or to Lamp1 to identify lysosomes. **Results:** C-peptide internalizes in the cytoplasm of cells within punctate structures identified as early endosomes. Internalization was clearly detectable after 10 min of incubation and was blocked at 4°C as well as with excess of unlabelled C-peptide. A minority fraction of vesicles, which increased with culture time, co-localized with lysosomes. Uptake of C-peptide was reduced by Monodansylcadaverine (MDC), a pharmacological compound that blocks clathrin-mediated endocytosis, and by Nocodazole, which disrupts microtubule assembly. **Conclusions:** C-peptide internalizes in the cytoplasm of cells via endocytosis as demonstrated by localization in early endosomes. Endosomes might represent a signaling station, through which C-peptide might achieve its cellular effects.

8.2 INTRODUCTION

Human C-peptide is a 31 amino acid long peptide released by pancreatic beta cells in equimolar amounts with insulin in response to elevated blood glucose levels (hyperglycaemia). Once secreted in the bloodstream, C-peptide circulates at low nanomolar concentrations in healthy individuals, but it is absent in the majority of type 1 diabetes patients². In recent years, C-

peptide has been shown to exert insulin-independent biological effects on a variety of cells, where it affects activation of several intracellular pathways, such as, but not limited to, those involved in cellular proliferation and inflammation⁶⁻⁸. Importantly, C-peptide has been demonstrated to be beneficial when administered as replacement therapy to type 1 diabetes patients who suffer from some diabetic complications¹²⁻¹⁵. How exactly C-peptide achieves its intracellular effects in target cells, however, is still unknown.

Several years ago, C-peptide was shown to specifically bind to plasma membranes from rat pancreatic beta cells¹⁴⁹, human renal tubular cells¹⁵⁰, human fibroblasts and endothelial cells¹⁰⁶. More recently, C-peptide was shown to bind and cross plasma membranes localizing in the cytoplasm of HEK-293 cells and Swiss 3T3 fibroblasts¹¹⁵, where it was detected up to 1 h after its uptake. A nuclear localization of C-peptide in HEK-293 cells and Swiss 3T3 fibroblasts has also been demonstrated by the same group¹¹⁵. These findings demonstrate that once internalized in the cytoplasm, C-peptide is not rapidly degraded but remains intact, possibly interacting with sub-cellular components through which it might achieve its cellular effects.

The process of internalization from the cell surface and sub-cellular localization of C-peptide in target cells have not yet been investigated. In particular, it is not known whether C-peptide passively diffuses across the cellular membrane or whether it is actively translocated by a specific pathway of internalization, such as endocytosis. In this study, we investigated the hypothesis that C-peptide internalizes in target cells by following a specific endocytic pathway.

C-peptide internalization was explored in HAEC and UASMC, two important targets of C-peptide activity especially in the context of vascular dysfunction leading to vascular complications in type 1 diabetes^{107,110}. We found that in these cells C-peptide internalizes from the cellular surface within punctate structures, a majority of them co-localizing with early endosomes. A minority fraction of C-peptide vesicles, which increases with culture time, is localized within the lysosomes for degradation. These results demonstrate that C-peptide internalizes in target cells by using a specific endocytic pathway. Endosome localization of C-peptide would support the proposal that C-peptide might achieve its cellular effects in part by signaling from these organelles.

8.3 RESULTS

C-peptide internalization was explored in human endothelial and smooth muscle cells by using fluorescently-labeled C-peptide¹²⁵. In these cells, C-peptide internalizes to punctate structures localized at the level of the cellular membrane and in the cytoplasm (Figure 25). Internalization of C-peptide was minimal after 5 minutes, clearly detectable after 10 minutes, resulted in bright staining after 30 minutes, and internalization was completed by 1 hour.

Consistent with the cellular trafficking of proteins in general, the internalization of C-peptide was blocked at 4°C. (Figure 26a). Accordingly, C-peptide internalization slowly recovered when cells that were incubated at 4°C were placed back at 37°C (Figure 26b-c).

As shown in Figure 27b, pre-incubation of HAEC with 30-fold excess of unlabelled C-peptide blocked uptake of the fluorescent C-peptide probe as compared to cells incubated with AlexaFluor488-labelled C-peptide only (Figure 27a). On the contrary, pre-incubation of HAEC with a scrambled version of unlabelled C-peptide did not interfere with AlexaFluor488-labelled C-peptide internalization (Figure 27d).

C-peptide uses a clathrin-mediated endocytotic pathway to enter HAEC. Pre-treatment of HAEC with MDC (43µmol/L) for 30 min completely blocked uptake of AlexaFluor488-labelled C-peptide ($p < 0.01$ versus control) (Figure 28). By contrast, Filipin pre-treatment of HAEC for 30 min (5µg/mL) lacked nearly completely inhibitory effect on fluorescent C-peptide probe internalization (Figure 28e). MDC is a pharmacological inhibitor of receptor-mediated endocytosis,^{117,118} while Filipin, which binds cholesterol in the plasma membrane, impairs the invagination and subsequent internalization of caveolae.^{122,123}

The involvement of the cytoskeleton network in C-peptide endocytosis was studied in HAEC with Cytochalasin D (30µmol/L) and Nocodazole (10µmol/L), which act by inducing depolymerization of actin filaments and microtubules, respectively.^{25,126} As shown in Figure 28, uptake of AlexaFluor488-labelled C-peptide following Cytochalasin D treatment was not significantly different from control cells. Conversely, Nocodazole drastically reduced fluorescent C-peptide uptake ($p < 0.01$ versus control) suggesting that entry of C-peptide into HAEC was dependent on microtubule integrity.

To explore the possibility that C-peptide localizes in early endosomes, HAEC and UASMC were transduced with Organelle Lights™ Endosome-GFP reagent, which targets expression of fluorescent Rab5a, an early endosome-specific marker. Live-cells were then labelled with 1 $\mu\text{mol/l}$ AlexaFluor546-labelled C-peptide and imaged under a confocal microscope. As shown in Figure 29a, early endosomes appear as green punctate structures in the cytoplasm and close to the cellular membrane of an endothelial cell. Figure 29b shows internalization of AlexaFluor546-labelled C-peptide as red punctate staining inside the cytosol. When the two images were merged, a yellow staining is evident, corresponding to co-localization of the green, early endosomes, with the red, C-peptide (Figure 29c, see arrows). In the majority of cases the red staining corresponding to the internalized C-peptide probe is evidently contained inside the endosome structures, observed as a bright yellow peripheral staining around the central red staining of the vesicles (Figure 29c-d).

As an additional technique to demonstrate co-localization of C-peptide to endocytic organelles, we performed immunofluorescence studies on PFA-fixed HAEC after exposure to 10 nmol/L of C-peptide. As shown in Figure 30a, C-peptide internalizes in HAEC as green punctate structures, the majority of which localize with the red early endosomes (Figure 30b) identified with a monoclonal antibody to the early endosome antigen 1 (EEA1), resulting in a yellow staining (Figure 30c).

To isolate early endosomes, we briefly incubated UASMC with AlexaFluor546-labelled C-peptide together with AlexaFluor488-conjugated human transferrin, and then proceeded to cellular fractionation. High-speed centrifugation allows plasma membranes and other cellular compartments to sediment in the pellet, while clathrin-coated pits and early endosomes, which are relatively small molecules¹²⁰ (100-200nm), remain in the supernatant. By using a scanning fluorimeter, we quantified the fluorescence present in the endosome-containing supernatant of the homogenized cells. As shown in Figure 31, the mean fraction of the AlexaFluor488-transferrin fluorescence (peak emission at 516), in the endosome-containing supernatant was 0.86 ± 0.06 ($n = 3$). The mean fraction of AlexaFluor546-C-peptide (peak emission at 568), in the endosome-containing supernatant was $0.77 + 0.08$ ($n = 3$). The fraction of each probe in the supernatant versus pellet was significantly different ($p < 0.001$), whereas the fraction of transferrin

and C-peptide in the endosomal fraction were statistically indistinguishable ($p>0.05$). The cell fractionation results further support the internalization of C peptide into early endosomes.

A final destination of internalized peptides along the endocytic pathway includes the lysosomes, where proteolytic degradation occurs. To visualize lysosomes, cells were transduced with Organelle Lights™ Lysosome-GFP reagent, which targets the lysosome-specific protein Lamp1, before labeling the cells with fluorescent C-peptide. By live-cell confocal microscopy, we found that a fraction of green AlexaFluor488-labelled C-peptide vesicles (Figure 32a) co-localized with the red lysosomes (Figure 32b), observed as yellow staining (Figure 32c). The fraction of C-peptide co-localized with lysosomes increased with culture time. We did not find evidence of localization of fluorescent C-peptide in mitochondria of live HAEC and UASMC.

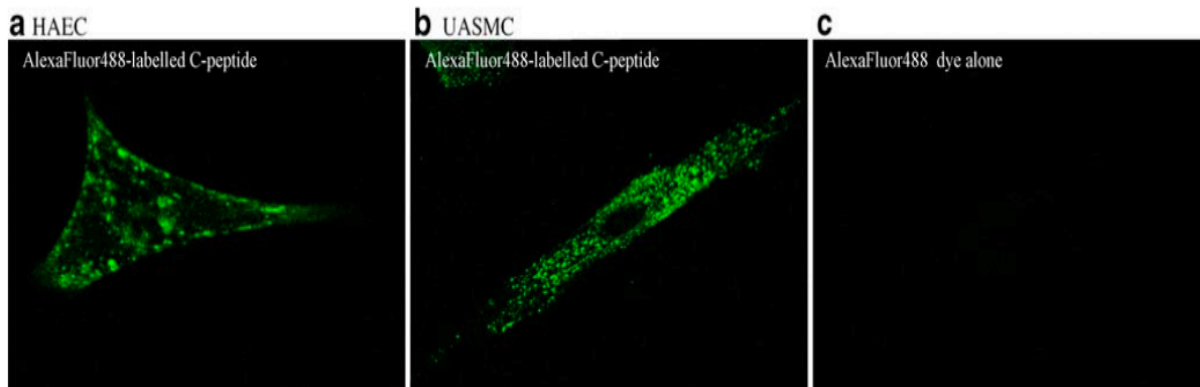


Figure 25. C-peptide internalizes in HAEC and UASMC as punctate structures. HAEC (a) and UASMC (b) were incubated for 30 min with 1 mmol/l AlexaFluor488-labelled C-peptide at 37°C, washed with medium and imaged by using confocal microscopy. The green punctate-staining corresponds to the C-peptide probe localized at the periphery of the cell and in the cytoplasm. In (c) as a control for the specificity of the staining, HAEC were incubated for 30 min with 1 mmol/l AlexaFluor488 dye at 37°C. Note the absence of green fluorescence staining. The Figure shows a representative z-section across one cell.

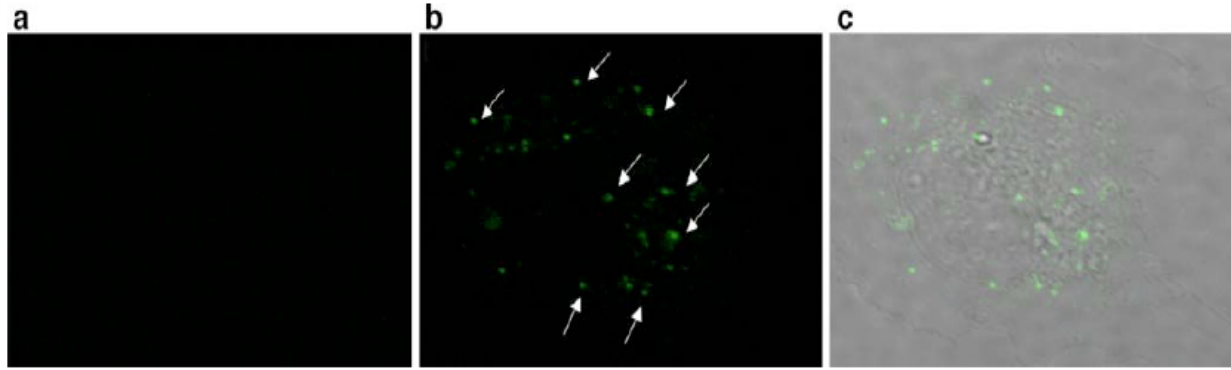


Figure 26. C-peptide internalisation is inhibited at 4°C. (a) HAEC were incubated for 30 min with 1 mmol/l Alexa Fluor 488-labelled Cpeptide at 4°C, washed, and immediately imaged by confocal microscopy. The figure shows absence of green fluorescence staining inside the cells, consistent with no internalisation of the probe. (b) Internalisation of green C-peptide probe slowly recovered when cells were put in the incubator at 37°C after being at 4°C. Arrows show examples of green punctate staining corresponding to the internalised C-peptide probe. (c) Differential interference contrast confocal image of the same z-section as in b merged with the fluorescence image to demonstrate localisation of green punctate staining in the cytoplasm.

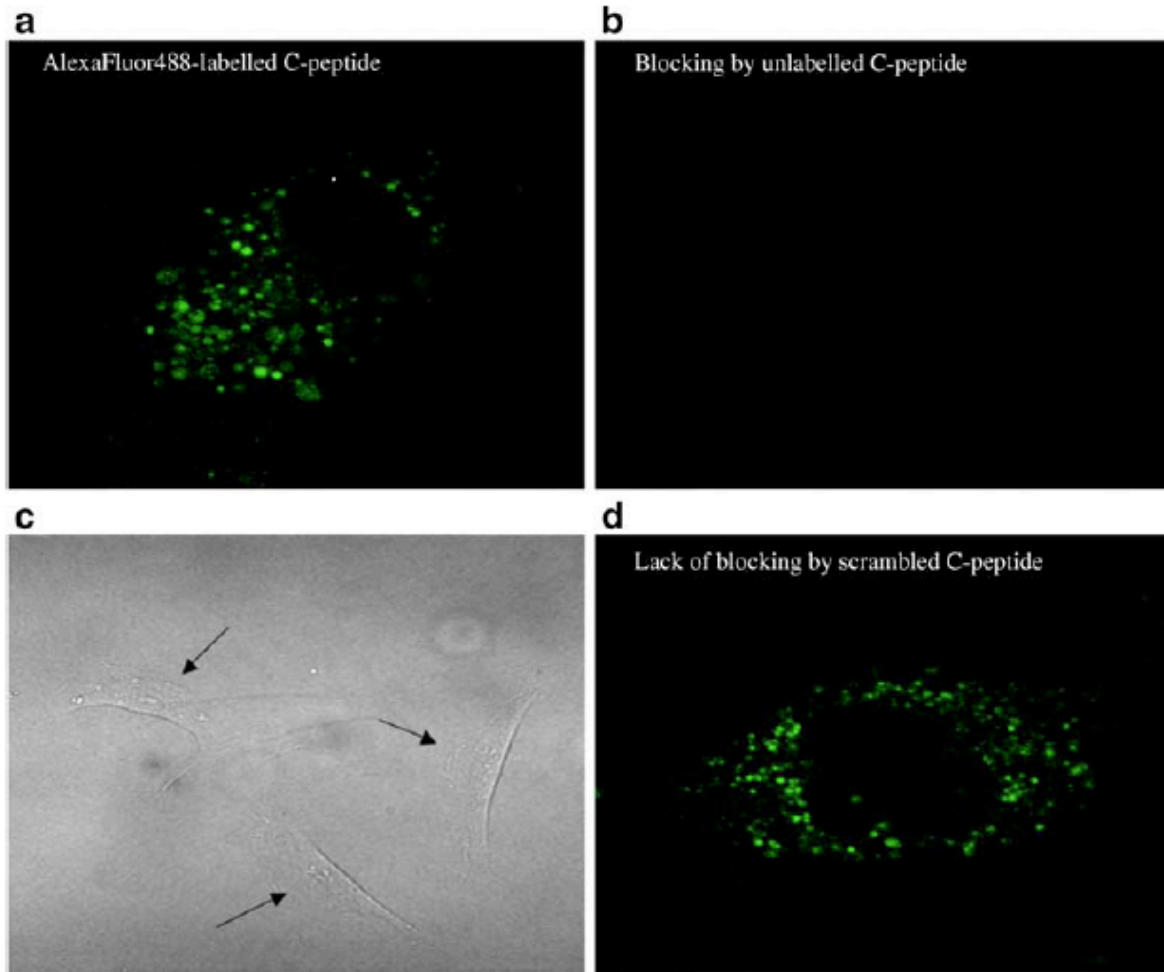


Figure 27. Alexa Fluor 488-labelled C-peptide internalisation is inhibited by an excess of unlabelled C-peptide. (a) HAEC were incubated for 30 min with 1 mmol/l Alexa Fluor 488-labelled C-peptide at 37°C, washed with medium, and immediately imaged by confocal microscopy. The figure shows green punctate staining inside the periphery and cytoplasm of the cell, consistent with internalisation of the probe. (b) Internalisation of the Alexa Fluor 488-labelled green C-peptide probe (1 mmol/l) was inhibited by preincubation with 30 mmol/l unlabelled C-peptide for 1 h at 37°C. (c) Differential interference contrast confocal image of the z-section shown in b. Arrows indicate examples of three different cells showing reduced green punctate staining in the cytoplasm. (d) Preincubation of cells with 30 mmol/l of a randomised version of C-peptide (scrambled C-peptide) did not affect internalisation of Alexa Fluor 488-labelled C-peptide, as demonstrated by the presence of green punctate staining inside the cytoplasm.

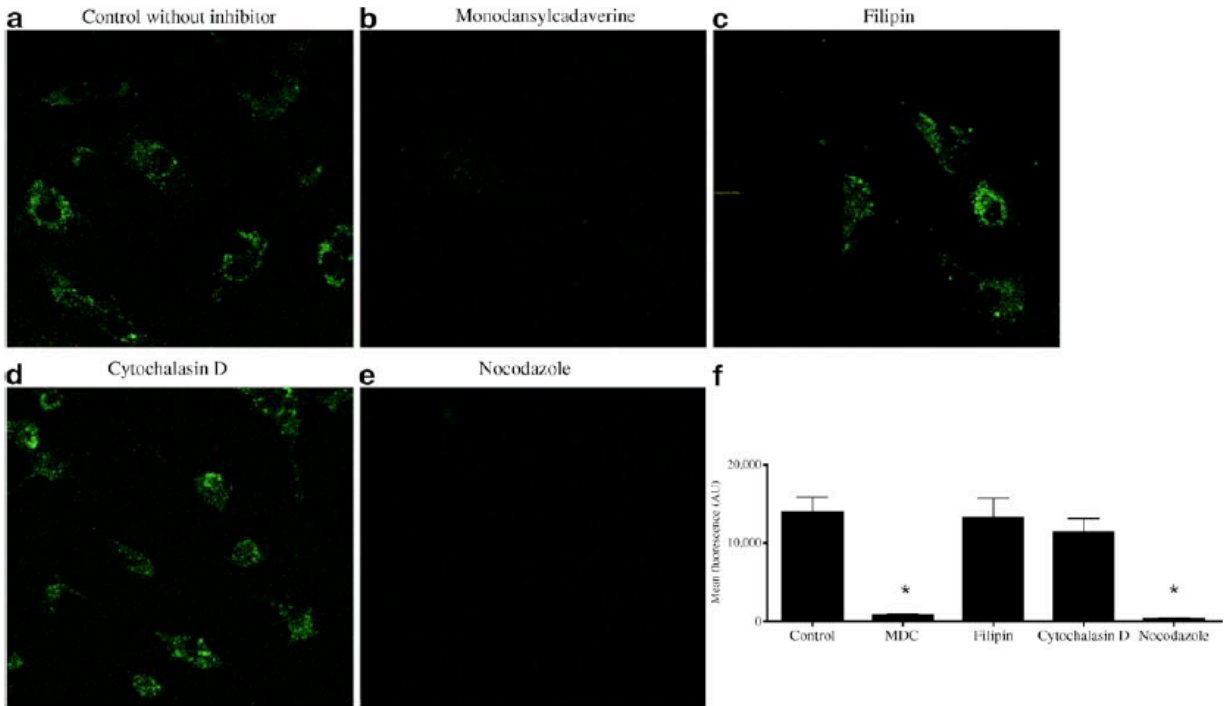


Figure 28. Effect of different pharmacological compounds on C-peptide entry into HAEC. Cells were either treated with 1 mmol/l Alexa Fluor488-labelled C-peptide for 30 min (control) or pretreated with the following compounds before addition of 1 mmol/l Alexa Fluor 488-labelled C-peptide: MDC (43 mmol/l), filipin (5 mg/ml), cytochalasin D (30 mmol/l) and nocodazole (10 mmol/l). As shown, pretreatment of HAEC with MDC, an inhibitor of clathrin-mediated endocytosis, inhibited entry of the C-peptide probe. Pretreatment with nocodazole, which prevents microtubule assembly, also impairs C-peptide internalisation. Filipin and cytochalasin D did not inhibit C-peptide internalisation. a–e Representative z-section across some endothelial cells. (f) The mean fluorescence (AU, arbitrary units) of Alexa Fluor 488-conjugated C-peptide internalisation measured in each experimental condition. The asterisk indicates that a significant decrease in uptake of fluorescent C-peptide was detected when HAEC were pretreated with MDC and nocodazole ($p < 0.01$ vs control cells)

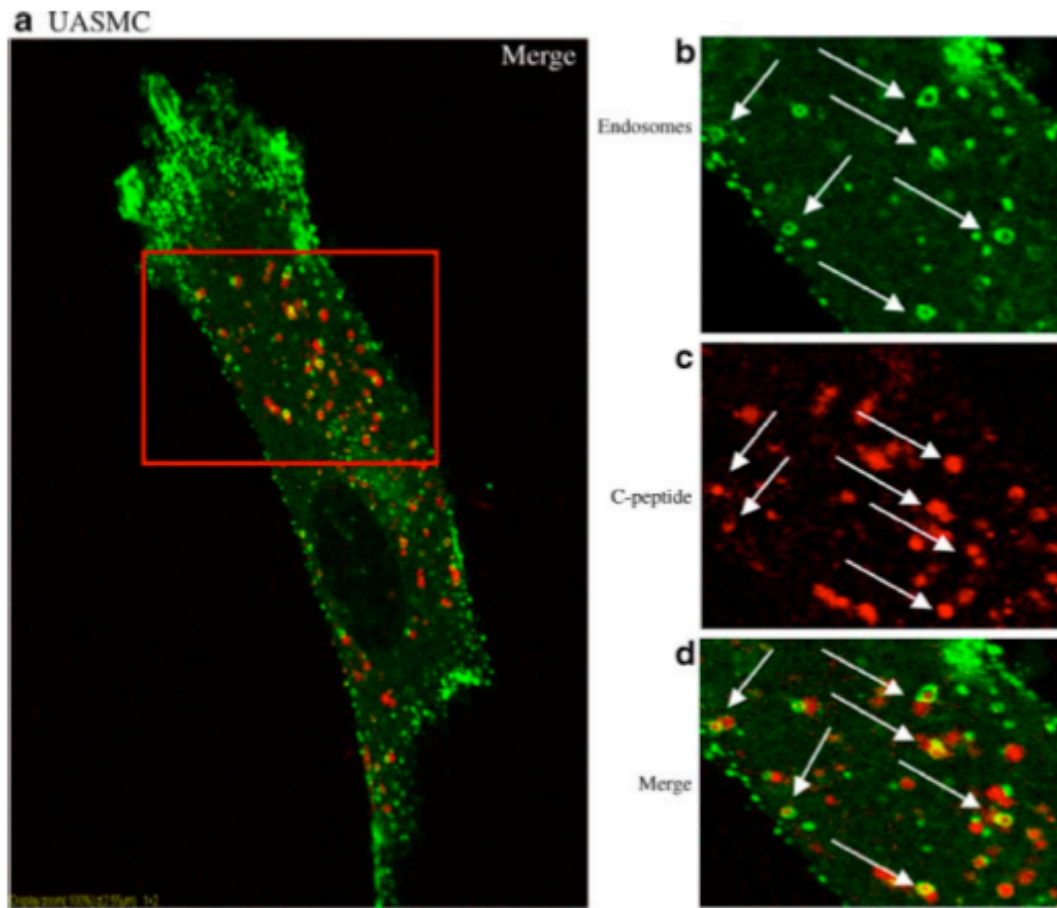


Figure 29. Internalized AlexaFluor546-labelled C-peptide co-localizes with early endosomes in UASMC. UASMC were transduced with Organelle Lights™ Endosomes-GFP, which induces expression of the fluorescent early endosomal marker Rab5a, and then incubated for 30 min with 1 mmol/l AlexaFluor546-labelled C-peptide at 37°C. After washing the cells with fresh medium, cells were imaged by confocal microscopy. In (a) the yellow staining corresponds to the merging of the green fluorescence (early endosomes) with the red fluorescence (C-peptide). In (b-d) images of part of the cell within the red quadrant. AlexaFluor546-labelled C-peptide co-localizes, or is in close proximity, with early endosomes (see arrows). Showing is one representative z-section across one smooth muscle cell.

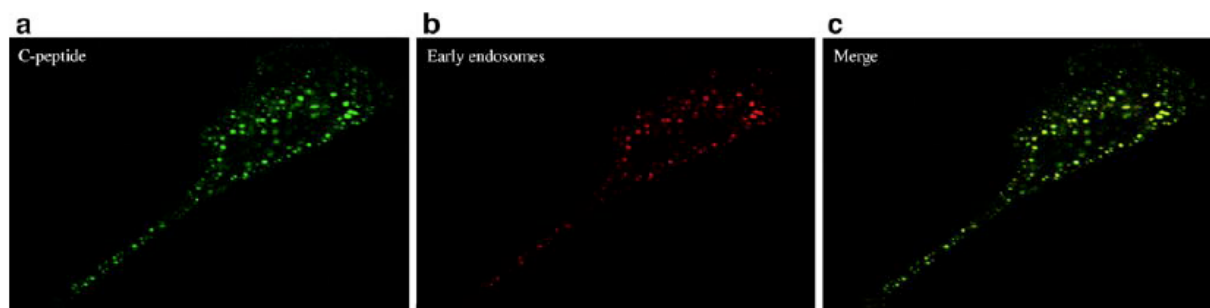


Figure 30. Immunohistochemistry of C-peptide internalisation and localization to early endosomes. HAEC were incubated for 3 h with 10 nmol/l C-peptide at 37°C. After fixation with paraformaldehyde, cells were incubated with rabbit anti-human antibody to C-peptide together with a mouse monoclonal antibody to the early endosome antigen 1 (EEA1) for 2 h and then with the appropriate secondary antibodies (see Methods). Cells were then washed and imaged by confocal microscopy. (a) Internalised C-peptide seen as green fluorescence vesicles. (b) Early endosomes, stained red. c Merging the two images shows colocalisation of most of the C-peptide with endosomes

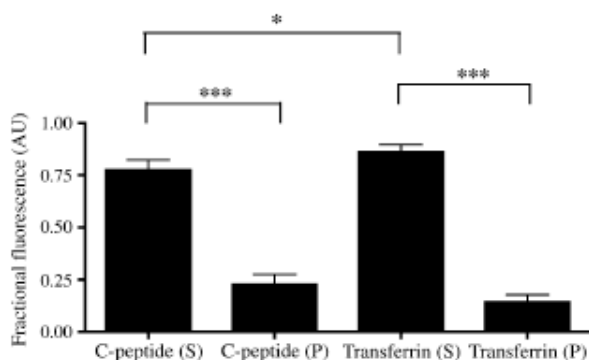


Figure 31. C-peptide co-localises with isolated early endosomes in UASMC. To identify early endosomes, we studied the internalization of Alexa Fluor 488-conjugated human transferrin, a specific marker of early endosomes, in the presence of Alexa Fluor 546-labelled Cpeptide in UASMC at 37°C, 5% CO₂ for 10 min. Endosomes were isolated from other subcellular compartments by high-speed centrifugation and an aliquot of both the pellet (P) and of the endosomecontaining supernatant fraction (S) was used to quantitate the AlexaFluor 488–transferrin and Alexa Fluor 546–C-peptide fluorescence spectra by using a scanning spectrofluorimeter. The fluorescence of each molecule was expressed as a fraction of the total for each probe. AU, arbitrary units. *p>0.05, ***p<0.001

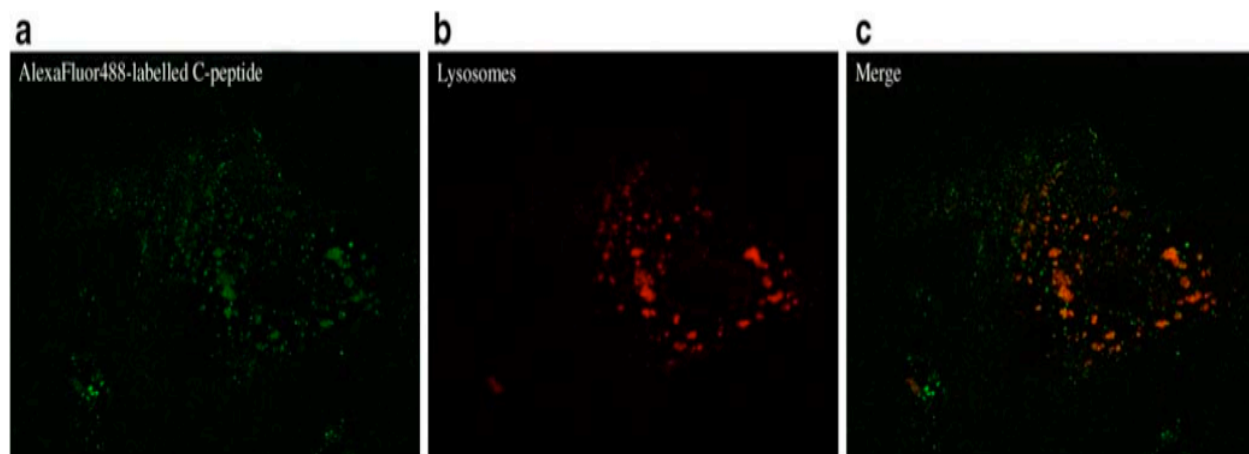


Figure 32. Internalized AlexaFluor488-labelled C-peptide traffics to lysosomes in UAMSC. UAMSC were transduced with Organelle Lights™ Lysosomes-RFP, which induces expression of fluorescent Lamp1 protein, a specific lysosomal marker. UAMSC were then incubated for 30 min with 1 mmol/l AlexaFluor488-labelled C-peptide at 37°C, washed with medium and imaged by using confocal microscopy. The yellow staining (c) corresponds to the merging of the green fluorescence (a; C-peptide) with the red fluorescence (b; Lysosomes) indicative of 82o-localization. The Figure shows images of a representative z-section across one vascular smooth muscle cell.

9.0 DISCUSSION

T1D is a well-known risk factor for both micro- and macro-vascular disease with inflammation and endothelial dysfunction being major contributors to this risk. Findings indicate that a generalized inflammatory response is already present in the very early stages of diabetes^{74,75}. Furthermore, T1D patients with microvascular complications exhibit increased production of inflammatory biomarkers, such as pro-inflammatory cytokines, over and above the levels detected in T1D patients without microvascular complications and healthy control subjects.^{68,71,77}

This risk is in part associated with the difficulty in maintaining euglycemic blood glucose conditions in the face of an appropriate exogenous insulin treatment.¹²⁷ Administration of recombinant insulin does not contain C-peptide, a product of insulin biosynthesis, which exerts beneficial effects on some of the microvascular complications associated with diabetes.¹²⁻¹⁴

In this study, we investigated the impact of human C-peptide specifically in the early process of atherogenesis in endothelial cells, vascular smooth muscle cells, and monocytes, three cellular target of vascular dysfunction. The few studies available on the topic, tested the effect of C-peptide on low and high glucose-induced proliferative activities of vascular smooth muscle cells, one major component involved in the formation of atherosclerotic plaque^{128,129}. Here, we wanted to expand these studies by evaluating the potential effects of C-peptide in all cellular components of the vessel wall - endothelial cells, smooth muscle cells, and immune cell during hyperglycemia-induced vascular insult.

The adhesion and migration of circulating monocytes into the subendothelial space is one of the key events in the early stages of atherogenesis¹³⁰. This process is in part regulated by the expression of adhesion molecules, such as VCAM-1, on the surface of endothelial cells,¹³¹ and by the release of chemotactic factors, including IL-8 and MCP-1¹³². We found that C-peptide exerts an inhibitory effect on high glucose-induced up-regulation of the adhesion molecule

VCAM-1 on HAEC *in vitro*. C-peptide at the physiological concentration of 0.5 nmol/L reduced high glucose-induced expression of VCAM-1 to basal levels observed under normal glucose conditions. The decrease in VCAM-1 expression induced by C-peptide on HAEC was detected both at the mRNA and protein levels. This result is in line with another study demonstrating that C-peptide reduces expression of the adhesion molecule P-selectin and ICAM-1 on the rat microvascular endothelium during acute endothelial dysfunction *in vivo*¹⁷. In another model of vascular injury, C-peptide was shown to decrease polymorphonuclear leukocyte infiltration into the myocardium and therefore improving cardiac dysfunction¹⁸. Overall, these data point to an anti-inflammatory effect of C-peptide on the endothelium in condition of insult. This hypothesis is supported by recent *in vivo* data showing that survival of mice following endotoxic shock is improved after C-peptide administration⁸. In these mice, plasma levels of the pro-inflammatory cytokines tumor necrosis factor(TNF)- α and MCP-1 were also decreased, suggesting a decreased inflammatory response⁸. In the context of T1D patients, endothelial dysfunction with upregulation of VCAM-1 and inflammatory changes of the vessel wall are early events in the course of the disease^{71,133-135}. These patients are insulin-dependent and take exogenous insulin to manage their blood glucose levels. It might well be that addition of physiological levels of C-peptide to the traditional exogenous insulin therapy could be beneficial as a means to “counteract” the negative effect of high glucose on the endothelial cells of the diabetic patients.

Another component of endothelial dysfunction that is affected by C-peptide is the secretion of the chemokines IL-8 and MCP-1 that facilitates endothelial cell interactions with circulating leukocytes. In support of other investigators^{91,136,137}, we observed an increased secretion of both chemokines in the supernatant of endothelial cells exposed to 25 mmol/L glucose. Unique to this study, however, is the finding that C-peptide reduced high glucose-stimulated IL-8 and MCP-1 secretion by endothelial cells to near or below the basal levels measured under normal glucose concentrations. In addition, adhesion of U-937 cells to endothelial cells stimulated with high glucose decreased after addition of C-peptide, an effect not detected when C-peptide was heat-inactivated. C-peptide at 0.5 nmol/L suppressed U-937 monocyte attachment to HAEC exposed to 25 mmol/L glucose by 50% due to a C-peptide-mediated inhibitory effect on VCAM-1, IL-8 and MCP-1 secretion by endothelial cells.

As predicted, another site of direct action of C-peptide are the U-937 cells. Previous studies from our laboratory⁷⁵ and others¹³⁷, have demonstrated that expression of several integrins, such as Mac-1 (CD11b), is increased on the surface of monocytes obtained from peripheral blood of T1D patients. Monocytes from these patients also show an increased adhesive capacity to endothelial cells *in vitro*^{75,137}. In this current study, we demonstrated that C-peptide reduces high glucose-stimulated secretion of IL-6, IL-8, MIP-1 α , and MIP-1 β from LPS-treated U-937 monocytes. Additionally, we observed that when C-peptide was added to 30mmol/L glucose, there were a decreased number of adherent monocytes as compared to high glucose alone. In low (5.6mmol/L) and intermediate (11 mmol/L) glucose conditions, C-peptide did not show any significant effects on the adherence of the treated U-937 monocyte to HAEC, thus suggesting that C-peptide exerts its most beneficial effects on the activated monocytes in conditions of insult from extreme hyperglycemia.

During the development of the atherosclerotic plaque, proliferating VSMCs migrate from the media into early atherosclerotic lesions, secrete pro-inflammatory mediators, up-regulate cell adhesion molecules, and promote synthesis of matrix molecules required for the retention of lipoproteins¹³⁸. In advanced human lesions, VSMCs and their secreted product constitutes up to 70 to 80% of the content of the atherosclerotic plaques. Moreover, there is evidence suggesting that VSMCs may also be important for the stability of the atherosclerotic plaque through a formation of a firm fibrous cap¹³⁹. Thus, the involvement of numerous VSMC functional abnormalities in diabetes, warrant the control of their proliferation to prevent diabetic complications.

In this study, we showed that short-term exposure to C-peptide inhibited excessive proliferation of UASMC and AoSMC induced by high glucose *in vitro*¹¹⁰. Although this evidence in human VSMC is reported here for the first time, a suppressive effect of C-peptide on glucose-induced proliferation of VSMCs has been previously described by Kobayashi *et al.* in a rat aortic smooth muscle cell line¹²⁸. Our and Kobayashi's results support the view that physiological concentrations of C-peptide may exert a protective action on VSMCs in conditions of hyperglycemia by targeting the excessive VSMC proliferation. This effect might be specific to conditions of hyperglycemia, as it was not detected under normal glucose. In fact, VSMC cultured in normal glucose in the presence of C-peptide showed an increased proliferation, a

result also reported by Walcher *et al.*¹²⁹. Based on these findings, it is tempting to speculate that C-peptide effects on proliferative activities of VSMCs *in vitro* is dependent on glucose concentrations in the culture medium, with stimulatory activity under normal glucose and inhibitory one in conditions of hyperglycemia.

The mechanisms underlying the effects of C-peptide on the human vasculature are still largely unknown. Nevertheless, the signal transduction pathways that lead to the enhanced gene expression of adhesion molecules and inflammatory cytokine secretion in endothelial cells and monocytes require the translocation of the transcription factor NF- κ B¹⁴⁰. Therefore, this study investigated C-peptide effects on NF- κ B activation in high glucose-stimulated model systems. In support of a previous study⁹¹, we confirmed that short-term high glucose exposure of endothelial cells stimulates NF- κ B activation, however, our work moves the paradigm forward by demonstrating that exogenous addition of C-peptide significantly reduced high glucose-induced nuclear translocation of canonical components of NF- κ B, p65 and p50. The suppressive effect on NF- κ B activation and high glucose-induced VCAM-1 expression and IL-8 and MCP-1 secretion in HAEC was specific for C-peptide since heat-inactivated C-peptide was not able to elicit the same phenotype. Similarly, our work demonstrates that exogenous addition of C-peptide significantly reduced high glucose-induced nuclear translocation of NF- κ B p65 and p50 subunits by reducing high glucose-induced phosphorylation of the cytoplasmic inhibitory protein I κ B α in VSMCs. The involvement of NF- κ B in VSMC proliferation in high glucose conditions is demonstrated by the fact that addition of PDTC and BAY 11-7082, two specific NF- κ B inhibitors, abolished UASMC and AoSMC proliferation *in vitro*. The inhibitory effects of PDTC and BAY 11-7082 were also tested on cytokines secretion on high glucose-stimulated HAEC.

In monocytes as well, C-peptide achieves its anti-inflammatory activity by leading to a reduction in NF- κ B activation. Western blot and ELISA analyses of nuclear extracts from LPS-treated U-937 cells exposed to high glucose showed a decreased nuclear translocation of NF- κ B p50 and p65 subunits through a decreased phosphorylation of the cytoplasmic inhibitory protein I κ B.

Although the exact mechanism by which C-peptide affects phosphorylation of I κ B is not known, one possible mechanism envisages that C-peptide turns off the cascade of

phosphorylation events ultimately leading to the activation of kinase proteins involved in the phosphorylation of the inhibitor protein I κ B. The phosphorylation cascade is carried through recruitment of several kinase proteins such as I κ B, IKK α and IKK β and it is initiated at the level of the plasma membrane after the binding of a ligand to a membrane receptor (e.g. Toll-like receptor). At which level of the phosphorylation cascade C-peptide might act is unknown.

Another NF- κ B dependent upstream event that could likely be affected by C-peptide is represented by ROS generation. High glucose damages endothelial cells by increasing ROS^{136, 141,142} and inducing apoptosis^{100,143}. Moreover, ROS are powerful cellular activators of the nuclear-factor(NF)- κ B pathway^{100,144-146}. We therefore examined the effect of C-peptide on high glucose-induced ROS generation as the mechanism underlying its beneficial effects on endothelial cell dysfunction and apoptosis.

We first assessed the level of apoptosis in condition of hyperglycaemia. We found that 24-h exposure to high glucose increased expression levels and activity of cleaved (activated) caspase-3, which was reduced by addition of C-peptide to HAEC *in vitro*. Moreover, expression levels of the anti-apoptotic molecule Bcl-2 were up-regulated by C-peptide as compared to high glucose alone in HAEC. Although this evidence in HAEC is reported here for the first time, a protective effect of C-peptide against apoptosis has been described in different models. Using human neuroblastoma SH-SY5Y cells, Li ZG *et al.* found that C-peptide reduced high glucose-induced apoptosis by promoting the expression of Bcl-2.

As expected, C-peptide reduced ROS generation, a crucial upstream signaling event in the NF- κ B pathway. The inhibitory effect of C-peptide on ROS generation in HAEC after overnight exposure to high glucose was observed immediately after the uptake of the dye and maintained overtime. By reducing ROS generation in HAEC, C-peptide reduces phosphorylation and degradation of the cytosolic NF- κ B inhibitor I κ B α , leading to a reduced nuclear translocation of the NF- κ B p50/p65 to the nucleus and reduced transcription of genes involved in inflammation and apoptosis. Moreover, we showed that C-peptide inhibits glucose-induced NAD(P)H oxidase activation, which is the major source of ROS in endothelial cells. This multi-component enzyme includes a membrane-bound cytochrome b₅₅₈, comprised of p22^{phox} and gp91^{phox} subunits, and the cytosolic adapter proteins p47^{phox} and p67^{phox} which are recruited to

the cytochrome during stimulation to form a catalytically active oxidase²³. Recruitment of p47^{phox} and p67^{phox} to the plasma membrane, requires presence of Rac-1, a member of the Rho family of small GTP-binding proteins, which complex with the cytosolic proteins to regulate NAD(P)H oxidase activity. In this study, we found that glucose-induced Rac-1 protein levels at the plasma membrane of HAEC was inhibited by treatment with C-peptide for 30 min *in vitro*. Glucose-induced Rac-1 GTP-ase activity was also reduced by C-peptide in HAEC. All together, our findings demonstrate that C-peptide reduces ROS generation in glucose-exposed HAEC by inhibiting Rac-1-dependent NAD(P)H oxidase activation.

Although there is a general consensus that C-peptide has physiological effects on several different cell types, the cell biology of C-peptide is for the most part unknown. In particular, it is not known how exactly C-peptides exerts intracellular activities in target cells. It was initially thought that C-peptide exerted its effect via nonchiral mechanisms rather than by binding to stereospecific receptors¹⁴⁸; though specific binding to cultured rat pancreatic beta cells was demonstrated earlier¹⁴⁹. More recently, specific binding of C-peptide to cellular membranes has been confirmed in several human cell types including human renal tubular cells, human fibroblast and saphenous vein endothelial cells^{106,150}. Furthermore, C-peptide binding reaches full saturation at 0.9 nM; thus in healthy subjects, receptor saturation is achieved already at physiologic levels¹⁰⁶. A specific C-peptide receptor has not been identified yet, although it is often suggested to be a G-protein-coupled receptor as deduced from effects of pertussis toxin^{106,151}.

C-peptide was shown to cross plasma membranes localizing in the cytoplasm of HEK-293 cells and Swiss 3T3 fibroblasts¹⁵¹, where it was detected up to 1 h after uptake of the peptide. A nuclear localization of C-peptide in HEK-293 cells and Swiss 3T3 fibroblasts has also been demonstrated by the same group¹⁵¹. These findings demonstrate that once internalized in the cytoplasm, C-peptide is not rapidly degraded but remains intact, possibly interacting with sub-cellular components through which it might achieve its cellular effects. Recently, C-peptide was detected in the nucleoli where it promoted transcription of genes encoding for ribosomal RNA¹⁵².

Given the lack of definitive knowledge on C-peptide cell biology, we investigated the process of internalization from the cell surface and sub-cellular localization of C-peptide in

target cells. In particular it was investigated whether C-peptide passively diffuses across the cellular membrane or whether it is actively translocated by a specific pathway of internalization, such as endocytosis. Our results showed that C-peptide binds to plasma membranes and internalizes in the cytoplasm of both cell types. The uptake of C-peptide was minimal after 5 min of incubation at 37°C with AlexaFluor488-labeled C-peptide probe and began to be clearly visible after 10 min. As a control for specificity of the staining, cells were incubated with the AlexaFluor488 fluorescent dye alone and this incubation resulted in the absence of staining¹²⁵. Further, when we tested whether C-peptide was directly translocated across the plasma membrane or whether it followed a vesicle-mediated pathway during internalization, we found that, the internalized C-peptide probe was evidently contained inside the endosome structures. C-peptide eventually trafficked to lysosomes in live HAEC and UASMC.

These findings indicate a process of C-peptide internalization from the cell surface within membrane-bound organelles of the endocytic pathway, and excluded direct translocation across the plasma membrane. Endosome localization of C-peptide would support the proposal that C-peptide might achieve its cellular effects in part by signaling from these organelles. Endosomes interact with a complex network of tubules and vesicles distributed throughout the cytoplasm interconnected by a tightly controlled transport system¹⁵³. In addition to their classical role as sorting stations for internalized activated receptor-peptides complexes on their way to lysosomal degradation, endosomes are emerging as crucial players in intracellular signaling¹⁵⁴. Examples of signaling endosomes are the ones associated with epidermal growth factor receptors (EGFRs) whose downstream signaling factors such as SHC-adaptor protein (SHC), growth factor receptor bound protein 2 (GRB2) and mammalian Son-of-sevenless (mSOS) were found not only on the plasma membrane but on early endosomes as well¹⁵⁵, suggesting that EGFR signaling continues in this compartment¹⁵⁶. Another example of signaling endosomes is the one associated with nerve growth factor (NGF) that was found bound to its activated receptor TrkA and phospholipase C- γ 1 (PLC- γ 1) in endocytic organelles⁴¹.

10.0 CONCLUSIONS

T1D patients lack physiological levels of insulin and C-peptide in their bloodstream due to the autoimmune destruction of their pancreatic beta cells. T1D patients are also at increased risk to develop both micro- and macro-vascular complications. Unfortunately, the standard of care for T1D patients is solely insulin-replacement therapy. Despite the recently published evidence of the beneficial effect of C-peptide replacement therapy on diabetes-associated vascular complications, C-peptide is not universally prescribed. In this study, we have presented the most updated findings showing that:

- C-peptide is internalized from the cell surface within early endosomes from which it affects intracellular signaling pathways;
- In a model of high glucose-induced vascular dysfunction, C-peptide reduces endothelial dysfunction and apoptosis in human aortic endothelial cells;
- C-peptide also reduces hyperglycaemia-induced proliferation in human vascular smooth muscle cells, a critical step in atherosclerosis;
- C-peptide reduces inflammatory cytokines secretion from human monocytes and inhibits their adherence to the activated endothelium;
- The molecular mechanism of C-peptide beneficial effects on the vasculature exposed to high glucose is through modulation of oxidative stress generation and downregulation of glucose-induced NF- κ B pathway.

Although there is still much to learn about the cell biology and specific mechanism(s) of action of C-peptide, C-peptide is emerging as a new molecule with therapeutic potential in the treatment of several diseases with a strong inflammatory component, such as sepsis, T1D and diabetes-associated vascular complications.

BIBLIOGRAPHY

1. Steiner DF, Cunningham D, Spigelman L, Aten B. Insulin biosynthesis: evidence for a precursor. *Science*. 1967;157:697-700.
2. Polonsky K, O'Meara N. Secretion and metabolism of insulin, proinsulin and C-peptide. In: DeGroot L, Jameson J, (eds). *Endocrinology*. WB Saunders, Philadelphia, 2001, pp. 697-711
3. Henriksson M, Nordling E, Melles E, Shafqat J, Stahlberg M, Ekberg K, et al. Separate functional features of proinsulin C-peptide. *Cell Mol Life Sci*. 2005; 62:1772-8
4. Kitabchi AE. Proinsulin and C-peptide: a review. *Metabolism*. 1977; 26:547-87
5. Polonsky KS, Rubenstein AH. C-peptide as a measure of the secretion and hepatic extraction of insulin. Pitfalls and limitations. *Diabetes*. 1984; 33:486- 94
6. Wahren J, Ekberg K, Jornvall H. C-peptide is a bioactive peptide. *Diabetologia*. 2007; 50, 503-509
7. Hills CE, Brunskill NJ. Intracellular signaling by C-peptide. *Exp Diab Res*. 2008; 635158.
8. Vish MG, Mangeshkar P, Piraino G, et al. Proinsulin C-peptide exerts beneficial effects in endotoxic shock in mice. *Critic Care Med*. 2007; 35, 1348-1355.
9. Libby P, Nathan DM, Abraham K, Brunzell JD, Fradkin JE, Haffner SM, et al. Report of the National Heart, Lung, and Blood Institute-National Institute of Diabetes and Digestive and Kidney Diseases Working Group on Cardiovascular Complications of Type 1 Diabetes Mellitus. *Circulation*. 2005;111:3489-93.
10. Zatz R, Brenner BM. Pathogenesis of diabetic microangiopathy. The hemodynamic view. *Am J Med*. 1986; 80:443-53.
11. Nathan DM. Long-term complications of diabetes mellitus. *N Engl J Med*.1993; 328:1676-85
12. Johansson BL, Borg K, Fernqvist-Forbes E. Beneficial effects of C-peptide on incipient nephropathy and neuropathy in patients with type 1 diabetes: a three-month study. *Diabet Med*. 2000; 17, 181-189.
13. Ekberg K, Brismar T, Johansson BL, Lindstrom P.C-Peptide replacement therapy and sensory nerve function in type 1 diabetic neuropathy. *Diabetes Care*. 2007; 30, 71-767.
14. Hansen A, Johansson BL, Wahren J, von Bibra H. C-peptide exerts beneficial effects on myocardial blood flow and function in patients with type 1 diabetes. *Diabetes*. 2002; 51:3077-30828.
15. Johansson BL, Wahren, J, Pernow J. C-peptide increases forearm blood flow in patients with type 1 diabetes via a nitric oxide-dependent mechanism. *Am J Physiol Endocrinol Metab*. 2003; 285, E864-8709.
16. Jensen T, Bjerre-Knudsen J, Feldt-Rasmussen B, Deckert T. Features of endothelial dysfunction in early diabetic nephropathy. *Lancet*. 1989;1:461-3
17. Scalia R, Coyle KM, Levin BL, Booth G, Lefer AM. C-peptide inhibits leukocyte endothelium interaction in the microcirculation during acute endothelial dysfunction. *FASEB J*. 2000;14:2357-236426.

18. Young LH, Ikeda Y, Scalia R, Lefer AM. C-peptide exerts cardioprotective effects in myocardial ischemia-reperfusion. *Am J Physiol Heart Circ Physiol.* 2000;279, H1453-459.
19. Nah DY, Rhee MY. The inflammatory response and cardiac repair after myocardial infarction. *Korean Circ J.* 2009;39(10), 393-398.
20. Sima AA, Zhang W, Kreipke CW, Rafols JA, Hoffman WH. Inflammation in Diabetic Encephalopathy is Prevented by C-Peptide. *Rev Diabet Stud.* 2009;6(1), 37-42.
21. Li ZG, Zhang W, Grunberger G, Sima A. Hippocampal neuronal apoptosis in type 1 diabetes. *Brain Res.* 2002;946(2), 221-231.
22. Sima AA, Li ZG. The effect of C-peptide on cognitive dysfunction and hippocampal apoptosis in type 1 diabetic rats. *Diabetes.* 2005;54(5), 1497-1505.
23. Ceriello A, dello Russo P, Amstad P, Cerrutti P. High glucose induces antioxidant enzymes in human endothelial cells in culture. *Diabetes.* 1996;45, 471-477.
24. Husebye H, Halaas O, Stenmark H, et al. Endocytic pathways regulate Toll-like receptor 4 signaling and link innate and adaptive immunity. *EMBO J.* 2006;25, 683-692.
25. Dodeller F, Gotar M, Huesken D, Iourhenko, V, Cenni B. The lysosomal transmembrane protein 9B regulates the activity of inflammatory signaling pathways. *J Biol Chem.* 2008;283, 21487-21494.
26. Sjöberg S, Gunnarsson R, Gjötterberg M, Lefvert AK, Persson A, Ostman J. Residual insulin production, glycaemic control and prevalence of microvascular lesions and polyneuropathy in long-term type 1 (insulin- dependent) diabetes mellitus. *Diabetologia.* 1987;30:208-13
27. Zerbini G, Mangili R, Luzi L. Higher post-absorptive C-peptide levels in Type 1 diabetic patients without renal complications. *Diabet Med.* 1999;16:1048
28. Panero F, Novelli G, Zucco C, Fornengo P, Perotto M, Segre O, et al. Fasting plasma C peptide and micro- and macrovascular complications in a large clinic-based cohort of type 1 diabetic patients. *Diabetes Care.* 2009;32:301- 5
29. Fiorina P, Folli F, Zerbini G, Maffi P, Gremizzi C, Di Carlo V, et al. Islet transplantation is associated with improvement of renal function among uremic patients with type I diabetes mellitus and kidney transplants. *J Am Soc Nephrol.* 2003;14:2150-8.
30. Fioretto P, Steffes MW, Sutherland DE, Goetz FC, Mauer M. Reversal of lesions of diabetic nephropathy after pancreas transplantation. *N Engl J Med.* 1998;339:69-75.
31. Bach JF. Insulin-dependent diabetes mellitus as an autoimmune disease. *Endocr Rev.* 1994; 15(4):516-42
32. Brownlee M. Biochemistry and molecular cell biology of diabetic complications. *Nature.* 2001; 414:813-20
33. Luppi P, Trucco M. Superantigens in insulin-dependent diabetes mellitus. *Springer Semin Immunopathol.* 1996;17(4):333-62
34. DIAMOND Project Group. Incidence and trends of childhood Type 1 diabetes worldwide 1990-1999. *Diabet Med.* 2006; 23(8):857-66
35. Borchers AT, Uibo R, Gershwin ME. The geoepidemiology of type 1 diabetes. *Autoimmunity Rev.* 2010; 9(5):A277-87
36. Redondo MJ, Rewers M, Yu L, Garg S, Pilcher CC, Elliott RB, Eisenbarth GS. Genetic determination of islet cell autoimmunity in monozygotic twin, dizygotic twin, and non-

- twin siblings of patients with type 1 diabetes: prospective twin study. *BMJ*. 1999; 318(7185):698-702.
37. Atkinson MA, Eisenbarth GS. Type 1 diabetes: new perspectives on disease pathogenesis and treatment. *Lancet*. 2001; 358(9277):221-9
 38. Todd JA. From genome to aetiology in a multifactorial disease, type 1 diabetes. *Bioessays*. 1999;21(2):164-74
 39. Singal DP, Blajchman MA. Histocompatibility (HL-A) antigens, lymphocytotoxic antibodies and tissue antibodies in patients with diabetes mellitus. *Diabetes*. 1973;22(6):429-32.
 40. Nerup J, Platz P, Andersen OO, Christy M, Lyngsoe J, Poulsen JE, Ryder LP, Nielsen LS, Thomsen M, Svejgaard A. *Lancet*. HL-A antigens and diabetes mellitus. 1974; 12;2(7885):864-6.
 41. Buzzetti R, Quattrocchi CC, Nisticò L. Dissecting the genetics of type 1 diabetes: relevance for familial clustering and differences in incidence. *Diabetes Metab Rev*. 1998;14(2):111-28
 42. Farid NR, Sampson L, Noel P, Barnard JM, Davis AJ, Hillman DA. HLA-D-related (DRw) antigens in juvenile diabetes mellitus. *Diabetes*. 1979; 28(6):552-7.
 43. Owerbach D, Lernmark A, Platz P, Ryder LP, Rask L, Peterson PA, Ludvigsson J. *Nature*. 1983; 303(5920):815-7.
 44. Thorsby E, Rønningen KS. Particular HLA-DQ molecules play a dominant role in determining susceptibility or resistance to type 1 (insulin-dependent) diabetes mellitus. *Diabetologia*.1993;36:371-7
 45. Erlich H, Valdes AM, Noble J, Carlson JA, Varney M, Concannon P, Mychaleckyj JC, Todd JA, Bonella P, Fear AL, Lavant E, Louey A, Moonsamy P; Type 1 Diabetes Genetics Consortium. HLA DR-DQ haplotypes and genotypes and type 1 diabetes risk: analysis of the type 1 diabetes genetics consortium families. *Diabetes*. 2008;57(4):1084-92
 46. Morel PA, Dorman JS, Todd JA, McDevitt HO, Trucco M. Aspartic acid at position 57 of the HLA-DQ beta chain protects against type I diabetes: a family study. *Proc Natl Acad Sci U S A*. 1988;85:8111-5.
 47. Lernmark A, Ott J. Sometimes it's hot, sometimes it's not. *Nat Genet*. 1998;19(3):213-4.
 48. Julier C, Hyer RN, Davies J, Merlin F, Soularue P, Briant L, Cathelineau G, Deschamps I, Rotter JI, Froguel P, et al. Insulin-IGF2 region on chromosome 11p encodes a gene implicated in HLA-DR4-dependent diabetes susceptibility. *Nature*. 1991;354(6349):155-9.
 49. Kennedy GC, German MS, Rutter WJ. The minisatellite in the diabetes susceptibility locus IDDM2 regulates insulin transcription. *Nat Genet*. 1995;9(3):293-8.
 50. Nisticò L, Buzzetti R, Pritchard LE, Van der Auwera B, Giovannini C, et al. The CTLA-4 gene region of chromosome 2q33 is linked to, and associated with, type 1 diabetes. Belgian Diabetes Registry. *Hum Mol Genet*. 1996 Jul;5(7):1075-80.
 51. Vaidya B, Pearce SH, Charlton S, Marshall N, Rowan AD, et al. An association between the CTLA4 exon 1 polymorphism and early rheumatoid arthritis with autoimmune endocrinopathies. *Rheumatology (Oxford)*. 2002;41(2):180-3.

52. Barreto M, Santos E, Ferreira R, Fesel C, Fontes MF, et al. Evidence for CTLA4 as a susceptibility gene for systemic lupus erythematosus. *Eur J Hum Genet.* 2004;12(8):620-6.
53. Mäurer M, Ponath A, Kruse N, Rieckmann P. CTLA4 exon 1 dimorphism is associated with primary progressive multiple sclerosis. *J Neuroimmunol.* 2002;131(1-2):213-5.
54. Lowe CE, Cooper JD, Brusko T, Walker NM, Smyth DJ, Bailey R, Bourget K, Plagnol V, Field S, Atkinson M, Clayton DG, Wicker LS, Todd JA. Large-scale genetic fine mapping and genotype-phenotype associations implicate polymorphism in the IL2RA region in type 1 diabetes. *Nat Genet.* 2007;39(9):1074-82.
55. Bottini N, Musumeci L, Alonso A, Rahmouni S, Nika K, et al. A functional variant of lymphoid tyrosine phosphatase is associated with type I diabetes. *Nat Genet.* 2004;36(4):337-8
56. Zimmet PZ, Elliott RB, Mackay IR, Tuomi T, Rowley MJ, Pilcher CC, Knowles WJ. Autoantibodies to glutamic acid decarboxylase and insulin in islet cell antibody positive presymptomatic type 1 diabetes mellitus: frequency and segregation by age and gender. *Diabet Med.* 1994; 11(9):866-71.
57. Patterson CC, Dahlquist GG, Gyürüs E, Green A, Soltész G; EURODIAB Study Group. Incidence trends for childhood type 1 diabetes in Europe during 1989-2003 and predicted new cases 2005-20: a multicentre prospective registration study. *Lancet.* 2009;13;373(9680):2027-33
58. Eehalt S, Dietz K, Willasch AM, Neu A; Baden-Württemberg Diabetes Incidence Registry (DIARY) Group. Epidemiological perspectives on type 1 diabetes in childhood and adolescence in germany: 20 years of the Baden-württemberg Diabetes Incidence Registry (DIARY). *Diabetes Care.* 2010;33(2):338-40.
59. Eisenbarth GS. Type I diabetes mellitus. A chronic autoimmune disease. *N Engl J Med.* 1986; 314:1360-8.
60. Conrad B, Weidmann E, Trucco G, Rudert WA, Behboo R, Ricordi C, et al. Evidence for superantigen involvement in insulin-dependent diabetes mellitus aetiology. *Nature.* 1994; 371:351-5.
61. Goodier MR, Nawroly N, Beyan H, Hawa M, Leslie RD, Londei M. Identical twins discordant for type 1 diabetes show a different pattern of in vitro CD56+ cell activation. *Diabetes Metab Res Rev.* 2006; 22:367-75.
62. Wilson SB, Kent SC, Patton KT, Orban T, Jackson RA, Exley M, et al. Extreme Th1 bias of invariant Valpha24JalphaQ T cells in type 1 diabetes. *Nature.* 1998; 391:177-81.
63. Adler T, Akiyama H, Herder C, Kolb H, Burkart V. Heat shock protein 60 elicits abnormal response in macrophages of diabetes-prone non-obese diabetic mice. *Biochem Biophys Res Commun.* 2002; 294:592-6.
64. Beyan H, Goodier MR, Nawroly NS, Hawa MI, Bustin SA, Ogunkolade WB, et al. Altered monocyte cyclooxygenase response to lipopolysaccharide in type 1 diabetes. *Diabetes.* 2006;55:3439-45.
65. Kolb-Bachofen V, Kolb H. A role for macrophages in the pathogenesis of type 1 diabetes. *Autoimmunity.* 1989; 3:145-54.

66. Hanenberg H, Kolb-Bachofen V, Kantwerk-Funke G, Kolb H. Macrophage infiltration precedes and is a prerequisite for lymphocytic insulinitis in pancreatic islets of pre-diabetic BB rats. *Diabetologia*. 1989; 32:126-34.
67. Eizirik DL, Colli ML, Ortis F. The role of inflammation in insulinitis and beta-cell loss in type 1 diabetes. *Nat Rev Endocrinol*. 2009;5:219-26.
68. Schalkwijk CG, Poland DC, van Dijk W, Kok A, Emeis JJ, Drager AM, et al. Plasma concentration of C-reactive protein is increased in type I diabetic patients without clinical macroangiopathy and correlates with markers of endothelial dysfunction: evidence for chronic inflammation. *Diabetologia*. 1999;42:351-7.
69. Kilpatrick ES, Keevil BG, Jagger C, Spooner RJ, Small M. Determinants of raised C-reactive protein concentration in type 1 diabetes. *QJM*. 2000;93:231- 6.
70. Lechleitner M, Koch T, Herold M, Dzien A, Hoppichler F. Tumour necrosis factor-alpha plasma level in patients with type 1 diabetes mellitus and its association with glycaemic control and cardiovascular risk factors. *J Intern Med*. 2000; 248:67-76.
71. Devaraj S, Cheung AT, Jialal I, Griffen SC, Nguyen D, Glaser N, et al. Evidence of increased inflammation and microcirculatory abnormalities in patients with type 1 diabetes and their role in microvascular complications. *Diabetes*. 2007; 56:2790-6.
72. Devaraj S, Glaser N, Griffen S, Wang-Polagruto J, Miguelino E, Jialal I. Increased monocytic activity and biomarkers of inflammation in patients with type 1 diabetes. *Diabetes*. 2006; 55:774-9.
73. Plesner A, Greenbaum CJ, Gaur LK, Ernst RK, Lernmark A. Macrophages from high-risk HLA-DQB1*0201/*0302 type 1 diabetes mellitus patients are hypersensitive to lipopolysaccharide stimulation. *Scand J Immunol*. 2002; 56:522-9.
74. Erbagci AB, Tarakcioglu M, Coskun Y, Sivasli E, Sibel Namiduru E. Mediators of inflammation in children with type I diabetes mellitus: cytokines in type I diabetic children. *Clin Biochem*. 2001; 34:645-50.
75. Cifarelli V, Libman IM, Deluca A, Becker D, Trucco M, Luppi P. Increased Expression of Monocyte CD11b (Mac-1) in Overweight Recent-Onset Type 1 Diabetic Children. *Rev Diabet Stud*. 2007; 4:112-7.
76. Litherland SA, Xie XT, Hutson AD, Wasserfall C, Whittaker DS, She JX, et al. Aberrant prostaglandin synthase 2 expression defines an antigen-presenting cell defect for insulin-dependent diabetes mellitus. *J Clin Invest*. 1999;104:515-23.
77. Schram MT, Chaturvedi N, Schalkwijk C, Giorgino F, Ebeling P, Fuller JH, et al. Vascular risk factors and markers of endothelial function as determinants of inflammatory markers in type 1 diabetes: the EURODIAB Prospective Complications Study. *Diabetes Care*. 2003;26:2165-73.
78. Saraheimo M, Teppo AM, Forsblom C, Fagerudd J, Groop PH. Diabetic nephropathy is associated with low-grade inflammation in Type 1 diabetic patients. *Diabetologia*. 2003; 46:1402-7.
79. Schalkwijk CG, Ter Wee PM, Stehouwer CD. Plasma levels of AGE peptides in type 1 diabetic patients are associated with serum creatinine and not with albumin excretion rate: possible role of AGE peptide-associated endothelial dysfunction. *Ann N Y Acad Sci*. 2005; 1043:662-70.

80. Schmidt AM, Hori O, Chen JX, Li JF, Crandall J, Zhang J, et al. Advanced glycation endproducts interacting with their endothelial receptor induce expression of vascular cell adhesion molecule-1 (VCAM-1) in cultured human endothelial cells and in mice. A potential mechanism for the accelerated vasculopathy of diabetes. *J Clin Invest.* 1995; 96:1395-403.
81. Yoder, M.C. Is endothelium the origin of endothelial progenitor cells? *Atheroscler Thromb Vasc Biol.* 2010; 30, 1094-1103.
82. Versari D, Daghini E, Viridis A, Ghiadoni L, Taddei S. Endothelial dysfunction as target for prevention of cardiovascular disease. *Diabetes Care.* 2009;S314-321.
83. Hartge MM, Kintscher U, Unger T. Endothelial dysfunction and its role in diabetic vascular disease. *Endocrinol Metab Clin North Am.* 2006; 35:551-560.
84. Widlansky ME, Gokce N, Keaney JF Jr; Vita, J.A. The clinical implication of endothelial dysfunction. *J Am Coll Cardiol.* 2003; 42,1149-1160.
85. Monnink SH, van Haelst PL, van Boven AJ, Stroes, et al. Endothelial dysfunction in patients with coronary artery disease: a comparison of three frequently reported tests. *J Investig Med.* 2002; 50, 19-24.
86. Bolton CH, Downs LG, Victory JG, et al. Endothelial dysfunction in chronic renal failure: roles of lipoprotein oxidation and pro-inflammatory cytokines. *Nephrol Dial Transplant.* 2001; 16,1189-1197.
87. Rizzoni D, Porteri E, Guelfi D, Muiesan ML, et al. Structural alterations in subcutaneous small arteries of normotensive and hypertensive patients with non-insulin-dependent diabetes mellitus. *Circulation.* 2001;103, 1238-1244.
88. Endemann DH, Pu Q, De Ciuceis C, Savoia C, et al. Persistent remodeling of resistance arteries in type 2 diabetic patients on antihypertensive treatment. *Hypertension.* 2004; 43,399-404.
89. Viridis A, Ghiadoni L, Cardinal H, Favilla S, et al. Mechanisms responsible for endothelial dysfunction induced by fasting hyperhomocystinemia in normotensive subjects and patients with essential hypertension. *J Am Coll Cardiol.* 2001;38, 1106-1115.
90. Green DJ, Walsh JH, Maiorana A, Best MJ, Taylor RR, O'Driscoll JG. Exercise-induced improvement in endothelial dysfunction is not mediated by changes in CV risk factors: pooled analysis of diverse patient populations. *Am J Physiol Heart Circ Physiol.* 2003;285, H2679-2687.
91. Piga R, Naito Y, Kokura S, Handa O, Yoshikawa T. Short-term high glucose exposure induces monocyte-endothelial cells adhesion and transmigration by increasing VCAM-1 and MCP-1 expression in human aortic endothelial cells. *Atherosclerosis.* 2007, 193, 328-334.
92. Johnstone MT, Creager SJ, Scales KM, Cusco JA, Lee BK, Creager MA. Impaired endothelium-dependent vasodilation in patients with insulin-dependent diabetes mellitus. *Circulation.* 1993;88, 2510-2516.
93. Harrison DG. Cellular and molecular mechanisms of endothelial cell dysfunction. *J Clin Invest.* 1997; 100, 2153-2157.
94. Duh E, Aiello LP. Vascular endothelial growth factor and diabetes: the agonist versus antagonist paradox. *Diabetes.* 1999; 48, 1899-1906.

95. Gerszten RE, Garcia-Zepeda EA, Lim YC, et al. MCP-1 and IL-18 trigger firm adhesion of monocytes to vascular endothelium under flow conditions. *Nature*. 1999; 398:718-723.
96. Wilcox JN, Nelken NA, Coughlin SR, Gordon D, Schall TJ. Local expression of inflammatory cytokines in human atherosclerotic plaques. *J Atheroscler Thromb*. 1994; 1, S10-S13.
97. Flier JS. Diabetes: the missing link with obesity? *Nature*. 2001;409, 292-293.
98. Ceolotto G, Gallo A, Papparella I, Franco L, et al. Rosiglitazone reduces glucose-induced oxidative stress mediated by NAD(P)H oxidase via AMPK-dependent mechanism. *Arterioscler Thromb Vasc Biol*. 2007; 27(12), 2627-2633.
99. Cohen RA. Dysfunction of vascular endothelium in diabetes mellitus. *Circulation*. 1993; 87 [Suppl 5], 67-76.
100. Du XL Sui GZ, Stockklauser-Färber K.; Weiss M, et al. Induction of apoptosis by high proinsulin and glucose in cultured human umbilical vein endothelial cells is mediated by reactive oxygen species. *Diabetologia*. 1998; 41, 249-256.
101. Barchowsky A, Munro SR, Morana SJ, Vincenti MP. Treadwell, M. Oxidant-sensitive and phosphorylation-dependent activation of NF-kappa B and AP-1 in endothelial cells. *Am J Physiol*. 1995; 269(6 Pt 1), L829-836.
102. Janssen-Heininger YM, Poynter ME, Baeuerle PA. Recent advances towards understanding redox mechanisms in the activation of nuclear factor kappaB. *Free Radic Biol Med*. 2000; 28(9), 1317-1327.
103. Nishikawa T, Eldestein D, Dux XL, Yamagishi S, et al. Normalizing mitochondrial superoxide production blocks three pathways of hyperglycaemic damage. *Nature*. 2000; 404, 787-790.
104. Martin-Gallan P, Carrascosa A, Gussinye M, Dominguez C. Biomarkers of diabetes-associated oxidative stress and antioxidant status in young diabetic patients with or without subclinical complications. *Free Radic Biol Med*. 2003;15, 34(12), 1563-1574.
105. Dandona P, Thusu K, Cook S, Snyder B, Makowski J, Armstrong D, Nicotera T. Oxidative damage to DNA in diabetes mellitus. *Lancet*. 1996;347(8999), 444-445.
106. Rigler R, Pramanik A, Jonasson P, et al. Specific binding of proinsulin C-peptide to human cell membranes. *Proc Natl Acad Sci*. 1999; 96:13318–13323
107. Luppi P, Cifarelli V, Tse H, Piganelli J, Trucco M. Human C-peptide antagonises high glucose-induced endothelial dysfunction through the nuclear factor-kappaB pathway. *Diabetologia*. 2008;51:1534-43
108. Grabner R, Till U, Heller R. Flow cytometric determination of E-selectin, Vascular cell adhesion molecule-1, and intercellular cell adhesion molecule-1 in formaldehyde-fixed endothelial cell monolayers. *Cytometry*. 2000; 40:238–244
109. Tse HM, Milton MJ, Piganelli JD. Mechanistic analysis of the immunomodulatory effects of a catalytic antioxidant on antigen-presenting cells: implication for their use in targeting oxidation-reduction reactions in innate immunity. *Free Radic Biol Med*. 2004; 36:233–247
110. Cifarelli V, Luppi P, Tse HM, He J, Piganelli J, Trucco M. Human proinsulin C-peptide reduces high glucose-induced proliferation and NF-kappaB activation in vascular smooth muscle cells. *Atherosclerosis*. 2008; 201:248-57.

111. Natarajan R, Gonzales N, Xu L, Nadler JL. Vascular smooth muscle cells exhibit increased growth in response to elevated glucose. *Biochem Biophys Res Commun.* 1992;187:552-560.
112. Graier WF, Grubenthal I, Dittrich P, Wascher TC, Kostner GM. Intracellular mechanism of high D-glucose-induced modulation of vascular cell proliferation. *Eur J Pharm* 1995;294:221-9.
113. Mustapha NM, Tarr JM, Kohner EM, Chibber R. NADPH Oxidase versus Mitochondria-Derived ROS in Glucose-Induced Apoptosis of Pericytes in Early Diabetic Retinopathy. *J Ophthalmol.* 2010;2010:746978
114. Zhao X, Carnevale KA, Cathcart MK. Human monocytes use Rac1, not Rac2, in the NADPH oxidase complex. *J Biol Chem.* 2003;278(42):40788-92.
115. Lindahal E, Nyman U, Melles E, et al. Cellular internalization of proinsulin C-peptide. *Cell Mol Life Sci.* 2007;64:479-486
116. Bradley JR, Johnson DR, Pober JS. Four different classes of inhibitors of receptor-mediated endocytosis decrease tumor necrosis factor-induced gene expression in human endothelial cells. *J Immunol.* 1993;150:5544-5555
117. Schutze S, Machleidt T, Adam D, et al. Inhibition of receptor internalization by monodansylcadaverine selectively blocks p55 tumor necrosis factor receptor death domain signaling. *J Biol Chem.* 1999; 274(15):10203-10212
118. Inal J, Miot S, Schifferli JA. The complement inhibitor, CRIT, undergoes clathrin-dependent endocytosis. *Exp Cell Res.* 2005;310:54-65
119. Uriarte SM, Jog NR, Luerman GC, Bhimani S, Ward RA, Mcleish KR. Counter-regulation of clathrin-mediated endocytosis by the actin and microtubular cytoskeleton in human neutrophils. *Am J Physiol Cell Physiol.* 2009; 296:C857-C867
120. Acosta EG, Castilla V, Damonte EB. Functional entry of dengue virus into *Aedes albopictus* mosquito cells is dependent on clathrin-mediated endocytosis. *J Gen Virol.* 2008; 89:474-484
121. Holroyd C, Kistner U, Annaert W, Jahn R. Fusion of endosomes involved in synaptic vesicle recycling. *Mol Biol Cell.* 1999; 10:3035-3044
122. Rothberg KG, Ying Y-S, Kamen BA, Anderson RG. Cholesterol controls the clustering of the glycopospholipidanchored membrane receptor for 5-methyltetrahydrofolate. *J Cell Biol.* 1990; 111:2931-2938
123. Schnitzer JE, Oh P, Pinney E, Allard J. Filipin-sensitive caveolae-mediated transport in endothelium: reduced transcytosis, scavenger endocytosis, and capillary permeability of selected macromolecules. *J Cell Biol.* 1994;127:1217-1232
124. Vasquez RJ, Howell B, Yvon AM, Wadsworth P, Cassimeris L. Nanomolar concentrations of nocodazole alter microtubule dynamic instability in vivo and in vitro. *Mol Biol Cell.* 1997; 8:973-985
125. Luppi, P.; Geng, X.; Cifarelli, V.; Drain, P.; Trucco, M. C-peptide is internalised in human endothelial and vascular smooth muscle cells via early endosomes. *Diabetologia.* 2009; 52, 2218-2228.
126. Meyer JA, Froelich JM, Reid GE, Karunarathne WK, Spence DM. Metal-activated C-peptide facilitate glucose clearance and the release of a nitric oxide stimulus via the GLUT1 transporter. *Diabetologia.* 2008; 51:175-182

127. Diabetes Control and Complications Trial Research Group. The effect of intensive treatment of diabetes on the development and progression of long-term complications in insulin-dependent diabetes mellitus. *N Engl J Med.* 1993;329:977-986
128. Kobayashi Y, Naruse K, Hamada Y, et al. Human proinsulin C-peptide prevents proliferation of rat aortic smooth muscle cells cultured in high-glucose conditions. *Diabetologia.* 2005; 48:2396-2401
129. Walcher D, Babiak C, Poletek P, et al. C-peptide induces vascular smooth muscle cell proliferation: Involvement of Src-Kinase, Phosphatidylinositol 3-Kinase, and Extracellular Signal-Regulated Kinase ½. *Circulation Res.* 2006; 99:1181-1187
130. Gerrity RG. The role of the monocyte in atherogenesis: II. Migration of foam cells from atherosclerotic lesions. *Am J Pathol.* 1981; 103:191-200
131. Dansky HM, Barlow CB, Lominska C, et al. Adhesion of monocytes to arterial endothelium and initiation of atherosclerosis are critically dependent on vascular cell adhesion molecule-1 gene dosage. *Arterioscler Thromb Vasc Biol.* 2001; 21:1662-1667
132. Gerszten RE, Garcia-Zepeda EA, Lim Y-C, et al. MCP-1 and IL-8 trigger firm adhesion of monocytes to vascular endothelium under flow conditions. *Nature.* 1999; 398:718-723
133. Jarvisalo MJ, Raitakari M, Toikka JO, et al. Endothelial dysfunction and increased arterial intima-media thickness in children with type 1 diabetes. *Circulation.* 2004; 109:1750-1755
134. Elhadd TA, Kennedy G, Hill A, et al. Abnormal markers of endothelial cell activation and oxidative stress in children adolescents and young adults with type 1 diabetes with no clinical vascular disease. *Diabetes Metab Res Rev.* 1999;15: 405-411
135. Toivonen A, Kulmala P, Savola K, Akerblom HK, Knip M. The Childhood Diabetes In Finland. Soluble adhesion molecules in preclinical Type 1 diabetes. The Childhood Diabetes in Finland Study Group. *Pediatric Research.* 2001; 49: 24-29
136. Srinivasan S, Yeh M, Danzinger EC, et al. Glucose regulates monocyte adhesion through endothelial production of interleukin-8. *Cir Res.* 2003; 92(4):371-377
137. Haubner F, Lehle K, Munzel D, Schmid C, Birnbaum DE, Preuner JG. Hyperglycemia increases the levels of vascular cellular adhesion molecule-1 and monocyte-chemoattractant-protein-1 in the diabetic endothelial cell. *Biochem Bioph Res Commun.* 2007;360:560-565
138. Ross R. Atherosclerosis-an inflammatory disease. *N Engl J Med.* 1999;340:115-26
139. Clarke MC, Figg N, Maguire JJ, et al. Apoptosis of vascular smooth muscle cells induces features of plaque vulnerability in atherosclerosis. *Nat Med.* 2006;12:1075-80.
140. Harada C, Okumura A, Namekata K et al. Role of monocyte chemotactic protein-1 and nuclear factor kappa B in the pathogenesis of proliferative diabetic retinopathy. *Diabetes Res Clin Practice.* 2006;74:249-256
141. Baynes JW. Role of oxidative stress in development of complications in diabetes. *Diabetes.* 1991;40:405-412
142. Li JM, Shah AM. Endothelial cell superoxide generation: regulation and relevance for cardiovascular pathophysiology. *Am J Physiol Regul Integr Comp Physiol.* 2004; 287(5):R1014-30
143. Baumgartner-Parzer SM, Wagner L, Pettermann M, Grillari J, Gessl A, Waldhäusl W. High-glucose--triggered apoptosis in cultured endothelial cells. *Diabetes.* 1995; 44(11):1323-7

144. Barchowsky A, Munro SR, Morana SJ, Vincenti MP, Treadwell M. Oxidant-sensitive and phosphorylation-dependent activation of NF-kappa B and AP-1 in endothelial cells. *Am J Physiol*. 1995;269(6 Pt 1):L829-36.
145. Aoki M, Nata T, Morishita R, Matsushita H, Nakagami H, Yamamoto K, Yamazaki K, Nakabayashi M, Ogihara T, Kaneda Y. Endothelial apoptosis induced by oxidative stress through activation of NF-kappaB: antiapoptotic effect of antioxidant agents on endothelial cells. *Hypertension*. 2001;38(1):48-55.
146. Janssen-Heininger YM, Poynter ME, Baeuerle PA. Recent advances towards understanding redox mechanisms in the activation of nuclear factor kappaB. *Free Radic Biol Med*. 2000;28(9):1317-27.
147. Li ZG, Zhang W, Grunberger G, Sima A. Hippocampal neuronal apoptosis in type 1 diabetes. *Brain Res*. 2002;946(2), 221-231
148. Ido Y, Vindigni A, Chang K, Stramm L, et al. Prevention of vascular and neural dysfunction in diabetic rats by C-peptide. *Science*. 1997; 277, 563-566.
149. Flatt PR, Swanston-Flatt SK, Hampton SM, Bailey CJ, Marks V. Specific binding of the C-peptide of proinsulin to cultured B-cells from a transplantable rat islet cell tumor. *Biosci Rep*. 1986;6, 193-199.
150. Pramanik A, Ekberg K, Zhong Z, Shafqat J, et al. C-peptide binding to human cell membranes: importance of Glu27. *Biochem Biophys Res Commun*. 2001;284, 94-98.
151. Lindahl E, Nyman U, Melles E, Sigmundsson K, et al. Cellular internalization of proinsulin C-peptide. *Cell Mol Life Sci*. 2007; 64, 479-486.
152. Lindahl E, Nyman U, Zaman F, Palmberg C, et al. Proinsulin C-peptide regulates ribosomal RNA expression. *J Biol Chem*. 2010; 285, 3462-3469.
153. Gruenberg, J. The endocytic pathway: a mosaic of domains. *Nat Rev Mol Cell Biol*. 2001; 2, 721-730.
154. Miaczynska M, Pelkmans L, Zerial M. Not just a sink: endosomes in control of signal transduction. *Curr Opin Cell Biol*. 2004;16:400-406.
155. Di Guglielmo GM, Baass PC, Ou WJ, Posner BL, Bergeron JJ. Compartmentalization of SHC, GRB2 and mSOS, and hyperphosphorylation of Raf-1 by EGF but not insulin in liver parenchyma. *EMBO J*. 1994;13:4269-4277.
156. Baass PC Di Guglielmo GM, Authier F, Posner BL, Bergeron JJ. Compartmentalized signal transduction by receptor tyrosine kinases. *Trends Cell Biol*. 1995;5, 465-470.
157. Grimes ML, Zhou J, Beattie EC, Yuen EC, et al. Endocytosis of activated trkA: evidence that nerve growth factor induces formation of signaling endosomes. *J Neurosci*. 1996;16, 7950-7964.